Parametrization of learning tasks for the analysis of switch-dependent memory consolid

Auteur : Kellens, Emmy
Promoteur(s) : Drion, Guillaume
Faculté : Faculté des Sciences appliquées
Diplôme : Master en ingénieur civil biomédical, à finalité spécialisée
Année académique : 2022-2023
URI/URL : http://hdl.handle.net/2268.2/17980

Parametrization of learning tasks for the analysis of switch-dependent memory consolidation

Master thesis realized with the aim of obtaining the degree of Master in Biomedical Engineering

Emmy Kellens

Promotors:
Guillaume Drion
Pierre Sacré

Jury members:
Guillaume Drion
Pierre Sacré
Gilles Vandewalle
Kathleen Jacquerie

University of Liège
Faculty of Applied Sciences
Academic year 2022 - 2023

Parametrization of learning tasks for the analysis of switch-dependent memory consolidation

Emmy Kellens

Supervisor: G. Drion
Master in Biomedical Engineering, University of Liège
Academic year 2022-2023

Abstract

When we learn something new, our brain initially forms a fragile memory. Then, this memory needs to be consolidated so that it can be stored more permanently. Memory consolidation describes the process by which our memories strengthen to become durable in our brain. But what influences this process?

One hypothesis of consolidation is the impact of activity switches on the reinforcement of neuronal connections. This property of neurons encoding information is known as synaptic plasticity. Experimental evidence in cognitive neuroscience has shed light on the mechanisms by which plasticity is triggered. By employing modeling techniques that replicate these experimental findings, we take another approach to understanding the processes underlying memory. Experimental studies have provided compelling evidence for the correlation between the transition of neuronal firing patterns in the brain and the formation and consolidation of memory.

To study the impact of these different activities, it is necessary to define a learning task. However, the literature on plasticity modeling is extensive. To gain insight into how to design a learning task, a literature review is conducted. The implementation of these tools is then combined with the choices of free parameters related to the tasks. The mechanisms of potentiation and depression based on the frequencies of neuronal input signals are also explored.

By applying this parametrization, limiting phenomenons of models have been highlighted, namely the spike transmission and its influence on network connectivity. This refers to the "erroneous" increase in synaptic plasticity for non-activated presynaptic neurons. From these limitations, implementations of solutions have been explored. Two of them made it possible to overcome this problem. The first one was the definition of a maximum synaptic capacity, and the second one was a simplified approach to a homeostasis mechanism for the excitability of postsynaptic neurons.

Finally, once parameterization was done and limitations were overcome, learning tasks on neuronal circuits were carried out. First, the network was presented with a grid pattern without overlapped pixels and showed a consolidation consistent with memory shaping. Then, patterns with overlapped pixels were shown. Depending on the simulation parameters chosen, two results were observed: total or partial consolidation of overlapped pixels.

Such sensitive parameterization of plasticity rules can be seen on the one hand as an inherent fragility of those models. On the other hand, the differences between the results obtained by changing the parameters could reflect the different situations occurring in the brain under the action of external parameters such as mood. The question of the right learning method remains open and merits further investigation. A noted perspective might be to combine the strengths of several research fields.

Acknowledgements

First of all, I would like to express my deep gratitude to my promoter, Guillaume Drion, whose expertise and precious advice played an essential role in the realization of this work. I would also like to thank Kathleen, whose many ideas and daily help were invaluable. Her energy, motivation and positive attitude have continually encouraged me and pushed me to give my best.

I would like to acknowledge my parents' understanding and acceptance of my difficult days. I would also like to thank my grandfather for his attentive reading.

Special thanks to Basil, whose timeless support and faith in me have been of great importance. His constant encouragement has strengthened my determination to persevere in my efforts.

Finally, I would like to express my heartfelt gratitude to my friends Caroline and Sika, with whom I have spent many hours of hard work and convivial meals. Your company has kept my mood up not only throughout this work but throughout the years.

Liège, June 9^{th}, 2023

Emmy Kellens

Acronyms

- ALIF: Adaptative Leaky Integrate-and-Fire
- AMPAr : α-amino-3-hydroxy-5-methyl-4-isoxazolepropionic acid receptor
- AP: Action potential
- CNN: Convolutional Neural Networks
- EEG: Electroencephalography
- E-LTP: Early Long-Term Potentiation
- EPSP: Excitatory Post-Synaptic Potential
- GABA: Gamma-Aminobutyric Acid
- GABA-A receptor: type A of Gamma-Aminobutyric Acid receptor
- GABA-B receptor: type B of Gamma-Aminobutyric Acid receptor
- fMRI: functional Magnetic Resonance Imaging
- IPSP: Inhibitory Post-Synaptic Potential
- LIF: Leaky Integrate-and-fire
- LTD: Long-Term Depression
- L-LTP: Late Long-Term Potentiation
- LTP: Long Term Potentiation
- MNIST: Modified National Institute of Standards and Technology
- NMDAr: N-methyl-D-aspartate receptor
- RF: Receptive Field
- SD: Standard Deviation
- SDSP: Spike-Driven Synaptic Plasticity
- SNNs: Spiking Neural Networks
- SO: Slow Oscillations
- STDP: Spike Timing Dependent Plasticity
- SWS: Slow wave sleep

Contents

Chapter 1

Introduction

1.1 Motivation

Researchers have long been fascinated by the intricate relationship between memory and brain activity. The process of memory formation relies on the remarkable ability of neurons to adapt and remodel their connections, through a phenomenon known as synaptic plasticity. In the brain, the combined activities of these neurons enable us to move from one state to another, for example from sleep to wakefulness. Numerous studies have highlighted the impact of switches of activity on this process of cognitive memory consolidation.

Early investigations of this influence began with the transition from wakefulness to sleep. In a seminal study by Jenkins and Dallenbach (1924), participants were asked to memorize a list of meaningless syllables. Their results were remarkable: those who had the opportunity to sleep after learning performed significantly better than their counterparts who remained awake for the same period. The field of cognitive neuroscience has continued the work of this seminal study, exploring the various links between neurobiological mechanisms - the functions of the nervous system - and cognitive processes such as perception, attention, memory and learning.

In this project, we will focus on one of the interfaces of cognitive neuroscience, namely computational neuroscience. Cognitive and computational neuroscience are like detectives trying to solve the mystery of how the brain works. Cognitive neuroscience can be compared to investigators who study the various clues left by the brain during experiments in cognition and memory. They analyze behaviors, reactions and cognitive abilities, and use brain imaging techniques to observe brain activity during these tasks. These detectives try to understand the brain's internal mechanisms by influencing our thoughts, emotions and behaviors. On the other hand, computational neuroscientists are like coders who create computer simulations of the brain. They use biophysical and mathematical models to reproduce observed cognitive processes and behaviors. These coders try to piece together a puzzle using codes to represent neuronal connections and interactions between different brain regions.

In this field, the principles of synaptic plasticity are translated into models that attempt to represent the brain's physiological mechanisms with varying degrees of reliability. These studies complement experimental research by simulating different theories and exploring the diverse mechanisms involved. But how can a memory task for neural networks be realized with modeling? This is where the problematic of my master thesis comes in, namely the design of memory tasks in the study of the relationship between activity switches and memory consolidation.

1.2 Structure

The computational neuroscience journey takes this global structure (aboarding points?)....

Part I presents the neurological and modeling elements that will be used throughout this project. With regard to the neurological bases, the different types and mechanisms of synaptic plasticity will be outlined. An overview of the different brain rhythms will also be provided, according to the different zoom levels in the brain (CHAPTER 2). In the same section on the background, an introduction is given to the various techniques for modeling synaptic plasticity, with details of the models which will be used in this project. The transition from biology to modeling is then made for the various neuronal rhythms. The modeling of neural networks and activity switches is also clarified. Finally, the combined application of plasticity, neural network and switch models will highlight the phenomenon of "homeostatic reset", which will be exploited for memory consolidation (CHAPTER 3)

Part II is dedicated to the literature review of learning tasks in computational neuroscience. The detailed analysis of these papers then enabled the formulation of a *checklist* of tools to be combined and specified for the design of these tasks (CHAPTER 4).

Part III focuses on the whole computational part and the experiments done during this thesis, whose general aim is to analyze brain-state-dependent memory consolidation across various tasks. This begins with the design of our own learning protocol, based on the checklist drawn up during the literature review. Then, when this protocol is tested on a simple task, a phenomenon not compatible with memory consolidation is observed. Solution scenarios will be analyzed in order to address this limitation. Once our parameterization is complete, we will compare the learning of different patterns by the network (from the grid pattern to the MNIST dataset) (CHAPTER 5).

Part IV draws a final conclusion to this work, concerning the fragility of the application of plasticity rules in memory consolidation protocols, as well as subjectivity in task design. Perspectives and reflections will also be discussed. (CHAPTER 6).

Part I

Background

Chapter 2

Biological background

2.1 Synaptic plasticity

The brain is a complex organ that serves as the control center of the body. It is the seat of the coordination of motor movement, the regulation of emotions, the process of information, and the support of cognitive functions such as memory and learning. The primary functional units of the brain are neurons, specialized cells that communicate with each other through electrical impulses called action potentials.

The *synapse* is a specialized junction between two neurons, allowing the transfer of information from one cell to the other. It includes the presynaptic terminal, the postsynaptic dendrites, and the space between them, called the synaptic cleft. The synapse plays a critical role in neural circuits in the nervous system.
The *synaptic transmission*, in chemical synapses, is the fundamental process by which chemical messengers are released in the synaptic cleft and bind to target cells to modulate their activity. It involves the synthesis, storage, and release of chemical messengers called *neurotransmitters*, which are stored in vesicles at the presynaptic terminal (Cotman and McGaugh, 1980; Fon and Edwards, 2001). The information transfer process can be divided into three main steps, as illustrated by Figure 2.1 (Holz and Fisher, 1999).

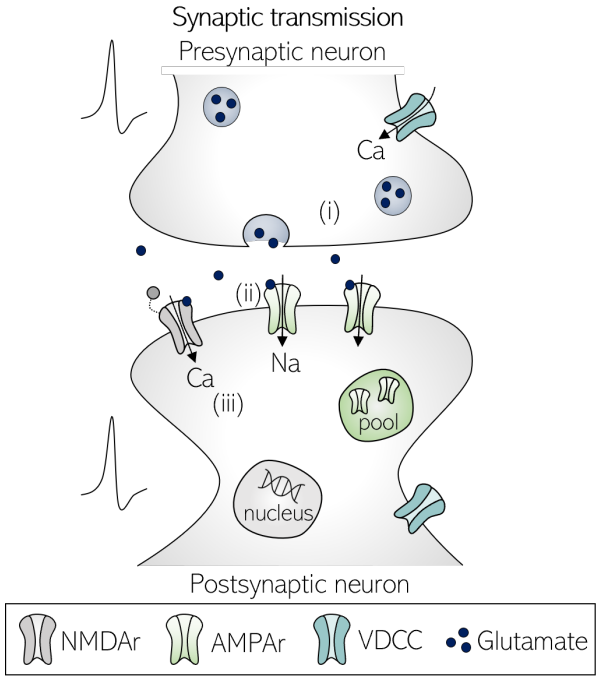

Figure 2.1 – **Synaptic transmission**: (i) After an action potential, calcium enters the cell through VDCC and leads to the endocytosis of vesicles filled with neurotransmitters. (ii) The neurotransmitters bind to their specific receptor located on the postsynaptic dendrite. (iii) The binding of the transmitter allows the ion to flow inside the cell. *Taken from (Jacquerie, 2023)*

(i) **Action Potential & neurotransmitter release**: The action potential (AP) in the presynaptic neuron causes the entry of *calcium* into the cell by opening voltage-dependent calcium channels (VDCC). This influx of calcium ions trig-

gers the fusion of the vesicles with the membrane,
leading to the release of neurotransmitters in the synaptic cleft.

(ii) **Neurotransmitters binding**: After their diffusion across the synaptic cleft, neurotransmitters bind to specific postsynaptic receptors. The primary excitatory neurotransmitter in the brain is the *glutamate*, which binds to receptors called NMDA receptors, *NMDAr* (N-methyl-D-aspartate receptor), and AMPA receptors, *AMPAr* (α-amino-3-hydroxy-5-methyl-4-isoxazolepropionic acid receptor). The latter is activated when glutamate binds to it, unlike the NMDAr which requires both glutamate binding and depolarization of the postsynaptic membrane.

(iii) **Postsynaptic transmission**: Activation of AMPAr allows cations to flow through the membrane. The voltage increase caused by this ion influx leads to the opening of the NMDAr, whose activation enables the influx of calcium ions into the postsynaptic neuron. Calcium can then trigger downstream signaling events. The increase in membrane potential of the postsynaptic neuron response due the to presynaptic action potential can be measured by the excitatory postsynaptic potential (EPSP).

The transmission explained here leads to an excitatory response of the postsynaptic neuron due to the binding of excitatory neurotransmitters on their receptors. Now consider an inhibitory neurotransmitter that binds to one of its associated receptors, located on the postsynaptic membrane. In this case, the response measured will be an inhibitory postsynaptic potential (IPSP). The major inhibitory neurotransmitter in the central nervous system is gamma-aminobutyric acid (*GABA*). It can bind to either GABAa or GABAb receptors.

Following transmission of information, neurotransmitters are removed from the synaptic space to avoid over-stimulation of the postsynaptic neuron. This process can take place via three main mechanisms: diffusion, degradation, or reuptake by the presynaptic neuron (Knapp et al., 2003).

A particular feature of these synapses is that they are extremely plastic, meaning that their strength is capable of evolving over time. Synaptic strength is defined as "the efficiency of signal propagation from one cell to another" (Vandeginste et al., 1998). The evolution of this efficiency reflects the ability of neurons to adapt and modify their structure and function in response to experience. This modification of the intensity of neuronal connections through activity-dependent mechanisms is called *synaptic plasticity* (Magee and Grienberger, 2020). This capacity of synapses is fundamental to understanding of the mechanisms of memory and learning (Takeuchi et al., 2014).

2.1.1 Plasticity mechanisms

Synaptic plasticity can occur over a wide range of timescales, from milliseconds to hours, days, and even longer. This temporal flexibility enables the brain to adapt to changes in the environment and to learn from experience in a dynamic, reactive way. The synaptic plasticity mechanism has been divided into two main timescales, namely short-term plasticity and long-term plasticity (Citri and Malenka, 2008).

Short term plasticity

On the fastest time scale, *short term plasticity* is defined as changes in the strength of synaptic connections that occurs in milliseconds or seconds. This plasticity is the response to a variety of mechanisms including changes in the level of neurotransmitter stored by the presynaptic neuron, the activity of ion channels, or the availability and concentration of calcium ions (Regehr, 2012).

Short-term plasticity can be either *facilitation* or *depression*, one being the opposite effect of the other. Facilitation refers to a transient increase in the strength of synaptic connections due to an increase in neurotransmitters released by the presynaptic neuron. On the other hand, depression refers to a transient decrease in the strength of synaptic connections due to a decrease in neurotransmitter exocytosis (Fioravante and Regehr, 2011; Zucker and Regehr, 2002).

Long term plasticity

On the slowest time scale, *long-term* plasticity refers to more persistent and long-lasting changes in the strength and efficiency of synapses (can occur over hours, days, or weeks). As for short-term plasticity, it can be divided into two main forms. Either the strengthening of synapses called *LTP* for long-term potentiation, or their weakening, called *LTD* for long-term depression (Abraham et al., 2019). Long-term plasticity can lead to the recruitment of new synapses, the insertion or removal of receptors, and the restructuring, consolidation, and modification of neural circuits in response to experience. LTP can be classified in two categories based on the time scale and the dynamics of protein synthesis, namely *Early Long Term Potentiation* (E-LTP) and *Late Long Term Potentiation* (L-LTP) (Baltaci et al., 2019; Lamprecht and LeDoux, 2004).

- E-LTP is the early phase of long-term changes. The process by which E-LTP occurs is explained by the influence of NMDAr mediated calcium influx into the postsynaptic neuron. In the case of high calcium influx, the signaling cascade triggered by calcium will lead to the potentiation of the synapse in two ways. The first is an increase in the efficiency of postsynaptic receptors, while the second is the insertion of new AMPAr from exocytosis of AMPAr-containing vesicles, called *pool*. It does not involve protein synthesis or structural changes at the synapse (Becker and Tetzlaff, 2021)

- L-LTP is the late phase, where stabilization of potentiated synapses occurs through morphological changes. The signaling cascade triggered by the high calcium influx goes one step further and leads to the expression of new proteins, such as AMPAr and growth factor. Therefore, it induces new AMPAr synthesis and insertion on the postsynaptic membrane but also structural changes, such as dendritic spine enlargement and growth or formation of new synapses (by spine creation) (Smolen, 2007; Toni et al., 1999). Dendritic spines are small protrusions that extend from the dendrites of neurons, and are highly dynamic structures that can undergo structural changes in response to neuronal activity and synaptic input (Hayashi and Majewska, 2005).

Figure 2.2 summarizes all the changes induced by E-LTP or L-LTP. These categories can also be applied to LTD, which will cause the opposite effect of LTP and decrease the synapse strength.

2.1.2 Types of plasticity

All types of plasticity are not mutually exclusive and can interact with each other. This particularity makes synapse evolution a very complex mechanism. An overview of the most studied forms of plasticity is provided in this subsection.

Hebbian plasticity

Hebbian plasticity is based on the principle of associative learning. The idea behind this plasticity comes from Hebb's postulate, which states that "neurons that fire together, wire together" (Hebb, 1949). This quote means that if two neurons are activated simultaneously, the strength of the synapse between them will be enhanced, resulting in increased efficiency of communication between them. In

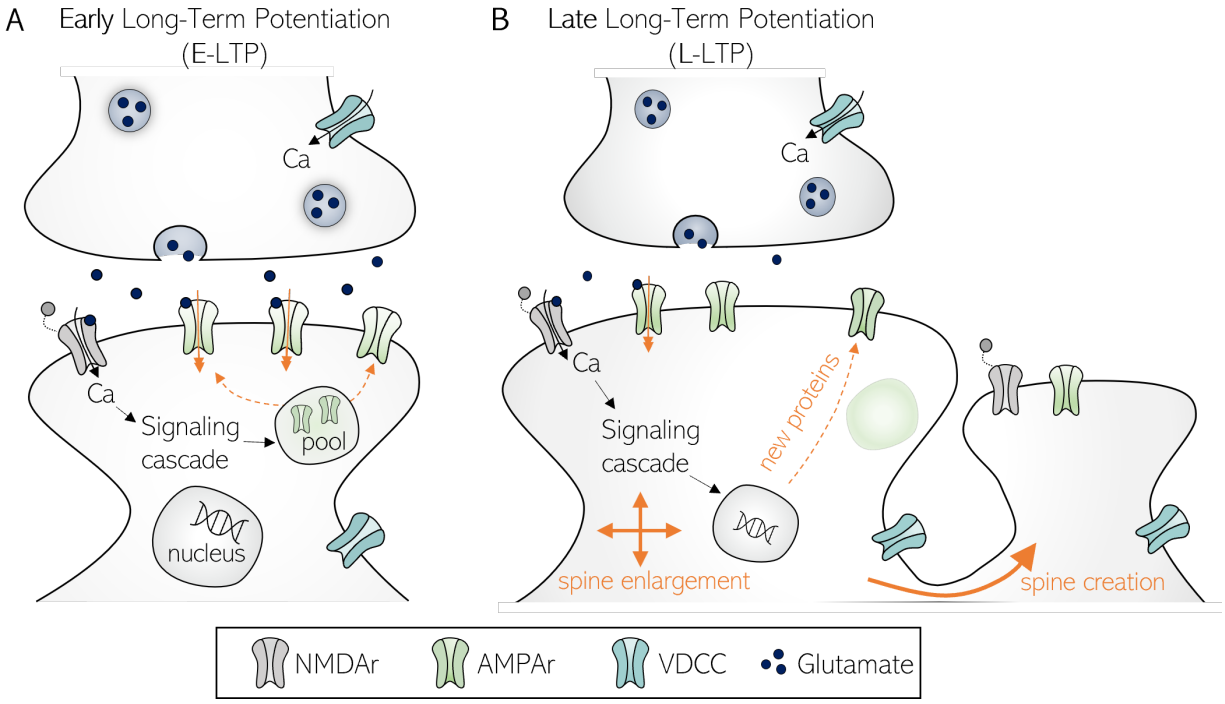

Figure 2.2 – **Mechanisms of early and late LTP**: Changes induced by processes are colored in orange in both figures **A.** High calcium influx into the postsynaptic neuron triggers a signaling cascade that will lead to the insertion of new receptors, coming from the pool, as well as the increase of the efficiency of receivers. **B.** For late-LTP, the signaling cascade leads to the synthesis and expression of new receptors and their efficiency increase, as well as morphological changes such as spine enlargement or creation. (*Adapted from Jacquerie (2023)*)

other words, if a presynaptic neuron fires repeatedly just before a postsynaptic neuron, the synaptic strength will increase. Conversely, if the postsynaptic neuron always fires before the presynaptic neuron, the synaptic strength will decrease. This Hebbian plasticity has been widely accepted as a fundamental principle of neuronal plasticity and has been refined and extended over the years (Bi and Poo, 2001).

A particular Hebbian plasticity rule is *Spike-Timing-Dependent plasticity* (*STDP*). STDP is a form of long-term plasticity that depends on the presynaptic and postsynaptic relative timing of spikes (Timofeev and Chauvette, 2019; Feldman, 2020). The relative timing between these activities determines the magnitude and direction of changes in synaptic strength (Zhang et al., 1998). Specifically, when the presynaptic neuron fires just before the postsynaptic neuron, it results in an increase of the synaptic strength through LTP. Conversely, when the postsynaptic neuron fires before the presynaptic neuron, synaptic strength decreases according to the LTD mechanism (Bi and Poo, 1998).

Homeostatic plasticity

Turrigiano and Nelson (2004) were the first to introduce the concept of homeostatic plasticity in neural circuits. They suggested that homeostatic plasticity helps ensure that neurons maintain an appropriate level of activity. This form of plasticity is often seen when inputs or environmental conditions change. It may happen that, if input is reduced over a long period, the neurons in the circuit increase the strength of their synapses to compensate for this input reduction and maintain stable activity levels. Homeostatic plasticity is mediated by several mechanisms, such as changes in the expression and function of ion channels, changes in the properties of synaptic connections (number or strength), and

adjustments in the release of neurotransmitters. All of these mechanisms act in the same way to help neurons maintain stability and adapt to changing conditions over time (Vitureira et al., 2012).

Extrinsic vs intrinsic plasticity

Extrinsic plasticity refers to changes in strength and efficiency of the synaptic connection between neurons, which can occur through LTP or LTD.

Intrinsic plasticity, also called plasticity of intrinsic excitability, is an activity-dependent plasticity driven by changes in the intrinsic properties of neurons, without involving changes at the synapses. This can occur through changes in the expression and function of ion channels or neurotransmitter receptors, resulting in changes in the excitability of the membrane potential (and therefore in a change in the firing rate of the neuron) (Daoudal and Debanne, 2003; Shim et al., 2018; Debanne et al., 2019).

Heterosynaptic vs homosynaptic plasticity

Heterosynaptic plasticity is defined as the change in strength between a presynaptic and a postsynaptic neuron as a result of the activity of a neighboring synapse, rather than from their own activity as in homosynaptic plasticity (Chistiakova et al., 2014).

Structural plasticity

Structural plasticity is defined as the ability of neurons to undergo physical changes in their morphology or connectivity. These changes occur at the level of individual synapses and more precisely, on the scale of small synaptic structures, such as dendritic spines (Holtmaat and Svoboda, 2009). Structural plasticity occurs in response to changes in neural activity or experience and can lead to the formation of new synapses or the elimination of existing ones, ultimately altering the functional connectivity of neural circuits (Butz et al., 2009; Muller et al., 2002). Actin filaments play a crucial role in regulating the structural plasticity of dendritic spines. They are the primary component of the spine's cytoskeleton and are responsible for maintaining spine morphology, stability and flexibility (Bosch and Hayashi, 2012).

2.1.3 Synaptic plasticity in the context of this thesis

In the context of this master thesis and according to the notations used in computational neuroscience (Jacquerie, 2023), the expression of synaptic plasticity will be classified into two categories.

The E-LTP process, leading to AMPAr insertion and increased receptor efficiency, will be associated with the notion of *traditional synaptic plasticity*, as often used in computational neuroscience. It does not involve morphological changes, or protein synthesis, since the AMPAr comes from the pool. As for the L-LTP process, affecting synapse morphology and the expression of new receptors, it will be modeled by *structural plasticity* (Butz et al., 2009).

2.1.4 Neuronal assemblies

Neuronal assemblies are ensembles of transiently active neurons that underlie various brain operations, including memory encoding and reasoning. These assemblies, composed of interconnected and synchronized neurons, form functional circuits of brain activity. They constitute as the fundamental units of information processing in the brain (Badin et al., 2017; Deolindo et al., 2018; Buzsáki, 2010).

The concept of cell assemblies results from Hebbian plasticity. Indeed, Hebb (1949) suggested that the simultaneous firing of neurons is strengthening their connection, thus leading to the formation of functional cell assemblies.

2.2 Cerebral rhythms and activities

The various behaviors and cognitive processes that take place over the course of a day are dictated by our brains. These activities range from sleeping and dreaming to wakefulness including learning, walking, or thinking. *Brain states* correspond to different functional or behavioral states, reflected by distinct patterns of neuronal activity. These states mirror different levels of arousal, cognitive processing, and overall functional connectivity within neural networks.

The brain is transitioning between the states in response to internal and external stimuli and can also be influenced by factors such as stress and various neurological or psychiatric disorders. Abnormal brain states may be characterized by disrupted activity patterns, altered connectivity, or impaired information processing.

These states can be observed and measured at the level of the brain and neurons through various neuroimaging techniques, providing insights into the dynamic nature of brain activity and its relationship to cognitive and behavioral processes (Bradley et al., 2022). Figure 2.3 schematize the different brain states and measurement techniques, as described below.

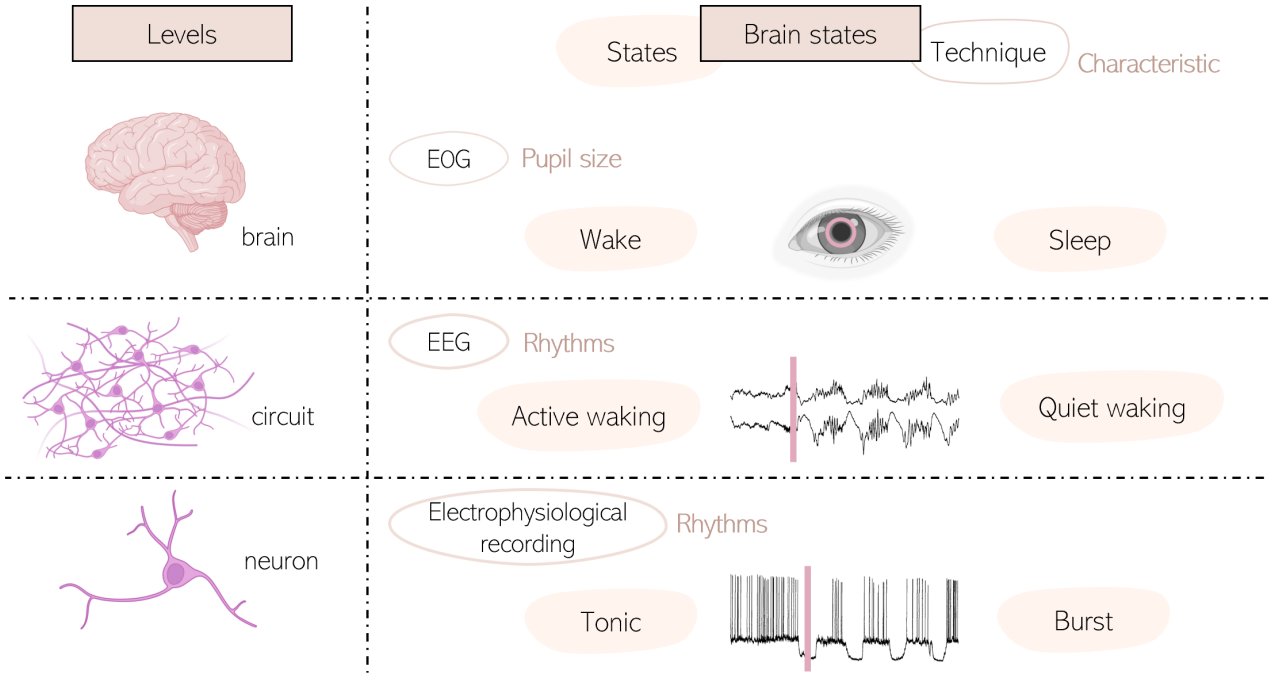

Figure 2.3 – **Characterization of brain states at different levels**: Brain states can be characterized at different brain levels. The brain can switch from sleep to wake state, which is for example reflected in the size of pupils. By looking at neural networks, the rhythm recorded by an EEG can switch from quiet waking to active waking. At the level of the neuron, the neuronal rhythm can go from bursting activity to a tonic firing, detected by electrophysiological recording. *Inspired from (Jacquerie, 2023)*

2.2.1 Brain level

Brain activity can be detected by analyzing the frequency and amplitude of electrical signals, recorded by electroencephalography (EEG). Other methods can complement the detection of the brain-behavior, such as the fluctuations in pupil diameter or eye-opening, or heart rate recorded by ECG.

If we focus only on the electrical activity of the brain, during wakefulness, the brain is in an active state and exhibits small amplitude and high-frequency EEG signals (Poulet and Crochet, 2019).

This state is associated with a high level of vigilance and cognitive processing. During sleep, the EEG signals from the brain show slow-wave sleep oscillations, corresponding to high amplitude, low frequency signals. As biologically points out, this brain state is also associated with memory consolidation (Sun et al., 2020).

2.2.2 Neuronal circuit level

Let us now consider a neuronal circuit, formed by the connections between individual neurons. They form an interconnected group of several neurons, that works together to process and transmit information. At this scale, brain states can range from active to quiet waking, detected by switches in Local Field Potential (LFP) oscillations or by EEG, from small amplitude and fast to large amplitude and slow oscillations (Figure 2.4).

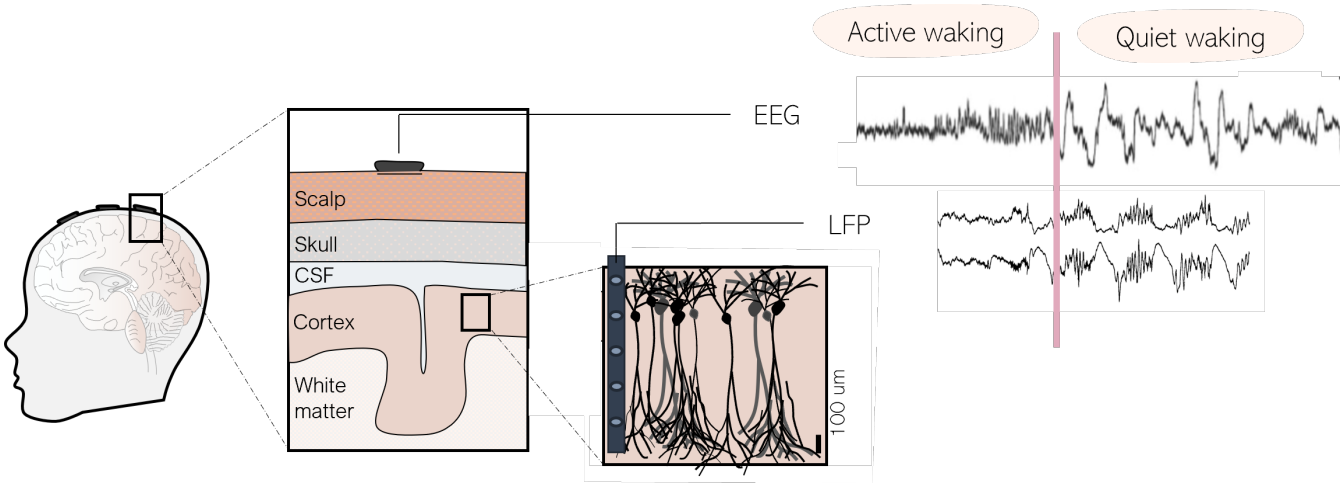

Figure 2.4 – **Active and quiet waking measured by EEG and LFP**: The electrodes for the EEG are placed on the scalp. For both rhythms, there is a transition between a small amplitude and fast to large amplitude and slow oscillations. *(Adapted from Jacquerie (2023))*

Box 1 - EEG and LFP

Electroencephalography (EEG) is a non-invasive technique that uses electrodes placed on the scalp to provide a global view of the brain's electrical activity. It records the summation of electrical potentials generated by the synchronized activity of neurons across different brain regions.
Local Field Potential (LFP) refers to the electrical signals recorded from a small group of neurons or a specific brain region. They provide valuable information about the synchronous activity and functional connectivity of neuronal populations in a specific brain region. They are typically recorded using microelectrodes.

2.2.3 Neuron level

At the level of the neurons, the different electrical patterns recorded are ranging from *tonic firing* to *bursting* (Beurrier et al., 1999), as shown in Figure 2.5. These two neuronal rhythms are part of a large list of patterns found in biology, but these are the ones that will be used and studied in this thesis.

Tonic firing is defined by a continuous and regular sequence of action potential generated by a

neuron in response to a sustained input or an external stimulus. This firing pattern is associated with a state in which neurons receive continuous input from sensory stimuli and cognitive processing.

The *bursting* electrical activity corresponds to a rapid succession of grouped spikes. More precisely, this pattern is characterized by high-frequency action potentials followed by a period of quiescence, longer than typical inter-spike intervals. This rhythm, often associated with sleep but also found in wakefulness, reflects an intense cerebral activity during which memory consolidation and other cognitive processes happen. (Peirano and Algarín, 2007)

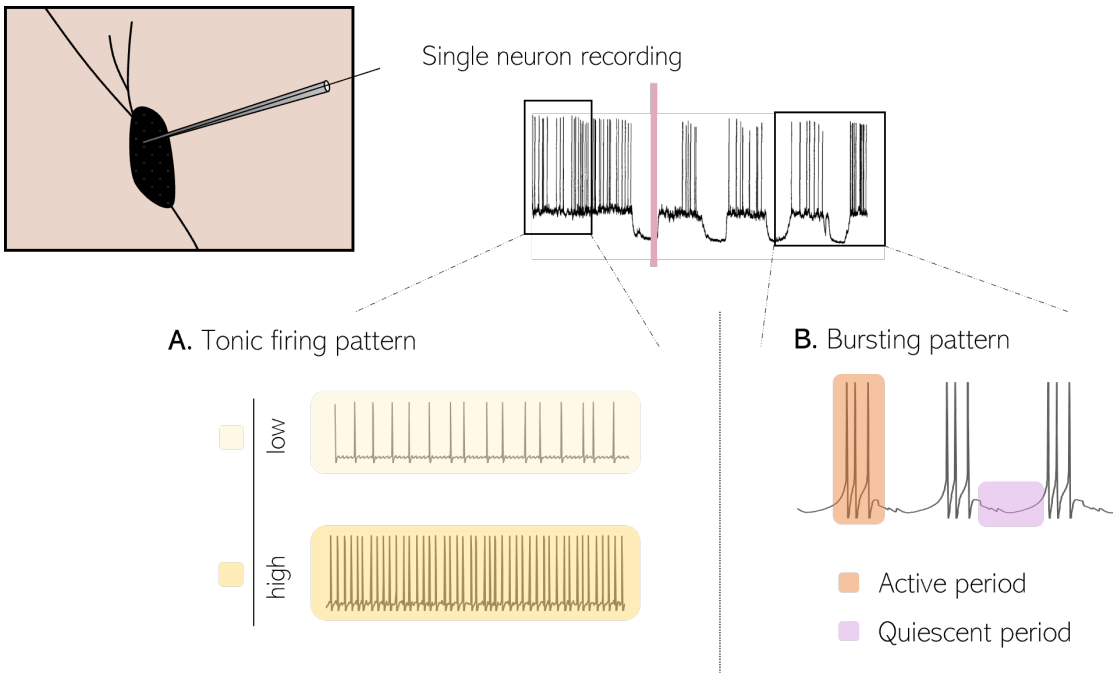

Figure 2.5 – **Tonic and Burst firing patterns**: **A.** Neuronal response to an external stimulus or input current, in the form of successive action potentials. The frequency can vary from low to high. **B.** Alternating between active periods, consisting of a rapid succession of spikes, and periods of silence, without any spikes. *(Inspired by Jacquerie (2023))*

The transition between brain states requires a change in the neuronal or networking activity in different brain regions, which can occur spontaneously or be triggered by external or internal factors. The exact mechanism underlying this change in cognitive and motor states is not fully understood. However, this transition is mainly modulated by neuromodulators present in the brain, such as acetylcholine or serotonin (Lee and Dan, 2012). They act in a complex way to regulate the switches from one state to another (Pedrosa and Clopath, 2017).

Chapter 3

Computational neuroscience background

In order to investigate all the complex notions described in the biological background and to understand how plasticity occurs, modeling is employed. Computational models of neurons, neuronal rhythms, and synaptic plasticity will be described in this chapter.

3.1 Plasticity rules

3.1.1 Traditional plasticity rules

From a mathematical point of view, synaptic plasticity can be considered as the evolution of the synaptic strength between two neurons of a synapse, noted w. The synaptic plasticity rules can be modeled by a black box with pre- and post-synaptic neuron activities as inputs and variations of the synaptic strength as output. Many models exist to represent this black box and particularly the way in which inputs are implemented to govern the evolution of the synaptic weight. They are divided into two categories with fairly explicit names: *biophysical* models, which take biological measures as input, and *phenomenological* models, based on the relationship between "phenomena" occurring within the synapse (Jacquerie, 2023). This is illustrated in Figure 3.1.

In order to be used in the modeling of artificial neural networks, these models need to be implemented. In the literature, various implementations exist, varying according to the choice of input data, such as different biological variables or neuronal events. In this chapter, selected implementations are reviewed, with a particular focus on those that will be mostly used in the computational part.

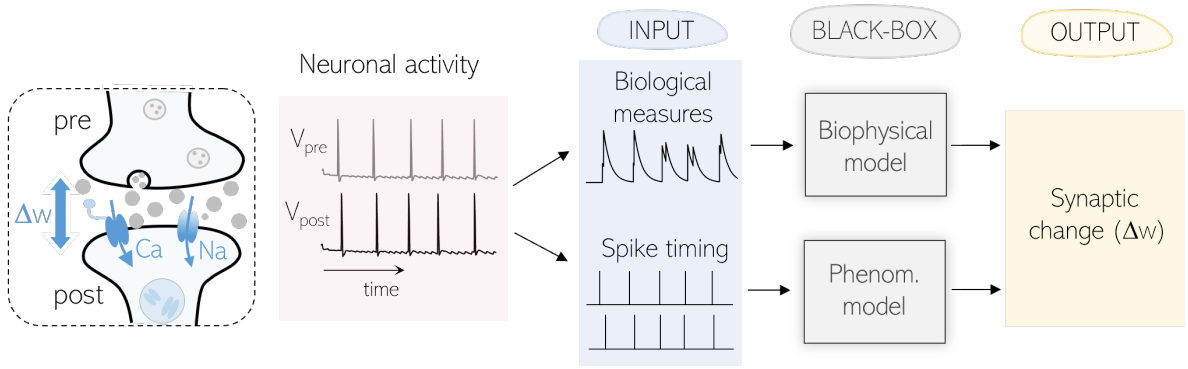

Figure 3.1 – **Categories of synaptic plasticity rules**: Synaptic plasticity can be modeled by a black box, taking neuronal activity as input and giving the synaptic strength change as output. Two categories of rules are modeling this synaptic plasticity: the biophysical model, based on biological measures arising from the neuronal activity, and the phenomenological model, based on the spike timing of synaptic neurons. *Adapted from (Jacquerie, 2023)*

Biophysical models

Biophysical models use biological measures as input signals to estimate the change in synaptic strength Δw. In particular, a calcium-based plasticity rule is a biophysical model that uses calcium as a key signal to modify w. It takes as input of the black box the calcium dynamics, that is, the influx of calcium as a function of time.

In the context of calcium-based rules, the relationship between pre- and postsynaptic spiking and calcium changes is implemented in various ways, so that model features can be very different from one model to another. Three main categories of model features can be distinguished. Firstly, to implement the calcium in a neuron model, several *source of calcium* can be taken into account, such as NMDAr, VDCC, or other pumps. Various ways of implementing *NMDAr dynamic* can also be considered, using pre-and postsynaptic neurons voltage or a more complex process to describe it. A third feature that can be modeled differently is the *calcium dynamics*, where calcium change can describe calcium current sources or by a more biophysical description.

In this thesis, the implementation of traditional calcium-based plasticity rules is based on the equations of Graupner and Brunel (2012) and Graupner et al. (2016), where synaptic change is governed by calcium dynamics. More precisely, the temporal evolution of w is conducted by a two-threshold calcium-dependence rule, with different calcium levels triggering different forms of plasticity. They introduced the notion of thresholds, with a depression threshold θd and a potentiation threshold θp. In their model, $\theta d < \theta p$, so that a calcium level below θd does not lead to a change in synaptic weight, while an intermediate level, between θd and θp, leads to LTD, and once θp is reached, LTP occurs (Figure 3.2).

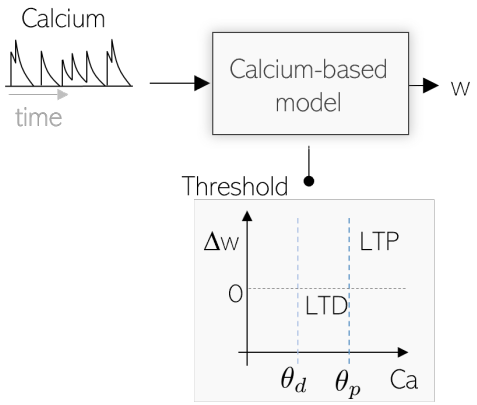

Figure 3.2 – **Exemple of calcium-based plasticity rule implementation**. In the implementation (Graupner and Brunel, 2012; Graupner et al., 2016), the evolution of the synaptic change depends on a two-threshold rule on the calcium level. *Adapted from (Jacquerie, 2023)*

.

Regarding the calcium dynamics, they decided to consider the contribution of NMDA receptors and also that of VDCCs. In this way, they take into account the calcium influx mediated by both pre-and post-spike, denoted by c_{pre} and c_{post}. The corresponding differential equations are:

$$\begin{aligned}
\dot{c}_{\text{pre}}\,(t) &= -\frac{c_{\text{pre}}}{\tau_{\text{Ca}}} + C_{\text{pre}} \sum_{\text{i}} \delta\,(t - t_{\text{pre}} - D) \\
\dot{c}_{\text{post}}\,(t) &= -\frac{c_{\text{post}}}{\tau_{\text{Ca}}} + C_{\text{post}} \sum_{j} \delta\,(t - t_{\text{post}}) \\
[\text{Ca(t)}] &= c_{\text{pre}}\,(t) + c_{\text{post}}\,(t)
\end{aligned} \tag{3.1}$$

where t_{pre} and t_{post} are the timings of pre and postsynaptic spikes. After each presynaptic (resp. postsynaptic) spike, the level of calcium of this neuron is increased by an amplitude C_{pre} (resp. C_{post}) and then decays exponentially, according to the time constant τ_{Ca}. The parameter D accounts for the slow rise time of the NMDAr-mediated calcium influx (a time-delayed increase of calcium after a presynaptic spike). The rule then considers the linear addition of these two levels of calcium to modify the

strength.

The equation representing this *two-threshold* is then given by:

$$\tau_w \dot{w} = \gamma_p(1-w)\Theta([\text{Ca}]-\theta_p) - \gamma_d w\Theta([\text{Ca}]-\theta_d) \tag{3.2}$$

where γ_d and γ_p are respectively the depression and potentiation rates. The two thresholds θ_d and θ_p are represented in the scheme of Figure 3.2. The function Θ can take two values, 1 if the calcium concentration is above the considered threshold and 0 otherwise.

It has been shown that this equation can be rewritten as a first-order differential equation (Ponnet, 2022; Jacquerie, 2023)

$$\tau_w([\text{Ca}])\dot{w} = \Omega([\text{Ca}]) - w \tag{3.3}$$

where $\tau_w([\text{Ca}])$ is the calcium-dependent time constant and $\Omega([\text{Ca}])$ the calcium-dependent steady-state value. This writing of ODE allows us to know directly the steady-state value in this calcium region and the associated time constant. There are three possible values for the steady states and the time constants, based on the threshold of the three calcium regions, such as:

$$\begin{aligned} [\text{Ca}] < \theta_d \quad & \tau_w^0 \dot{w} = \Omega^0 - w \\ [\text{Ca}] \in [\theta_d, \theta_p] \quad & \tau_w^d \dot{w} = \Omega^d - w \\ [\text{Ca}] > \theta_p \quad & \tau_w^p \dot{w} = \Omega^p - w \end{aligned}$$

This writing also allows to predict the convergence value of w, according to this equation:

$$w = \frac{\alpha^p \Omega^p + \alpha^d \Omega^d}{\alpha^p + \alpha^d} \tag{3.4}$$

where variables α corresponds to the time spent in each zone and Ωp and Ωd respectively to the maximum and minimum convergence values of w.

Phenomenological models

Phenomenological models of synaptic plasticity are rules according to which synaptic connections are modified by neuronal activity, such as the spike timings or frequencies. These models are based on experimental observations without incorporating a detailed description of the underlying biological mechanisms and processes. Three different implementations existing in the literature and which will be useful in this project are reviewed, namely pair-based, triplet, and voltage-based models (Figure 3.3).
The *pair-based model*, better known as spike-timing-dependent plasticity (STDP), modulates the evolution of the strength as a function of the relative timing of pre- and postsynaptic spikes. This model is based on the Hebbian theory which, as a reminder, states that synaptic connection between neurons repeatedly activated at the same time will be strengthened. Therefore, it involves two variables: the synaptic weight change Δw and a variable that describes the timing of the pre- and postsynaptic spikes Δt (Abbott and Nelson, 2000; Morrison et al., 2008).

Other phenomenological models are used in the literature, such as the triplet or the voltage-dependent synaptic plasticity. The *triplet* model is also based on the spike timing of presynaptic and postsynaptic neurons, like the pair-based model, but it considers a set of 3 successive spikes, called spike triplet. It can be either post-pre-post or pre-post-pre, as in the Figure 3.3 (triplet) (Pfister and Gerstner, 2006;

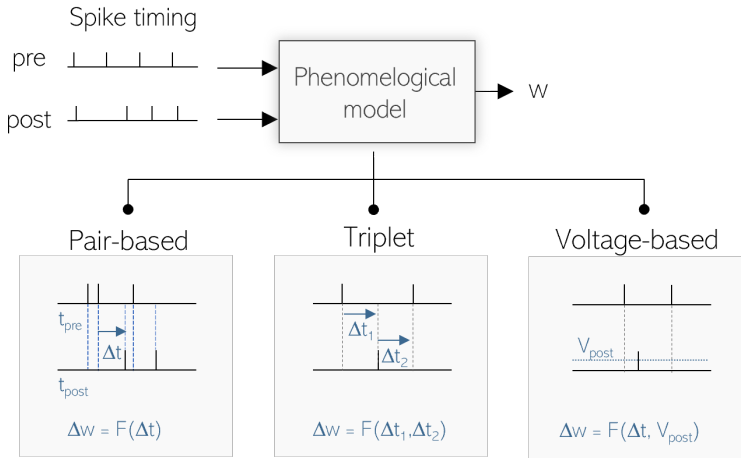

Figure 3.3 – **Phenomenological models**: Three different models of synaptic plasticity among those considering the neural activity as input of the rule. *Adapted from (Jacquerie, 2023).*

Gjorgjieva et al., 2011).

Lastly, the *voltage-dependent synaptic plasticity (VDSP)* suggests that the efficiency of synaptic transmission can be modulated by the voltage level of the postsynaptic neuron and the presynaptic spike arrival (Garg et al., 2022; Clopath et al., 2010). It thus involves three variables: the synaptic weight Δw, the variable that describes the timing of the pre-and postsynaptic spikes Δt, and also the postsynaptic membrane potential V_{post}.

3.1.2 Structural plasticity rule

It has recently been shown that to study the interaction between tonic/burst rhythms and plasticity, additional plasticity modeling is required. Therefore, in addition to traditional rules, structural plasticity (Jacquerie, 2023) is added. Traditional plasticity rules will model the Early LTP, related to LTP expression and leading to changes in temporary synaptic efficiency. The variable driven by these traditional rules will still be denoted w but it will refer to the *early weight*. The structural synaptic plasticity rule will model the Late LTP, serving to maintain this LTP expression. Another variable is therefore introduced to represent structural changes in the synapse and will be called the *late weight*, denoted by l. This late weight will be governed by early weight during rhythm changes.

Previous studies have led to the creation of several structural plasticity rules, used in the study of activity switches. In this thesis, we are using a rule recently developed in Justine Magis' thesis, which will highlight the benefits of this rule over existing ones. The equations are based on the calcium rule, where evolution of the early weight is described according to

$$\dot{w} = \frac{1}{\tau_w([\mathrm{Ca}])}(\Omega([\mathrm{Ca}]) - w \tag{3.5}$$

From this equation, we get the temporal evolution of late weight, governed by the following equation:

$$\tau_l \dot{l} = -\frac{1}{\tau_w([\mathrm{Ca}])}(\Omega([\mathrm{Ca}]) - w) \tag{3.6}$$

The main assumption of this model (discussed in Justine Magis' thesis) is that the *late weight* is only evolving in bursting mode.

3.1.3 Use of plasticity models

It is important to bear in mind that these plasticity models are computational tools. Indeed, given that the mechanisms taking place in the brain are still not fully understood, these tools enable us to try to understand things in a different way from tests on living beings. These rules attempt to model reality with varying degrees of rigor, but are not perfect and will therefore be tested and discussed in the experimental part of this thesis.

3.2 Neuronal rhythms

3.2.1 Modeling neuron spiking activity

To model neurons, and in particular their membrane potential V_m, we use a conductance-based model. This model, developed by Hodgkin and Huxley (1952), is compatible with activity switches and will therefore be the basic assumption for the experiments. The model represents neuronal activity mathematically by considering the conductance of ion channels in the neuronal membrane. It describes the behavior of ion channels using conductance values, which reflect the ease of ion movement through the channels, and explains how ions like sodium, potassium, and calcium contribute to the electrical properties of neurons.

In the formalism of Hodgkin and Huxley, the evolution of membrane potential V_m is described according to:

$$C_{\mathrm{m}}\dot{V}_{\mathrm{m}} = -\sum_i I_{\mathrm{ion}} + I_{\mathrm{app}} \tag{3.7}$$

where I_{app} is the applied current, C_m the membrane capacitance and I_{ion} the voltage-dependent ionic currents. Details about the different ion channels considered in this thesis can be found in Jacquerie (2023). The current flowing through an ion channel can be precise for each ion and is modeled by:

$$I_{\mathrm{ion}} = \bar{g}_{\mathrm{ion}} m_{\mathrm{ion}}\left(V_{\mathrm{m}}\right) h_i\left(V_{\mathrm{m}}\right)\left(V_{\mathrm{m}} - E_i\right) \tag{3.8}$$

where m_{ion} and h_i are respectively the variable that describes the activation and inactivation of the ion channel gates, modeling the opening or closing of the ion channel. The maximal conductance $\bar{g}_{\mathrm{ion}}$ represents a situation where all ion channels are open and E_i is the reversal potential also called Nernst potential. The equation governing gate activation and inactivation can be found in (Jacquerie, 2023).

3.2.2 Modeling neuronal networks

To now connect the neurons together, a variable representing synaptic currents must be added to the equation 3.7, which becomes :

$$C_{\mathrm{m}}\dot{V}_{\mathrm{m}} = -\sum_i I_{\mathrm{ion,i}} + I_{\mathrm{app}} + I_{\mathrm{syn}} \tag{3.9}$$

The different synaptic I_{syn} currents that will be considered here are those associated with the postsynaptic receptors AMPA, $\mathrm{GABA_A}$, and $\mathrm{GABA_B}$. They are defined as:

$$\begin{aligned} I_{\mathrm{AMPA}} &= \bar{g}_{\mathrm{AMPA}} s_{\mathrm{AMPA}}\left(V_{\mathrm{m}} - 0\right) \\ I_{\mathrm{GABA_A}} &= \bar{g}_{\mathrm{GABA_A}} s_{\mathrm{GABA_A}}\left(V_{\mathrm{m}} - E_{\mathrm{Cl}}\right) \\ I_{\mathrm{GABA_B}} &= \bar{g}_{\mathrm{GABA_B}} s_{\mathrm{GABA_B}}\left(V_{\mathrm{m}} - E_{\mathrm{K}}\right) \end{aligned} \tag{3.10}$$

where $\bar{g}_{\mathrm{AMPA}}, \bar{g}_{\mathrm{GABA_A}}$ and $\bar{g}_{\mathrm{GABA_B}}$ are the synaptic conductances, and $s_{\mathrm{AMPA}}, s_{\mathrm{GABA_A}}$ and $s_{\mathrm{GABA_B}}$ gating variables of the synaptic receptors. The dynamics of the gating variables and the reversal potentials of these three receptors can be found in Jacquerie (2023).

3.2.3 Modeling switches of activity and applied currents

Polarization-induced switching of inhibitory neurons

To model neuron activity switching, an inhibitory neuron is integrated into a circuit of excitatory neurons. Synaptic transmission is univocal, from the inhibitory neuron to the excitatory one through synaptic current from $\mathrm{GABA_A}$ and $\mathrm{GABA_B}$ receptors. The inhibitory neuron is capable to switch from tonic firing to burst due to an applied hyperpolarizing current step. First, as shown in Figure 3.4, a depolarizing current drives the neuron into tonic activity, which in turn drives the excitatory neurons into a hyperpolarized state. Then, when the inhibitory neuron is hyperpolarized, it switches all neurons of the circuit into burst mode.

Generation of excitatory neuron action potentials by applying an external current

The frequency of action potentials imposed on pre and postsynaptic neurons will be mainly done by applying brief current pulses to these neurons. In the simulation shown in Figure 3.4, a short depolarizing pulse is applied to the excitatory neuron at 1000ms, resulting in the generation of a single action potential. By applying many similar pulses, the wanted frequency can be achieved.

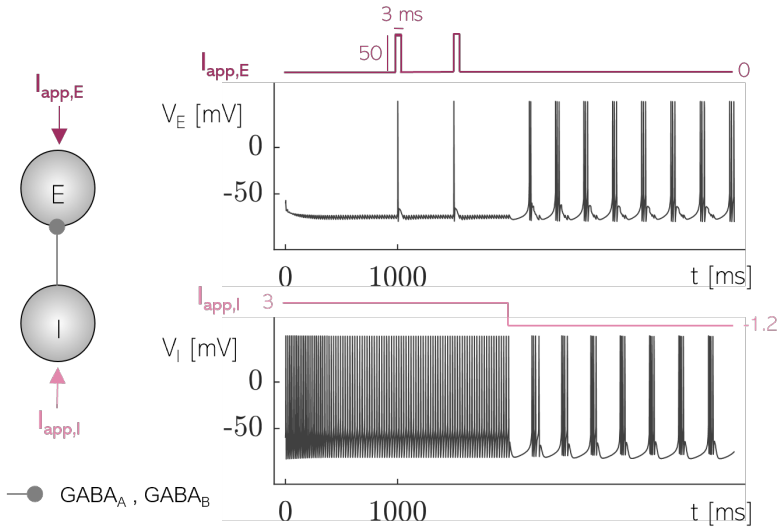

Figure 3.4 – **Simulation of neuron circuit switching activity**. Inhibitory connection from an inhibitory neuron to an excitatory neuron. The value of applied current to the inhibitory neuron is modulating the switch of the circuit, going from tonic spiking to burst. A pulse of applied current to the excitatory neuron triggers its response, in the form of a simple action potential. *Adapted from (Jacquerie, 2023)*

3.3 Homeostatic reset

3.3.1 Origins and consequences of the homeostatic reset

With the aim of understanding the role of burst on plasticity, (Jacquerie et al., 2022) used a three-cell circuit capable of switching from tonic to burst firing, using a current applied on the inhibitory neuron. Different implementations of traditional synaptic plasticity rules, including those introduced above, were tested during these switches of activity. The goal was to see how the fluctuations in neuronal rhythms influence the evolution of the weight in the case of traditional plasticity rules. Concerning the protocol, the tonic phase was representing a learning period, where pre- and post-synaptic neurons fired at a given frequency. During this phase, weights were free to evolve according to the chosen plasticity rule and to the initial level of correlation of neurons, either correlated or uncorrelated. Correlated neurons are defined by a high firing rate of both pre and post-neurons, while uncorrelated neurons are defined by low neuronal activity.

The simulation focused mainly on the bursting evolution of strong and weak synaptic weights, acquired after tonic firing.

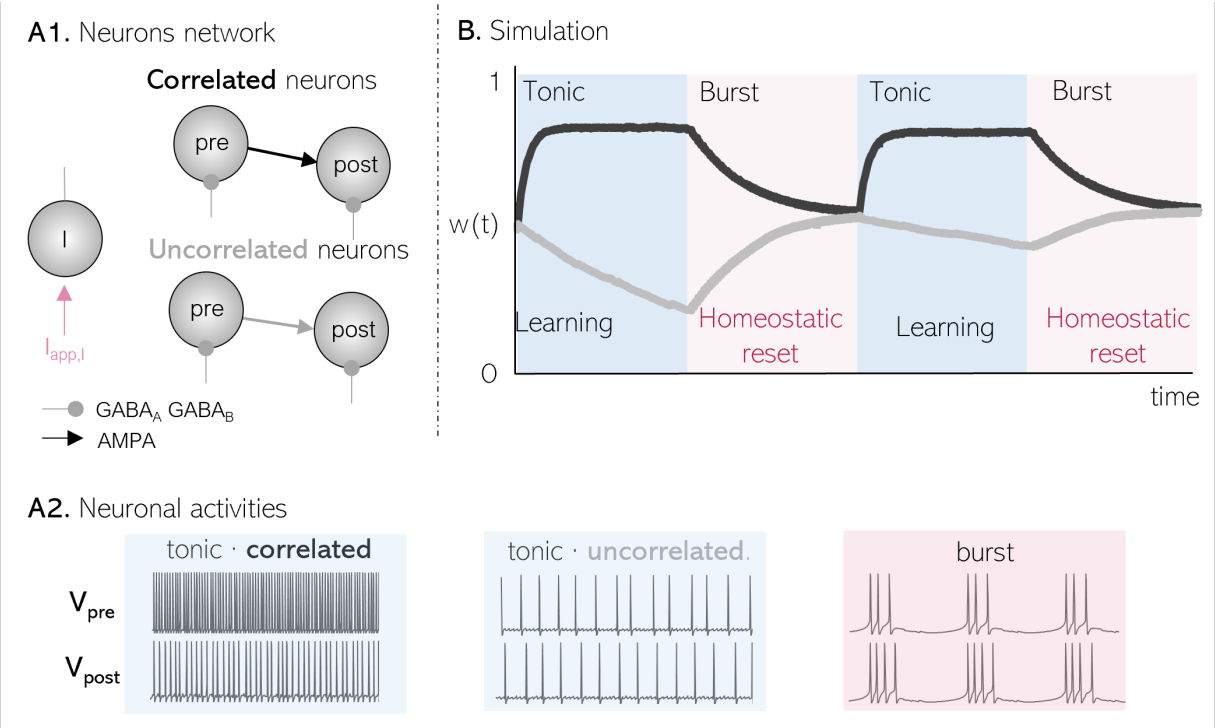

Figure 3.5 – **"Homeostatic reset" of synaptic weights during burst activity**: **A1.** Representation of the connection between neurons. **A2.** Definition of correlated and uncorrelated neurons, by their tonic frequency rates. **B.** Evolution of the synaptic weights shows convergence towards a reset value during the burst phase. This value is the same for correlated or uncorrelated neurons activity

This analysis of the results revealed a convergence of all synaptic weights towards a basal value during each burst period. This phenomenon has been called the *homeostatic reset* and occurs in the same way whatever the correlation level. This means that the convergence value is the same regardless of the initial weight at the start of the burst phase (Figure 3.5).

Reset explanation

This burst-induced homeostatic reset occurs for both biophysical and phenomenological models, making it robust to the synaptic plasticity model used. In all cases, strong weights decrease and weak weights increase towards the homeostatic reset value. However, the analytical explanation of this reset differs according to the rule. In biophysical models, the rhythmic burst activities of all neurons lead to a particular overall calcium dynamic. Indeed, calcium oscillations contribute to the balance between potentiation and depression, which further drives the synaptic weight to its steady state value. In the case of phenomenological models, since the parameters of the synaptic rule are weight-dependent, low potentiate and high weights depress to finally reach a steady state value.

Reset utility

Therefore, the usefulness of this reset has therefore been called into question. *Is this a good feature or an artifact of sleep-dependent memory consolidation?* (Jacquerie et al., 2022). On the one hand, the reset is a good feature because it allows the weight to return to a control value and avoids the saturation of the connection. It can be seen as a *wash out* during the switching activity before starting a new learning period and being able to learn and consolidate again. On the other hand, because of this reset, memory consolidation never lasts longer than a tonic period. Whenever the neurons burst, the neural network forgets everything, whether it is a strengthening or a weakening of the synapse. The use of these traditional plasticity rules in bursting is therefore incompatible with memory consolidation theories.

3.3.2 Exploitation of the reset to drive structural plasticity

It was proven that traditional plasticity rules were leading to a homeostatic reset of all synaptic weight when switching from tonic to burst activity (Jacquerie et al., 2022; Ponnet, 2022). To bring together the two sides of this reset, i.e. restoring weight while at the same time being able to consolidate memory, the implementation of *structural plasticity* is incorporated.

Henceforth, the synaptic weight is calculated by multiplying the early weight, modeled by the traditional plasticity rule, and the late weight, adjusted by structural plasticity. The reset will therefore be exploited to vary the *late weight* according to the *early weight* and consolidate learning information while avoiding system saturation.

The variable w can evolve or decrease during the tonic phase, according to the level of correlation between neurons. Once the neurons are bursting, all w above the reset value, w_{reset}, will contribute to the increase of l. While low values of w below the w_{reset} will lead to the decrease of the late weight l. The reset is still happening but only for the early weight w, along with its consolidation into the late-weight l, keeping all learning information in that former variable as can be seen in Figure 3.6.

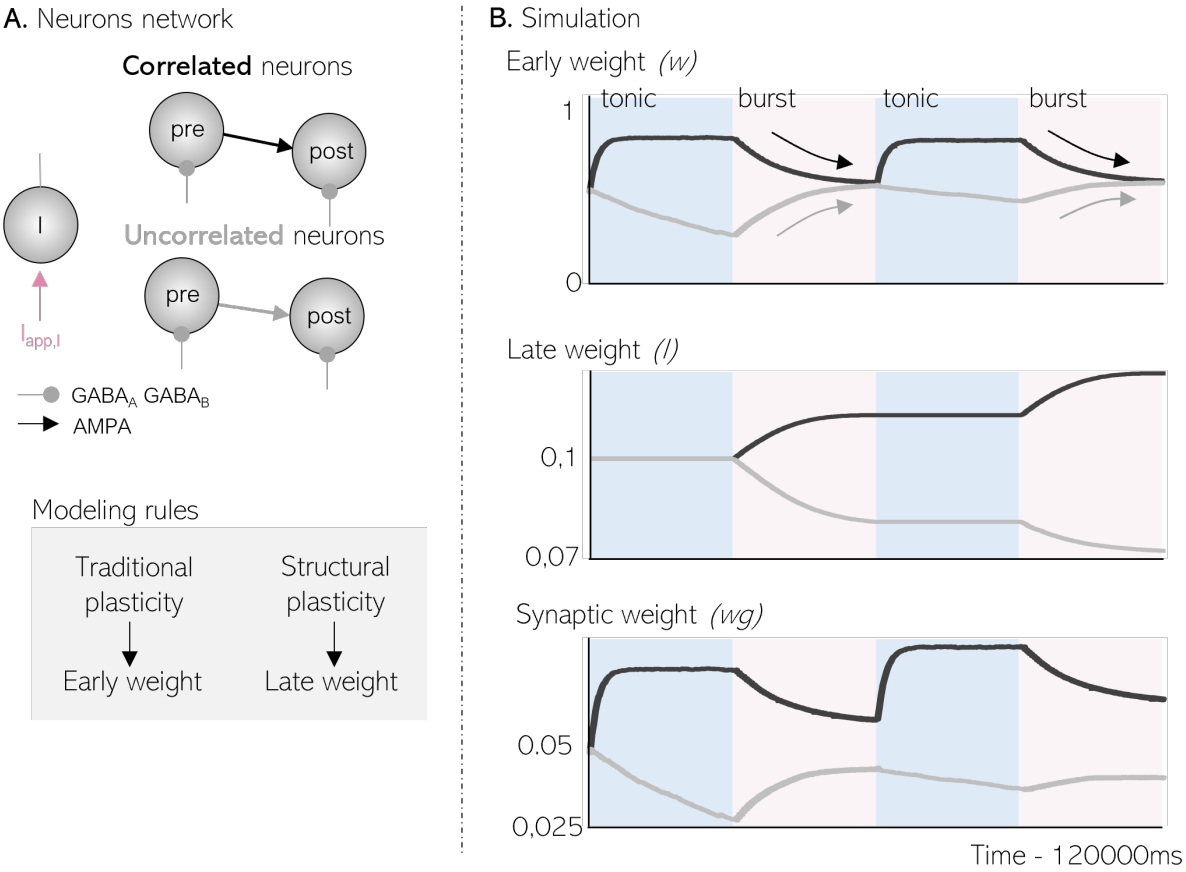

Figure 3.6 – **Structural plasticity**: **A.** Representation of the connection between neurons (same as in Figure 3.5) and of the modeling rules (black box). **B.** Use of the reset in early weight to modify the late weight. For $w > w_{reset} : l$ increases and $w < w_{reset} : l$ decreases.

Part II

Literature review on learning tasks

Chapter 4

Design of learning protocols: an overview of the literature

4.1 Research topic

The overall aim of this project is to understand how memory works and, in particular, how brain rhythms affect its consolidation. The neural activity we will be focusing on for this consolidation is the quiet waking rhythm. In other words, the research question can be formulated as follows: *How can the role of quiet waking on memory be determined?* . This question, if we refer to the literature, is studied at different scales.

At one end stands *cognitive neuroscience*, defined as "an interdisciplinary area of research that combines measurement of brain activity (mostly by means of neuroimaging) with a simultaneous performance of cognitive tasks by human subjects" (Pereira Jr, 2007). Cognitive tasks used in cognitive neuroscience can include remembering the identity or location of a stimulus, reproducing in the correct order a sequence of presented elements, recalling a list of words read beforehand, or recognizing visual patterns or motifs (Anderson and Craik, 1974; Musen and Treisman, 1990).

These are sometimes combined with periods of relaxation, arousal, or drowsiness, to which different cerebral or neuronal rhythms are associated. Between these periods, memory tests are performed to assess the impact of the different states and rhythms. Neuroimaging techniques are then used to measure brain activity (Debas et al., 2010). In the literature, evidence of the importance of rhythms in the memory consolidation process has been put forward, notably by showing the activation of certain parts of the brain via fMRI or EEG (Rauchs et al., 2011; Wamsley, 2019), but also via cognitive tests. However, while this evidence of a link between rhythms and cognitive brain activity helps guide research, it does not provide the exact cellular mechanisms that lead to this memory formation and reinforcement. The limitation of human studies lies in the non-invasive analysis of the brain and in the impact of quantifying the human response.

On the other end, neural networks in *machine learning* can be an option, taking only the mathematical part to free oneself from human constraints. For example, in machine learning, they are using convolutional neural networks (CNN) to make their artificial network learn images (Gu et al., 2018). CNNs are defined as "a particular type of feed-forward neural network in AI, widely used for image recognition" (Shajun Nisha and Nagoor Meeral, 2021). This area of research is of great interest because it enables learning processes, but the neural models used in these networks are highly simplified and do not necessarily reproduce all the activities present in biological neurons. As our focus here is on

tonic and burst activities, the limiting factors in these networks are the inability of neural networks to reproduce the quiet-waking electrical activity.

Between the study of cognition in living beings and the machine learning of artificial networks lies *computational neuroscience*. It is the meeting point between biological and mathematical points of view, through the use of biophysical models. Biophysical models are defined as *"a simulation of a biological system using mathematical formalizations of the physical properties of that system."*[1] These methods can be used to model reality with different approaches and levels of accuracy.

In computational neuroscience, no general formalism has been established for the parameterization of learning tasks. This is where my project comes in. Inspired by literature experiments using biophysical models, we will be able to choose the protocol and parameters of our learning tasks. These can then be used to guide further experiments, with the aim of obtaining models that are increasingly faithful to reality.

Box 2 - fMRI
Functional magnetic resonance imaging (fMRI) is a non-invasive brain imaging technique that measures changes in blood flow and oxygenation levels to infer brain activity. It is based on the different magnetic properties of oxygenated and deoxygenated hemoglobin.

4.2 Computational neuroscience and biophysical models

Considering the world of computational neuroscience, the study context can be refined in the following focused topic: *Role of the bursting activity in plasticity*. Synaptic plasticity is the basis of learning and memory formation in the brain. It can manifest itself in several forms and across different time scales, as covered in Chapter 2. When we learn something new, the brain is able to modify and adapt its synaptic connections. This ability is essential to form, encode, store, and retrieves memories. New synapses can be formed, and existing ones can be either strengthened or weakened. On the one hand, strengthening of synaptic connections between neurons facilitates their communication, which is important for the initial encoding of new memories. On the other hand, the weakening is important to the pruning of unnecessary information and allows more efficient memory storage (Miehl et al., 2022; Lamprecht and LeDoux, 2004).

In order to understand how the burst electrical activity of neurons is involved in synaptic plasticity, a learning task must be defined. Therefore, the main objective guiding my master's thesis will be the **parametrization of a learning protocol** to perform learning tasks. In neuronal networks, learning tasks can be achieved through changes in synaptic strength. Learning also involves the coordination of activity across multiple brain regions and can be performed through various forms of synaptic plasticity. Indeed, biophysical models are using different implementations and rules to model plasticity, as we saw in Chapter 3. In the literature, these learning tasks are performed on several different neuronal networks, from the basic one only formed by a few neurons (Gurunathan and Iyer, 2020), to the complex network formed by many layers of interconnected neurons that process information and learn patterns from input data (Zenke et al., 2015). One example of learning patterns in neuronal networks is the ability to recognize digits in the MNIST dataset. In this task, the network is trained to classify and recognize thousands of handwritten digits (Garg et al., 2022; Capone et al., 2019).

[1] https://www.nature.com/subjects/biophysical-models

In this section, a review of existing studies on learning patterns in neuronal networks is carried out in order to identify commonalities and differences among approaches. In fact, researchers have developed a variety of protocols, selected parameters, and performed validation methods to study the behavior of these networks and their learning capabilities. All these parameters, which each author can play with for each study are grouped under the name *free parameters*. A further complication arising from the lack of consensus on the study of plasticity is the diversity of terms used to describe the same concept. A description of all simulation parameters will therefore first be provided in order to unify the different terms and notations used in the literature. Then, for each paper of this literature review chapter, a schematic representation of the network, parameters, and protocol will be presented according to the information it provides.

4.2.1 Computational tools and networks for learning tasks

Computational approaches to biology are quite diverse, ranging from modeling a neuron and its activity, to modeling its plasticity and learning. The tools available for studying the behavior of neurons during memory consolidation are therefore numerous.

For simulations, the choice of learning protocol can be divided into two main categories: the *parameterization of the neuronal circuit*, including its size and the choice of stimulation parameters, and the actual *running of the learning task* and its various phases.

Then, the validation method will be explained. It corresponds to the way in which the circuit performances will be evaluated.

Neural circuit and parameters

The basic architecture of neural networks, representing a non-exhaustive list of all the free parameters that authors can modify, is shown in Figure 4.1 Some elements, or free parameters, will therefore change according to the paper. Here is an overview of the parameters and their notations.

First of all, the neural circuits used will vary in *size*, with more or fewer pre- and post-synaptic neurons. The notations n_{pre} and n_{post} will be used to describe these variables respectively. Then, the choice of *frequencies*, an important free parameter for characterizing the protocol, will vary. These will be denoted f_{pre} and f_{post}, following the same logic as the number of synaptic neurons.

Sequence of phases and activities

The protocol is often divided into distinct parts, the most frequently found of which are the learning phase and the testing phase.

Learning

The learning phase may comprise a single neuronal activity or a succession of neuronal activities. These are called *state*, and have different durations (T_{state}). With regard to plasticity in the learning phase, different models and types of plasticities are used.

During learning, certain neurons will receive external stimulation, according to the frequencies defined by the author. Simulations will be carried out by selecting a number of presynaptic neurons to be stimulated, which in most cases will be stimulated according to patterns. *Patterns* will correspond in this context to a certain number of active and inactive pixels, forming a visual image when these pixels are arranged in a grid. For stimuli based on a visual pattern, each presynaptic neuron will correspond to a pixel in the pattern. Active presynaptic neurons (part of the pattern) are also referred to as ON pixels. Inactive neurons (outside the pattern) are called OFF pixels. As far as postsynaptic neurons

are concerned, each of them will often code for a defined pattern or for a defined pattern class. A class is defined as a region of the grid encompassing several patterns.

Testing
The testing section is used to test the learning of our network. In this section, presynaptic neurons are stimulated according to different patterns, and the response of the postsynaptic neuron, which no longer receives any stimulation, is measured. This step is based on the concept of spike transmission. When the value of the synaptic force is high enough, the presynaptic spikes generate the response, in the form of an action potential, of the postsynaptic neuron. This response can be calculated as a frequency.

Others
Sometimes, other phases are also implemented, such as a sleeping or an inactive phase. These are refined throughout the analysis of the papers.

Validation methods

Performance assessment methods appear in both learning and testing. They are based on different outcomes and are complementary.

In learning, a *receptive field* is constructed from the synaptic weight values obtained after each state. The receptive field defines the specific areas of the simulation to which the output neuron is more or less sensitive.

In other words, the receptive field visually represents the synaptic weight of each presynaptic neuron with a postsynaptic neuron. It is individually associated with each postsynaptic neuron. This receptive field will be formed by a grid of pixels, corresponding to the presynaptic neurons, and each pixel will have a different color depending on the synaptic strength it has with the postsynaptic neuron under consideration.

In testing, the frequency of the postsynaptic neuron is compared with a defined threshold. The threshold corresponds to the minimum frequency required for the pattern to be considered as recognized. The pattern associated with the postsynaptic neuron that fires the most will be considered the pattern predicted by the neuronal circuit.

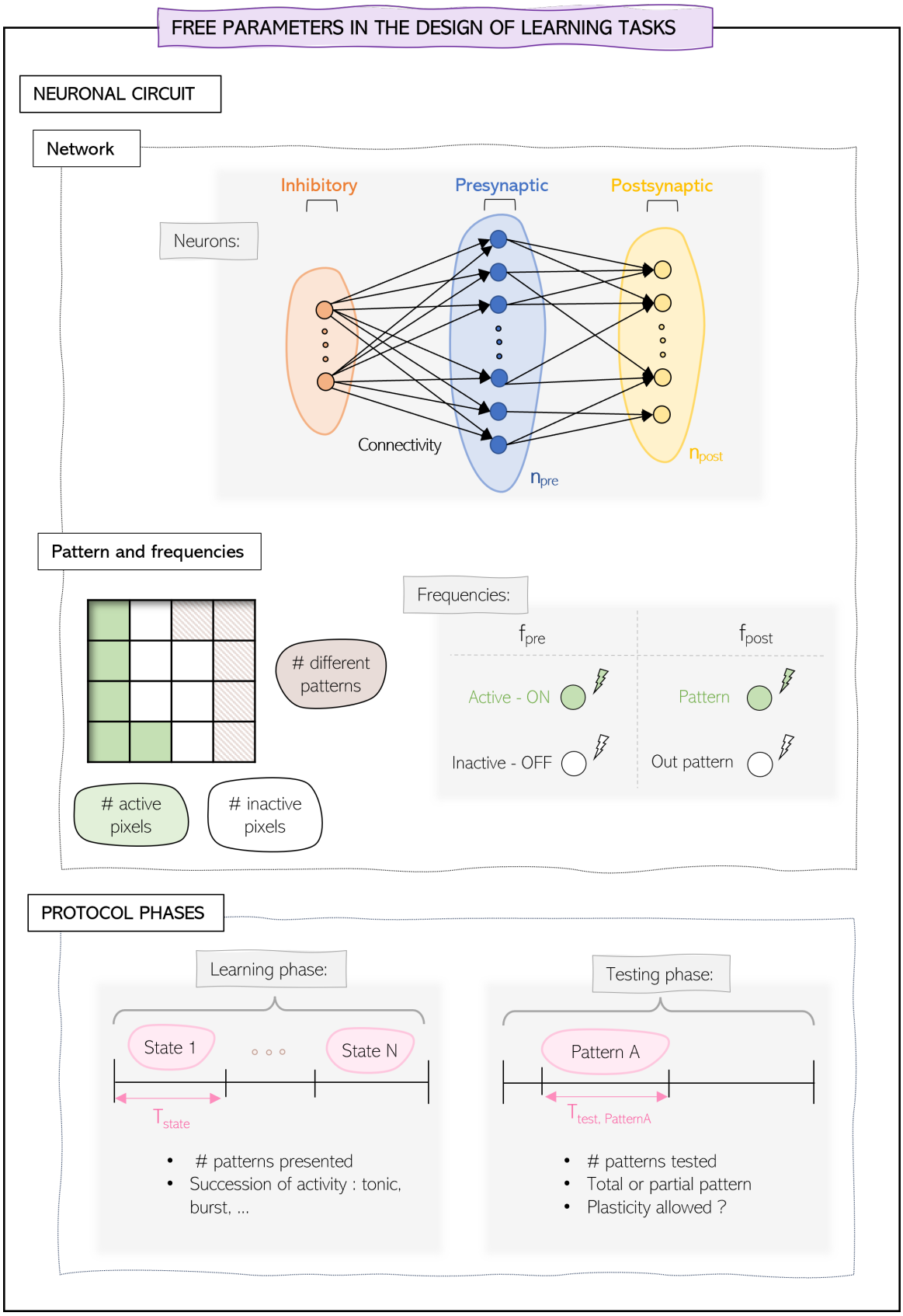

Figure 4.1 – **"Free parameters"**: Non-exhaustive list of the free parameters varying according to the paper. It can often be separated into categories such as the network architecture, the patterns shown to the network and the frequencies associated to them, and the protocol under which the patterns are presented.

4.3 Literature paper analysis

Some articles of interest to my subject are explored more closely in this literature section. There is clearly a large number of articles on learning tasks using biophysical models. The selected articles cover different types of protocols and patterns that can be implemented in our experiments but are not exhaustive of the content of the literature. An analytical view is used to highlight only those elements that have an impact on the design of memory tasks. An introduction to the purpose of the article is nevertheless provided, so as not to list parameters without context. The conclusion of each article specifies the characteristics and free parameters of the experiments that were useful in designing of my simulations. Extended versions of these article reviews can be found in Appendix C, where a more detailed analysis of some experiments that I found interesting is provided.

Finally, a cross-sectional analysis is presented, summarizing the main features and common points of the articles read. This analysis is presented in the form of a recipe for task design, based on literature practices.

4.3.1 GURUNATHAN 2020

Title

"Spurious learning in networks with Spike Driven Synaptic Plasticity", (Gurunathan and Iyer, 2020).

Goal

In this article, the authors used the SDSP (spike-driven synaptic plasticity) to study the spurious and incomplete learning of patterns in SNNs (Spiking Neural Networks). Their goal was to use simple network architecture and simple patterns to better understand the rule, which is not widely used at the moment. The learning in SDSP depends on a probability ρ of the postsynaptic membrane potential V_m to reach a certain voltage threshold V_{th}^w when a pattern presentation occurs. However, the probability of the membrane potential is not proportional to the amount of input current reaching the output neuron. Thus, they introduce the notions of *incomplete* and *spurious* learning. Spurious learning is associated with *false positive* learning. This is defined as a large increase in weight even when the input current is low, due to a large probability. Incomplete learning, inversely, reflects the cases when there is no learning where it should normally happen. This paper aimed to find out the impact of two model parameters on spurious and incomplete learning.

Experiments

The authors performed five experiments, the first of which aimed to show how the network works with simple data, and the following ones were focusing on the understanding of spurious learning with the plasticity rule.

First experiment specific features and methods (Figure 4.2):

- *Patterns* : 5 random patterns on a 3x3 grid with different overlaps. Each pattern is composed of 5 inactive and 4 active pixels and is associated with 1 output neuron, which brings the total to 5 output neurons.
- *Dataset*: The datasets for the learning and test phase are generated from the 5 initial random patterns with different frequency spike trains. In total, 2000 training patterns and 100 test

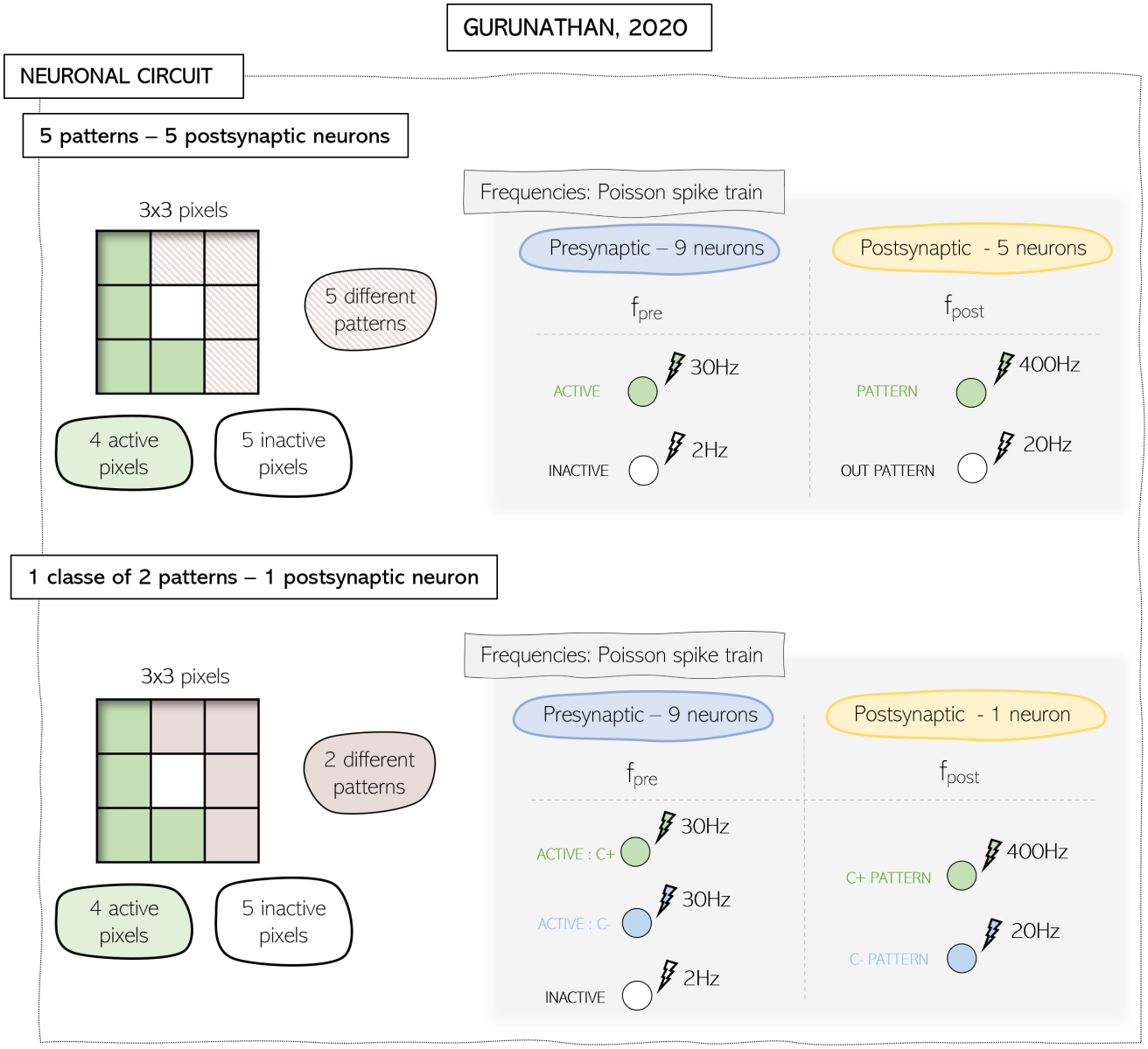

Figure 4.2 – **Gurunathan 2020**: The neuronal circuit is defined by 9 presynaptic neurons, corresponding to each pixel of the 3x3 grid, and a specific number of postsynaptic neurons, linked to the number of patterns. In the first experiment, five patterns with different degrees of overlap are generated and therefore 5 output patterns are used. In the other experiments, a class (from the size of the grid) of 2 patterns is used. The only output neuron encodes the class.

patterns are obtained.

- *Input neuron frequencies* - f_{pre}: Poisson spike trains of high (30Hz) and low (2Hz) frequency are respectively assigned to active or inactive pixels.

- *Output frequencies* - f_{post}: The first experiment is composed of 5 output neurons: a high-frequency spike train of 400Hz will be used for the output neuron associated with the presented pattern ("good" output), and a low-frequency spike train of 20Hz for the 4 other ("wrong") output neurons.

- *Simulation*: Each pattern runs for 400 ms and "between them, all voltages and current traces are reset"

- *Validation method*: Check of the pattern (in testing phase): The pattern associated with the output neuron that fires the most spikes is considered as the pattern predicted by the network. They obtained a mean accuracy of 99.97%

Other experiments
In the four other experiments, they took

- *Patterns*: 1 output neuron, encoding a pattern class. The pattern class in this article represents the entire grid and is composed of 2 patterns. This is to specifically study spurious learning. The pattern C^+ will be presented with a signal T^+, and C^- with a signal T^-. These categories are just representing the patterns that are supposed to be consolidated (C^+), associated with a high frequency, or not (C^-).

- *Dataset*: They used 2000 training patterns during the training of the network. Then, the network is tested on 100 testing patterns.

- *Input neuron frequencies* - f_{pre}: Poisson spike trains of high (30Hz) and low (2Hz) frequency are respectively assigned to active or inactive pixels.

- *Output frequencies* - f_{post}: 400Hz will be used as the T^+ signal (assigned to the C^+ pattern) and 20Hz as the T^- signal (for the C^- pattern).

In the second experiment, the values of parameters for which spurious or incomplete learning (grouped under the notion of "incorrect learning") occured is investigated. They used two ways to check the incorrect learning:
In the first one, they looked at the frequency of spikes fired by the output neuron for the two classes of patterns and checked the difference between them. The second one focused on the learned weights on a receptive field. The receptive field was built by looking at which portion of weight in the wrong category has learned (spurious learning) and those in the good category who did not learn. They showed the weights in the receptive field with different colors, corresponding to the different ranges of values of the weights.

In the other experiments, they studied the impact of their parameters on different aspects, such as the cause of spurious learning or the implementation of a stop-learning condition to avoid incomplete learning. Then, a longer period of learning was tested.

Conclusion

All those experiments aimed at understanding how the network is learning and how the neurons behave with the SDSP rule, and especially how the evolution of weights is directed by the values of the parameters. They made a review of V_{th}^{w} and τ_M parameters that were impacting this rule, for SDSP users to be able to use it properly.

This article has given me a better overview of the different patterns that can be taught to a circuit. Indeed, it proposes a simulation based on a pattern class comprising several patterns, thus showing that not all patterns are uniquely associated with a neuron output. The receptive field proposed is also interesting, as it demonstrates why using classes help to better understand consolidation mechanisms within a single neuron as a function of imposed frequencies. The first simulation carried out also informed me about network testing methods, and in particular about prediction and accuracy calculation.

4.3.2 ZENKE 2015

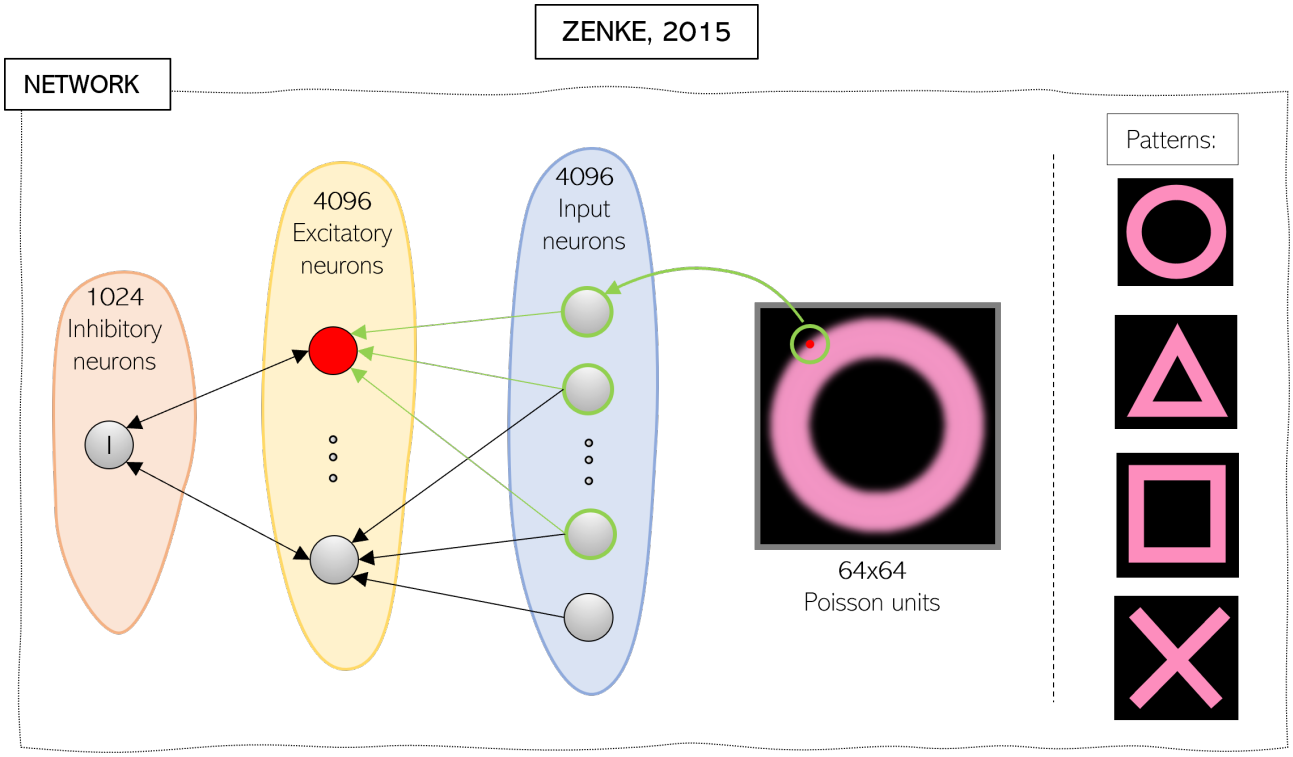

Figure 4.3 – **Zenke 2015**: The network is presented with different input patterns. Each input pattern is a 64x64 Poisson unit, where cells from a circular area (R=8) are projected to an individual input neuron. The center of the circle is randomly selected into the input space and associated with one excitatory neuron.

Title

"Diverse synaptic plasticity mechanisms orchestrated to form and retrieve memories in spiking neural networks", (Zenke et al., 2015).

Goal

The goal of this paper is to show that a combination of different plasticity rules is sufficient to form and recall assemblies in spiking neural networks. In particular, it concerns here a spiking recurrent neural model of inhibitory and excitatory neurons.
The different types of plasticity considered are the Hebbian homosynaptic and non-Hebbian (heterosynaptic and transmitter-induced) plasticity, combined with structural, short-term, and homeostatic plasticity. The latter are used to represent slow homeostatic changes and consolidation.

Experiments

Orchestrate plasticity to form stable cell assemblies
The article first discusses the concept of orchestrated plasticity in the formation of stable cell assemblies in a recurrent neural network. Stability refers to a state in which the firing rate of neurons in the network remains relatively constant over time. Plasticity mechanisms considered here are homosynaptic (triplet STDP), transmitter-induced potentiation, and heterosynaptic depression.

The network architecture for the stability experiment is the following (Figure 4.3):

- *Inputs*: 1 postsynaptic neuron received simultaneous inputs from an active pathway composed of 80 presynaptic neurons activated at 10 Hz and a control pathway with 80 background neurons at 1 Hz.
- *Protocol*: Localized stimulus that changes its position on average once every 20 s
- *Validation method*: Postsynaptic neuron develops a localized receptive field accorded to its stimulus

Assembly formation and recall
This experiment investigates whether inhibitory and excitatory plasticity could work together to enable stable assembly formation and recall. In this neural network model, each excitatory neuron received input from both other neurons in the network and from sensory neurons that represented specific locations in space. These small patches of sensory neurons are defining the receptive field of the excitatory neuron. The network was then stimulated with different patterns of input, and the plasticity allowed certain groups of neurons to become more strongly connected to each other, forming assemblies that responded to specific input patterns.

- *Network*: Composed of 5120 LIF neurons, including 4096 excitatory and 1024 inhibitory neurons randomly connected, with an overall connection probability of 10%.
- *Input*: Excitatory neurons receive stimulation from an external input. The input is a 64x64 Poisson units, where cells from a circular area (R=8) are projected to an individual input neuron. The center of the circle is randomly selected into the input space and associated with one excitatory neuron. All input neurons stimulated during activation of the circular area, go on to excite the excitatory neuron corresponding to the center of the circle.
- *Stimulation/Patterns*: The stimuli are 4 different geometric patterns, randomly presented and alternated with periods without stimulation. The patterns can overlap, which means that some neurons corresponding to the first pattern, can also fire for another pattern.
- *Protocol*: Only one phase with ongoing plasticity throughout the phase, allowing synapses to evolve freely. This phase was "separated" into 2 parts, wherein the first one, the network was

stimulated by applying "repeatedly and stochastically one of four possible full-filed input patterns". Then in the second part, the network was stimulated with partial input (up to three-quarters of the input field can be occluded). The identity and duration of the stimulus, as well as the time between successive stimuli, were randomized. However, the intensity of the stimulus remained constant.

- *Results*: The activity they record was the mean activity of all neurons *responding* to the stimulus

- *Validation method*: they counted the postsynaptic neuron as coding for the stimulus when its stimulus-evoked firing rate was $\geq$ 10Hz

Results show that these assemblies remained connected even after the input had stopped, and could be reactivated later by partial input that matched the original pattern. The authors found that the assemblies were stable over long periods of time and did not degrade. The network could spontaneously transition between different assemblies without external input.

By looking at the different timescales of plasticity mechanisms and how they contribute to stability in the model, they also proved that this stability is a result of the coordinated interplay of multiple plasticity mechanisms on different timescales.

Other small experiments were performed to see the effect of simulation parameters on learning. For example, one experiment aimed to see the effect of individual plasticity on the network (by blocking one of them). Another focused on increasing the learning time or adding new learning patterns.

Conclusion

This article allowed me to see patterns made with particular motifs (not just randomly activated pixels). Another interesting point is their test phase, where patterns are reactivated in full but also partially (up to three-quarters of the input field can be occluded). As a validation method, they do not just compare frequencies to find the post neuron with the highest frequency but consider that the frequency must exceed a certain defined threshold. It also highlights the importance of having several plasticity mechanisms, taking into account both short- and long-term changes, in order to better represent reality.

4.3.3 CAPONE 2019

Title

"Sleep-like slow oscillations improve visual classification through synaptic homeostasis and memory association in a thalamo-cortical model", (Capone et al., 2019).

Goal

The main idea of this paper is to explore the role of slow oscillations (SO) during sleep, and how they contribute to memory consolidation and restoration, from a computational point of view. Experimental studies have shown that this oscillation activity is beneficial for memory consolidation and task performances optimization.
The authors used Adex neurons in a thalamo-cortical network model and the STDP (or pair-based) for the plasticity rule.

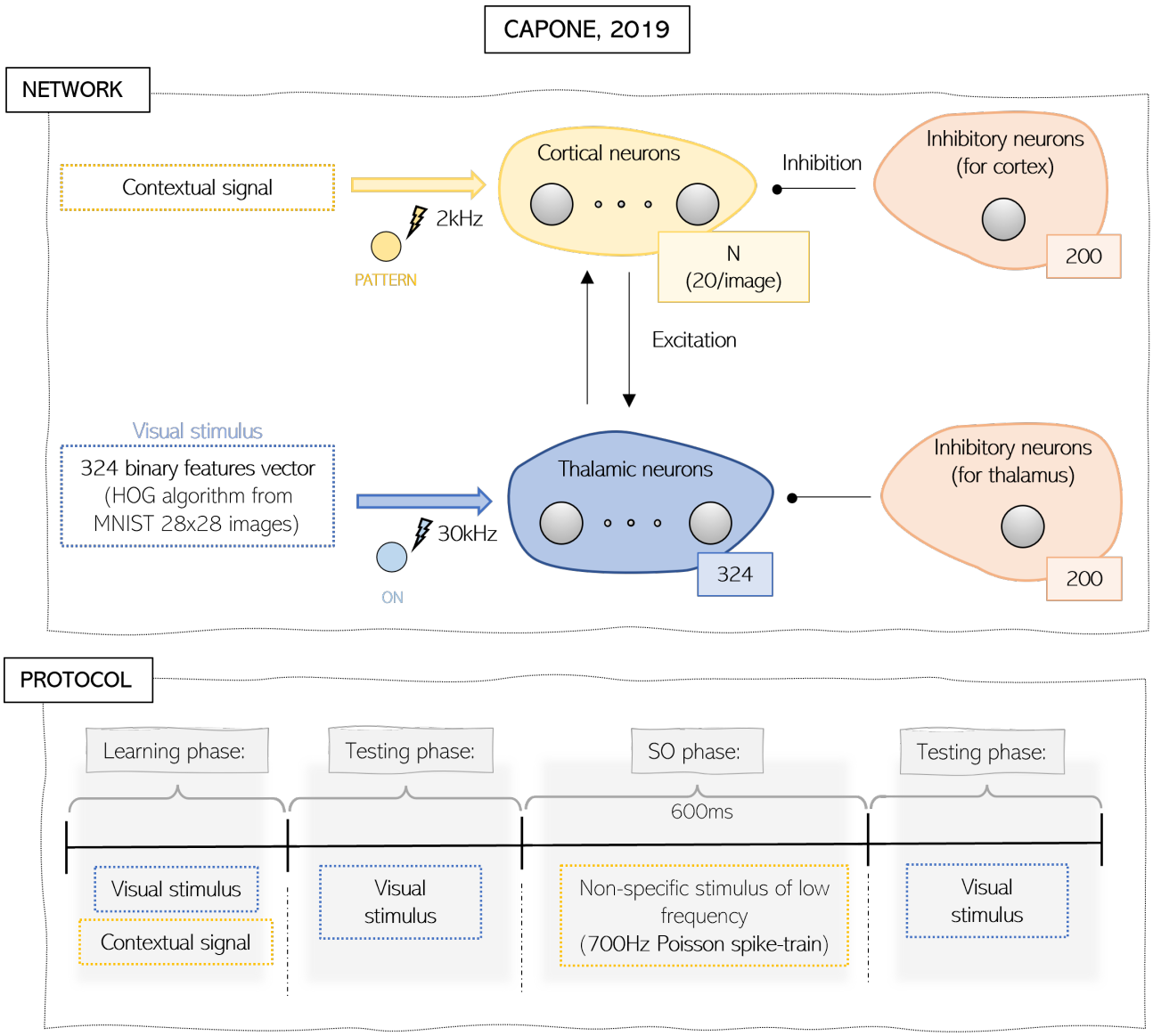

Figure 4.4 – **Capone 2019**: The network contains two populations of excitatory neurons: the thalamic, corresponding to the input neurons, and the cortical population, considered as the output. The number of cortical neurons depends on the number of images presented. A visual stimulus (associated with an MNIST image) and/or a contextual signal can simulate the thalamic or cortical population, respectively, depending on the phase considered.

Experiments

Network architecture and protocol (Figure 4.4)

- *Patterns*: The patterns shown to the network are handwritten digits from the MNIST dataset, including 28x28 pixels images. An algorithm is used to transform each image into a vector of 324 binary features. The number of images will be specified for the 2 different runs of the paper.

- *Network*: Number of thalamic neurons $N_{th} = 324$. Number of cortical neurons $N_{cort} = 20$ neurons for each image. Number of inhibitory neurons: $N_{in} = 200$ and $N_{re} = 200$, corresponding respectively to the cortical and the thalamic inhibition. All neurons are interconnected.

- *Frequencies*: The frequencies of input signals vary according to the stimulation and the target population. The thalamic neurons receive a visual stimulus, formed by a Poisson spike train with an average firing rate of $30kHz$ when the element of the vector is 1. An external stimulation ("contextual signal") provides a $2kHz$ Poisson spike train to cortical neurons.

- *Protocol*: The protocol is divided in 4 successive phases : *Training*, *pre-sleep testing*, *sleeping (slow-oscillation)*, *post-sleep testing*:

  - *Training phase*: In the training phase, the thalamic population receives a visual stimulus. More precisely, this stimulus is a Poisson spike train with an average firing rate of 30Hz only when the element of the vector is 1. At the same time, an external stimulus is applied to a subset of 20 cortical neurons, which allows them to code for this specific image. The STDP rules change the weight of connections in the network.
  - *Testing*: Images are presented without the contextual signal on the cortical neurons. Only the thalamic neurons are stimulated. The success of this phase is achieved when the population of cortical neurons responding to this stimulation is the same as in the training phase.
  - *Slow oscillation (SO) phase*: To obtain the slow oscillations of this phase, the parameters of the model are modulated. Especially, a non-specific stimulus of low frequency (700Hz Poisson spike-train) is provided inside the cortex. The network is disconnected from sensory stimuli, and driven by its internal activity. This phase lasts 600 seconds.

First set of runs
In this first set of runs, 9 images are presented to the network in the training phase. More precisely, 3 instances for each chosen digit (0,1,2) are used. They demonstrate that the slow oscillations enable the creation of stronger synapses between groups of neurons belonging to the same digit category. During this phase, the cortex is minimally simulated, but groups of neurons will spontaneously activate in a high-frequency regime. These neurons will activate the same thalamic neuron population that activated them in testing. Once the thalamic neurons are active, they recruit back all cortical neuron populations associated with similar thalamic representations.

Second set of runs
In the second group of runs, the network was presented with images from all ten-digit classes in the MNIST dataset, with three examples per digit. A total of 30 training instances are randomly picked from an initial dataset of 250 images. The goal here was to prove the post-sleep improvement for the classification task. The classification was achieved by identifying the pattern associated with the

neuron showing the highest firing rate. The accuracy of the classification task goes from 58% to 64% after sleep.

Conclusion

The authors demonstrated the interesting effects of deep-sleep-like slow oscillation activity on the model's performance in encoding, retrieval, and classification tasks.

This article also introduced me to different protocol variants. In this case, a slow oscillation phase is added to the testing and learning phases. In addition, the patterns use several output neurons to encode a single image. The network validation method is therefore based on the response of the entire output population. Here, they use a fairly high pattern complexity with the MNIST dataset. However, as we can observe, it is also possible to select just a few digits from the dataset to train our network.

4.3.4 GARG 2022

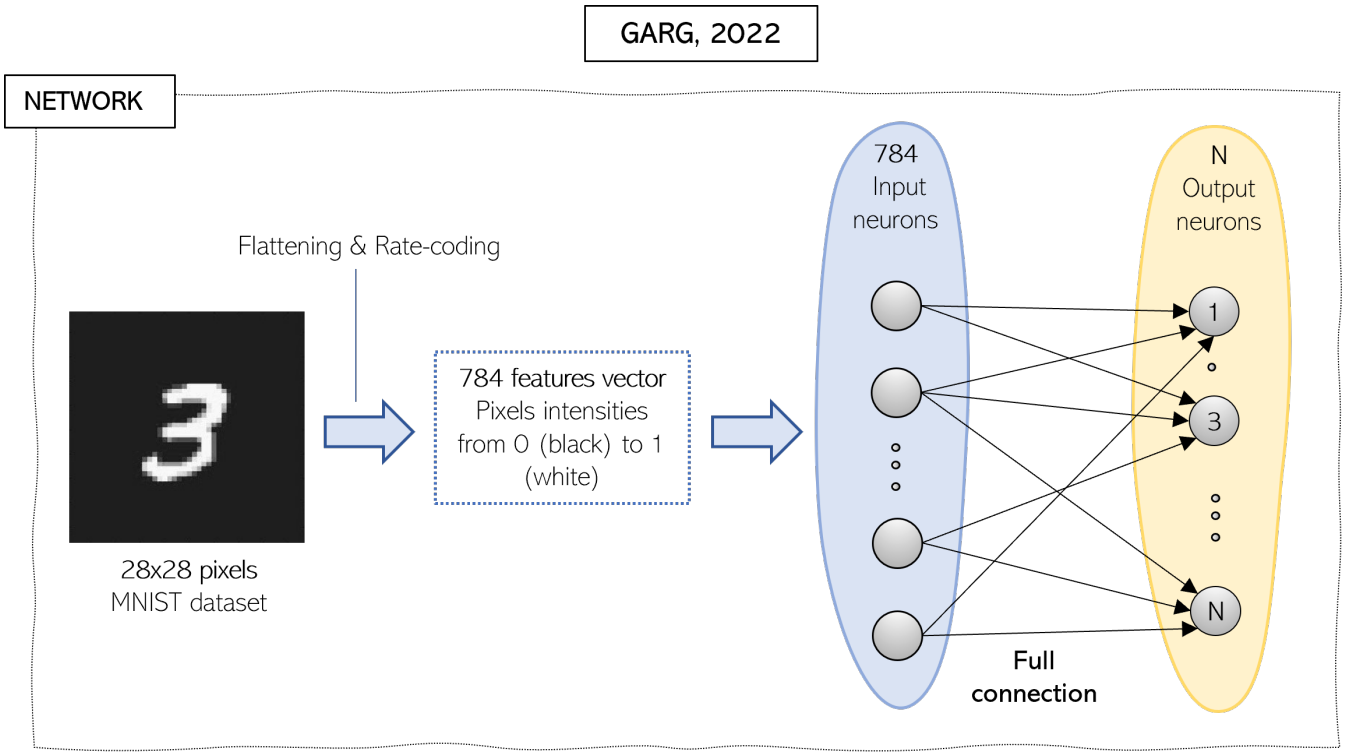

Figure 4.5 – **Garg 2022**: The input presented to the network is an MNIST image that has been flattened and rate-coded to obtain a vector of 784 features ranging from 0 to 1 as a function of pixel intensity. There are 784 input neurons, corresponding to each image pixel, and N output neurons. N is either equal to or greater than the number of digits presented, depending on the experiment.

Title

"Voltage-Dependent Synaptic Plasticity (VDSP): Unsupervised probabilistic Hebbian plasticity rule based on neurons membrane potential ", (Garg et al., 2022).

Goal

The authors of this paper wanted to test the *Voltage-Dependent Synaptic Plasticity*, or Voltage-based synaptic plasticity, using a spiking neural network (SNN) for the recognition of handwritten digits

(MNIST dataset). To simplify the STDP rule using only the presynaptic membrane potential $v(t_{post})$, the presynaptic neurons must be supplied with a constant positive current. This current is used to predict the spike dynamics.

The network and learning protocols for the classification task are described as follows (Figure 4.5):

- *Neuron model*: LIF input neurons and ALIF output neurons. The "A" stands for *adaptive* because an adaptation mechanism is included in the post-neurons to avoid the instability caused by excessive firing.
- *Patterns*: The patterns showed for the classification task are 28x28 images from the MNIST dataset. The training set is composed of 60000 images and the test set contains 10000 images, different from those of the training set.
- *Network*: The number of input neurons equals the total number of pixels in an image, i.e. 784. The number of output neurons varies according to the experiment. The input neurons are fully connected to every output neuron.
- *Input*: The magnitude of the input current used to stimulate the input neurons varies according to the intensity of the pixel, but goes from a magnitude of 0 (black pixel) to 1 (white pixel).
- *Protocol*: During the learning phase, the images are presented to the SNN for 350ms. Every instance of digits is shown without a waiting time between them. During the testing phase, the synaptic weights are fixed and the samples from the test set are proposed to the trained network.
- *Results/Validation method*: After the learning phase, a weight matrix for each of the ten output neurons is obtained and represented on a receptive field. To obtain the accuracy of the network in the recognition of patterns, a testing phase is done. The digit predicted by the network is assigned based on the output neuron class that presented the highest number of spikes during the presentation of the sample. Accuracy is then obtained by comparing this predicted digit with the digit actually presented.

Experiments

First experiment
To evaluate the efficiency of the VDSP rule in pattern recognition, the authors conduct a performance analysis by recognizing handwritten digits. In this experiment, the number of output neurons is equal to the number of digits of the MNIST dataset, i.e. 10.

Second experiment
Here, they test the impact of the network size and training time on the efficiency of the implemented learning rule. The network size is modified by changing the number of output neurons, ranging from 10 to 500. The training time is modulated by increasing the number of epochs (the number of times the dataset is run in its entirety) until 5.

Conclusion

This article uses a protocol quite similar to that of Capone et al. (2019). However, the validation phase is based on the cumulative frequency of all output neurons coding for the same digit, when several neurons are associated with 1 digit. Interestingly, they also show synaptic weights on a receptive field, giving a clearer, more visual representation of what is going on in our network.

4.3.5 GJORGJIEVA 2011

Title

"A triplet spike-timing–dependent plasticity model generalizes the Bienenstock–Cooper–Munro rule to higher-order spatiotemporal correlations", (Gjorgjieva et al., 2011).

Goal

The main goal of the research is to explore and overcome the limitations of a particular learning rule (BCM rule) by using the triplet model, which considers sets of three spikes instead of pairs. Indeed, the BCM rule is not able to account for the timing of pre-and postsynaptic spikes and has difficulty distinguishing input patterns based on temporal spiking structure. The researchers demonstrate that the triplet model improves the explanation of synaptic plasticity.

Experiments

Some network features are common for every experiment, and will be specified in each of their descriptions (Figure 4.6):

- *Network*: Feedforward network with n_{pre} input neurons as Dirac delta spike train and 1 output neuron.
- *Input*: The number of patterns differs in all experiments. The first 10 patterns are rate-based patterns, defined by different input firing rates. The second 10 are correlated-based patterns, associated with different correlation strengths between groups of input neurons in a pattern. The last 2 patterns are "third-order correlation"-based patterns. These patterns are defined by 3 specific input neurons (spatial correlation) having a spike exactly at the same time during the pattern presentation (temporal correlation).
- *Protocol*: Every 200 ms, the network was presented with a new randomly-chosen pattern.

First experiment: Selectivity with Rate-Based Patterns
To examine the level of pattern selectivity of the feedforward network, the authors designed the following experiment: 100 input neurons are divided into groups of 10, with each group coding for a specific pattern. The patterns are rate-based, meaning that they differ by their input firing rates. The input patterns presented to the network are 10 Gaussian profiles with different ratios of the background firing rate (r_{min}) to the peak firing rate (r_{max}), and different standard deviations (SD), resulting in different amounts of overlap. In this experiment, r_{min} was between 0 and 10 Hz, r_{max} was set at 55 Hz and the SD could vary from 5 to 15.

The amount of selectivity of the postsynaptic neuron is computed. The authors observed that higher selectivity is associated with higher values of the ratio (r_{min}/r_{max}) and a lower standard deviation (SD).

Second experiment: Selectivity with Correlation-Based Patterns
In this context, correlation-based patterns refer to patterns with identical firing rates but varying degrees of correlation strength. The firing rate of all inputs is thus set to 10Hz. There are 100 input neurons, each group of 10 coding for 1 pattern, as in the first experiment. The correlation strength was done by selective potentiation of a group of inputs. Weight of 10 input from 1 pattern potentiated while the other depressed at each time we show a new pattern.

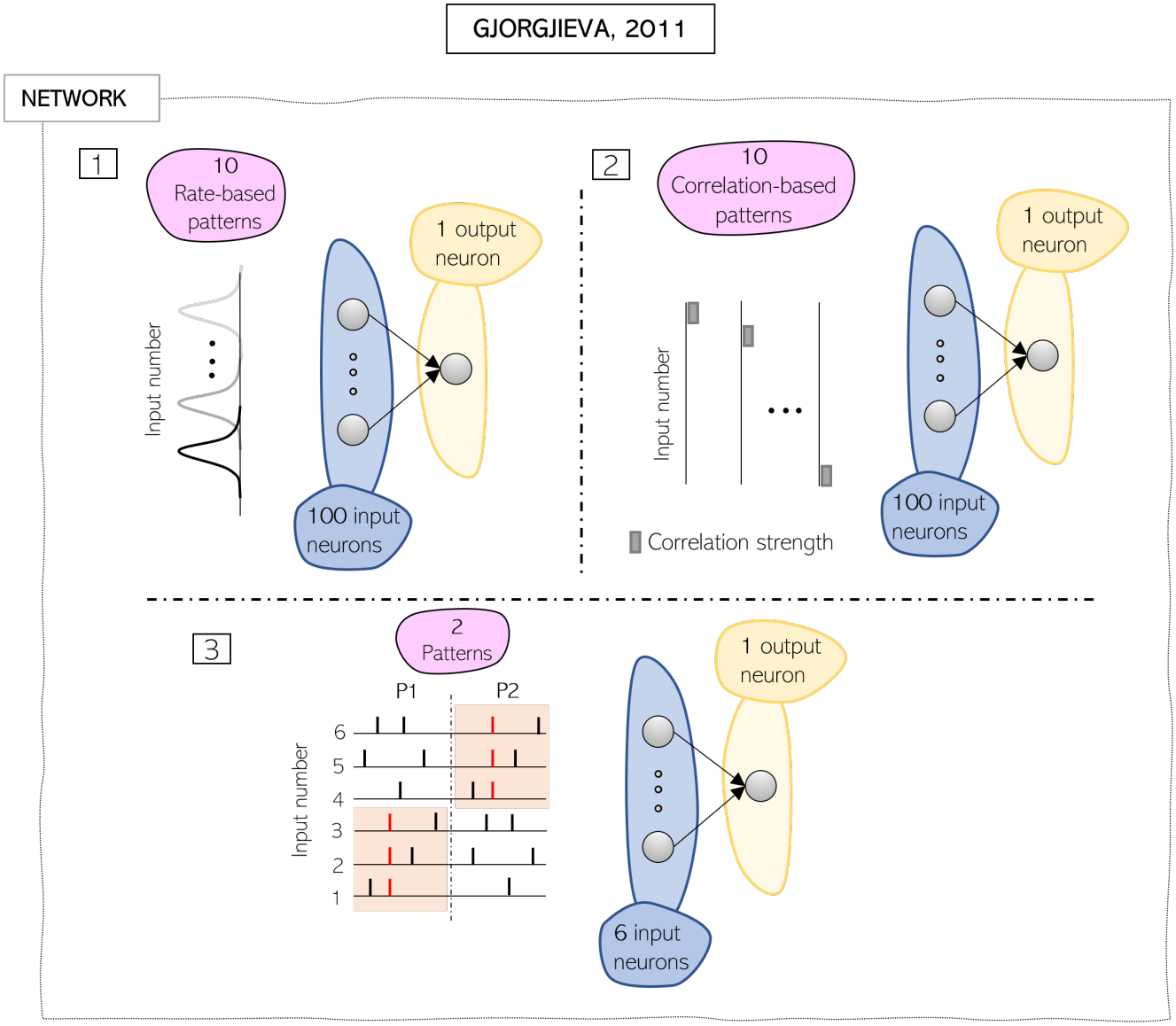

Figure 4.6 – **Gjorgjieva 2011**: The first two experiments use the same network and the same number of patterns. The 10 patterns each include 10 consecutive active input neurons (e.g., the first pattern includes neurons 1-10). **1.** The first one uses rate-based patterns defined by different input firing rates (represented by a Gaussian and a specific standard deviation). **2.** The 10 patterns used here are correlation-based patterns, each associated with different correlation strengths between groups of input neurons in a pattern. **3.** Only 2 patterns are used, defined by 3 specific input neurons spiking once simultaneously (red spike) during the pattern presentation. So there are 6 input neurons.

Third experiment: Selectivity driven by third order correlations
"Third-order correlations" of inputs used here describe a correlation of the postsynaptic neuron with 3 particular neurons based on the fact that they have simultaneous spike timing. Two patterns are presented to the network: P1 and P2. A total of 6 input neurons is used. The patterns consist of 2 pools of 3 input neurons. The first pattern P1 contained simultaneous spikes in inputs 1 to 3, while inputs 4-6 were randomly spiking. For the second pattern P2, it is the opposite. In other words, when the pattern P1 is presented, the weights according to the first 3 inputs potentiate, while the other inputs depress.

The analysis focuses on the probability of P1 winning, which means higher weights for inputs 1 to 3, when varying the presentation of patterns to the network.

Conclusion

This article has shown me that pixel consolidation can also be achieved in ways other than frequency-based association. Here, patterns can be defined in several ways, either by a priori reinforcement of the connection between several input neurons or by a simulation pattern made up of correlated spikes for the inputs corresponding to the pattern we want to consolidate. We note that this paper also uses pattern classes, as there is only one output neuron each time.

4.3.6 DELAMARE 2022

Title

"Intrinsic neural excitability induces time-dependent overlap of memory engrams", (Delamare et al., 2022).

Goal

The main goal of the study is to understand the mechanisms underlying the formation and linking of memory engrams in neural circuits, with a focus on the role of synaptic plasticity and intrinsic excitability. Indeed, memories are stored in neural ensembles called engrams, which are reactivated during memory recall. Engrams have been identified across multiple brain regions as the neural basis for memory storage and retrieval. They are defined as *" a subpopulation of neurons that is initially activated during the presentation of a stimulus, followed by transient physical and/or chemical changes that lead to its specific reactivation during memory recall"*.

The exact process behind engram overlaps, which are important for memory allocation, is still unclear. However, it has been suggested that intrinsic excitability, mediated by neural activity, may serve as a complementary mechanism for the formation of memory engrams.

For this purpose, the researchers developed a computational model that integrates synaptic plasticity and intrinsic excitability to explain the dynamics of overlapping memory ensembles. They are using a rate-based Recurrent Neural Network with feed-forward and recurrent connections, and Hebbian plasticity combined to excitability for plasticity mechanisms.

Experiments

Description of the network and protocol used in this study (Figure 4.7).

- *Network*: The network is divided into the input layer and the main region. The input layer is composed of 30 neurons and is projected to the main layer, which contains 60 neurons. Weights are then initialized to form 3 diagonal blocks in the receptive field.

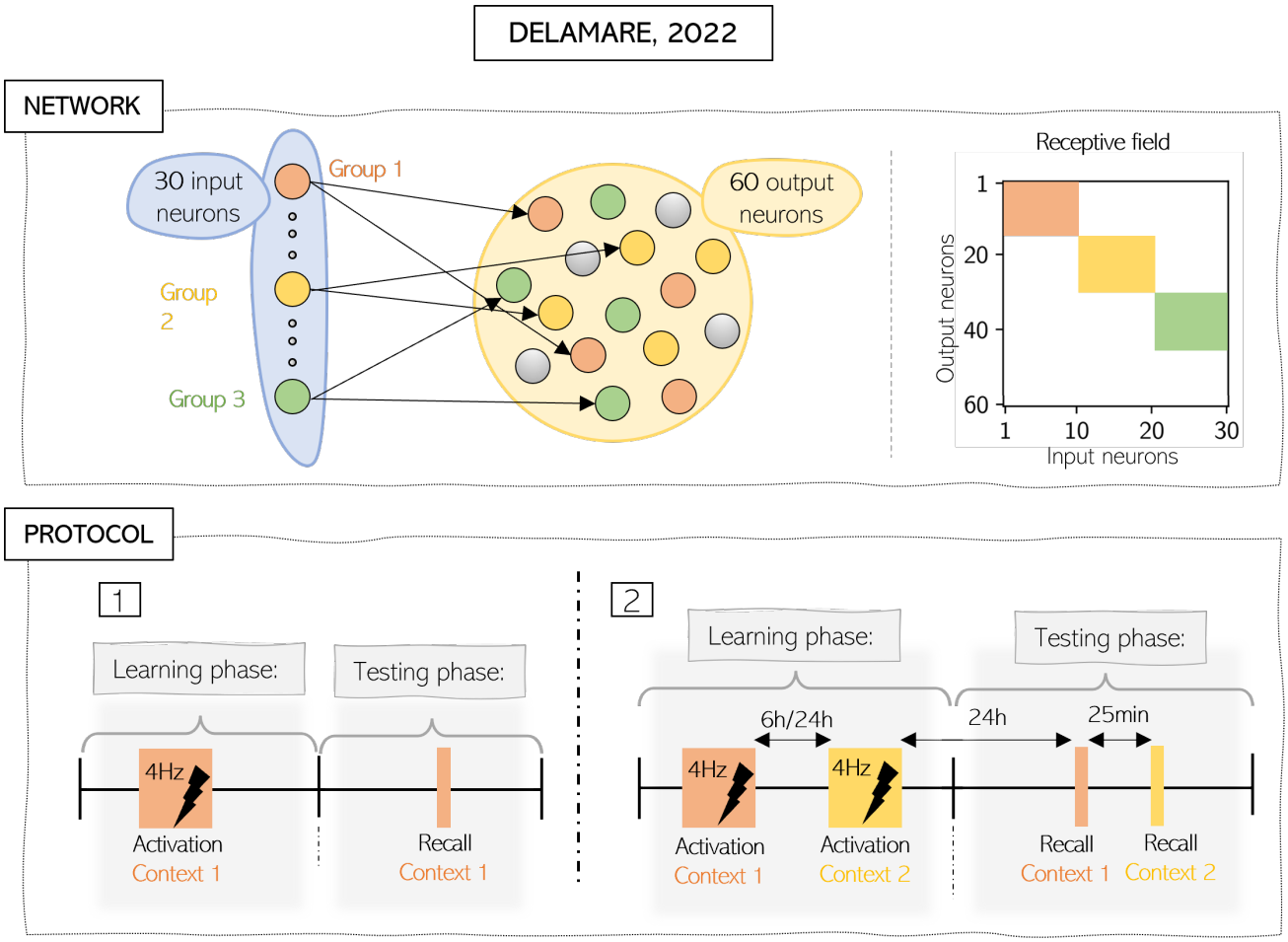

Figure 4.7 – **Delamare 2022**: In this network, 30 input neurons, divided into 3 groups of 10 consecutive neurons, are projected onto the main layer composed of 60 neurons. The weights are initialized according to the receptive field, with colored areas having a higher weight value than the white ones. Two learning/testing protocols are used. In the first one, only one context is presented (by simulating 1 of the 3 groups of neurons, here the first group is represented) and recalled. In the second, two contexts are presented, with a different time interval between them, and then recalled.

- *Inputs*: The inputs are one layer of neurons divided into 3 subsets, forming groups for different context presentations. Groups are formed by 10 consecutive neurons from the input layer.
- *Protocol*: Training and testing phases:
  - Training phase: Simulation of the network by presenting different contexts. One group of input neurons is activated by setting their firing rate to 4Hz. Each activation is repeated 20 times during 40ms, with an interstimulus interval of 150ms. The "active" threshold, where the neurons are classified as active, is set to 6Hz.
  - Testing phase (resp. *"memory retrieval phase"*: this phase test the ability of the network to do pattern recognition task. Some neurons from the assembly, that were tagged as active, are stimulated again during 40ms. The results are presented in the form of a firing rates graph..

Formation of a single memory engram

After showing the first context, only the firing rate of neurons associated with this context is above the active threshold. The memory retrieval phase is using only 4 of the 7 active neurons for pattern

completion. It displays that memories can be retrieved even when stimulated by a partial signal. This finding demonstrates that activating a subgroup of neurons within the assembly is enough to stimulate other neurons in the same assembly due to robust intra-assembly connections.

Link of intrinsic neural excitability and overlapped memory engrams
To study the overlap of memory engram, another experiment is made. During the learning, 2 different contexts are shown to the network to form 2 different memories. The contexts are spaced by time intervals of 6h or 24h. The memory retrieval phase happens 24h after the last learning and consists in showing the 2 contexts, separated by 25min. The intrinsic neuronal excitability is added in this experiment such that after learning, the neural excitability of the neurons involved in the newly established assembly is enhanced.

The authors found that when the contexts are presented with a 6h interval, both memories are stored using overlapping neural representations. This is not the case in 24h intervals. The overlap between the 2 assemblies can be quantified by the number of active neurons for both context recalls.

Conclusion

This article is characterized by a synaptic weight initialization process prior to learning. This step makes it possible to observe the impact of this initialization on consolidation. As for the patterns, no overlap is implemented and, as with those of Capone et al. (2019) and Garg et al. (2022), several output neurons represent the same neuron group. In the test phase, only certain neurons in the group are activated for simulation. The choice of these neurons is interesting in that it is made according to their activation, among the neurons considered to be active (whose firing rate is greater than a certain threshold).

With regard to plasticity, this study highlights the importance of considering not only synaptic plasticity but also intrinsic excitability in order to understand the mechanisms of memory formation and neuronal connectivity.

4.4 Cross-sectional analysis of literature

Figure 4.8 below shows a checklist of the essential elements for designing a task from scratch.

To start a task, a neural network composed of excitatory and inhibitory neurons must be chosen. Next, the stimulus to be presented to this circuit must be defined. This is done firstly by choosing the pattern to be presented, and secondly by encoding the pixels of this input: this can be done on the basis of frequencies, spike correlation, or a priori initialization of synaptic weights. For frequency-based pixel encoding, the pixels to be learned receive a high-frequency stimulus at the same time as activation of the postsynaptic neuron, while neutral pixels are not or only weakly stimulated. Encoding by spike correlations is based on adjusting the timing of spikes so that they lead to either consolidation or depression. The next step is to establish a protocol for presenting the pattern. This is often divided into 2 phases, learning and testing. The plasticity rule(s) that will modify the synaptic weight in these phases must also be chosen. Finally, a network validation method must be decided. Receptive field display and pattern recognition are the two most commonly used validation methods and can be combined.

The choice of free parameters is then specified for each feature of the checklist, using Figure 4.1 presented at the beginning of the chapter.

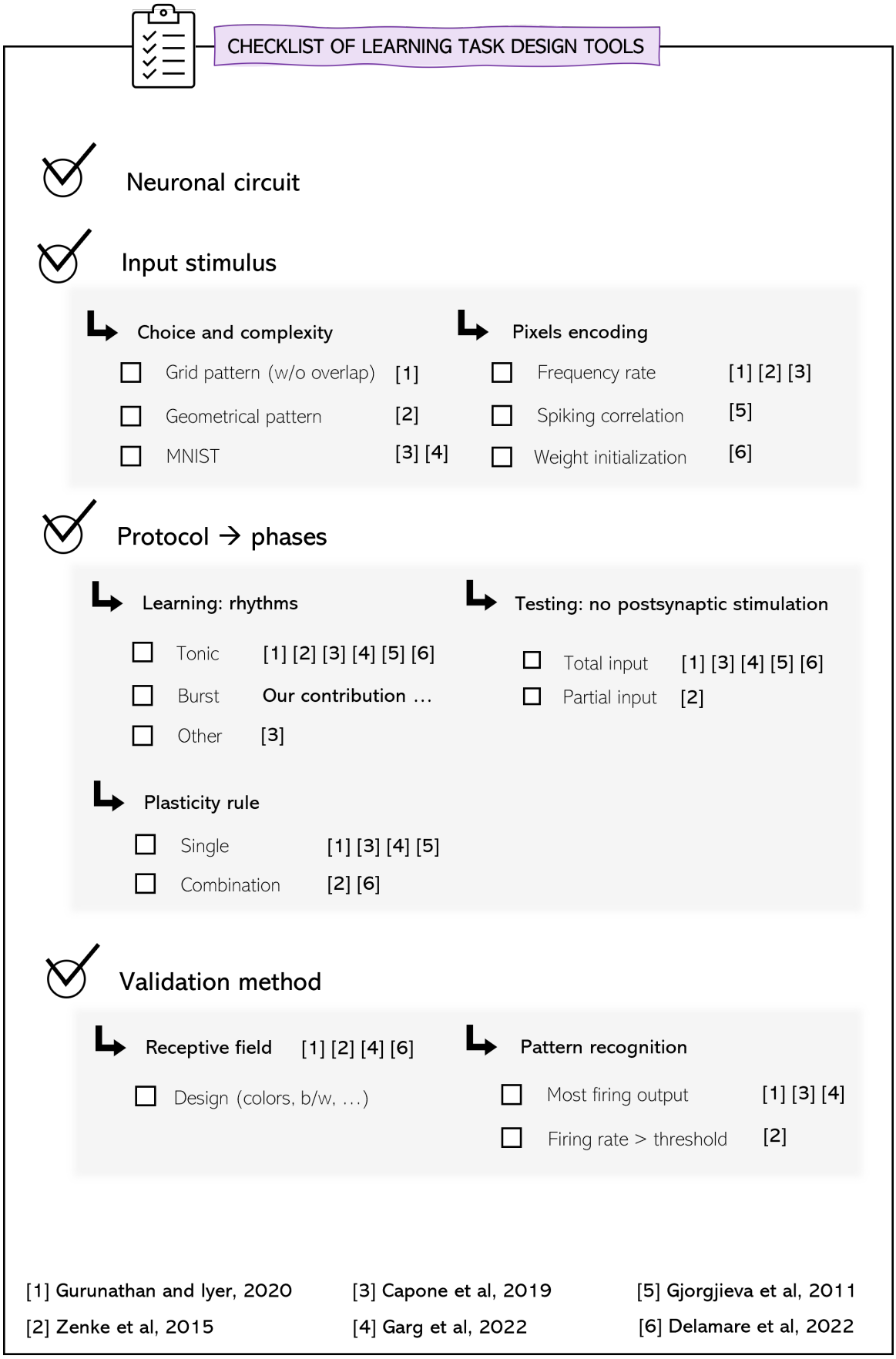

Figure 4.8 – **Checklist of tools and choices to design learning tasks**: Visual representation of the different items to choose from when designing a learning task

Part III

Computational study

Chapter 5

Robustness analysis of brain-state dependent memory consolidation on simple learning tasks

The learning tasks can be designed in various ways, as illustrated in the literature review. Based on the plasticity rules described in Chapter 3 and with the aim of finding out how the burst is involved in memory consolidation, I will draw upon the findings from the existing literature on learning protocols to inspire the parametrization of the protocol I will use. As a reminder, plasticity rules are designed to be validated experimentally and computationally. These models are powerful computational supports for trying to understand what is going on in the brain, with different degrees of reality representation. They allow us to guide experiments using computers, giving us access to more data and being faster than experiments on living beings. Given that no general consensus on plasticity exists, the parameters of these rules or their implementation can be discussed and adapted according to the experiments conducted in the literature and consequently in this project. In other words, our experiments allow us to re-parameterize models and then inspire new experiments, in an attempt to get closer and closer to a parametrization faithful to reality.

This chapter begins with a description of the network and the tools from which the experiments are conducted. Then, different approaches of learning protocol will be considered continuer à la fin.

5.1 Investigation of the parameterization of learning protocols

The identification of free parameters in the literature will now have an impact on our protocol. A description of the architecture, parameters, and simulation phases to be used in this computational part will now be detailed and is illustrated in Figure 5.1, according to the checklist made in the previous chapter.

5.1.1 Neural circuit and parameters

The network used will always comprise several excitatory neurons and at least one inhibitory neuron, used to model activity switches (see section 3.2.3). The main neuronal network characteristics that will be specified throughout the work are the size of the neural circuit, including n_{pre} and n_{Post}, and the frequencies imposed on each neuron.

In addition, the external current applied to excitatory neurons, $I_{app,E}$, will sometimes be modified. The initial values of the early and late weights, respectively $w(0)$ and $l(0)$, will also have an influence

on the experiments.

Regarding synaptic plasticity, a combination of rules will be used. In the majority of this computational part, the traditional calcium-based rule is combined with the structural plasticity rule. The implementation of early and late weights is as described in Chapter 3, where the l is shaped by w. If triplet and pair-based rules are to be used in certain tests, this will be specified.

5.1.2 Sequence of tasks

Our protocol will be divided into 2 separate parts, namely the learning, or training, and the testing.

Learning
During the learning phase, a succession of tonic and burst activities, with duration T_{tonic} and T_{burst}, will be performed. Each period of activity corresponds to a *state*. The combination of a tonic and a burst is called a *cycle*, whose number may vary from experiment to experiment. Regarding the plasticity in the learning phase, the early weight is free to evolve throughout tonic and burst firing, while the late weight will only evolve during burst activity. As a reminder, early weight is modeled by traditional plasticity rules, and late weight by structural plasticity.

During the tonic, input patterns are presented to the network. The size of the grid and the number of pixels ON and OFF are adjusted according to the experiment. The input frequencies used to define patterns during the learning process are chosen according to protocols used in the literature. This means either a learning protocol dependent on simulation frequencies, or a protocol based on the correlation of neuronal activities.

During the burst, all neurons adopt this endogenous rhythmic activity by applying the hyperpolarizing current to the inhibitory neuron. No pattern is presented during this period, leaving only time for consolidation through the evolution of late weight. The rhythmic activity switch is modeled as explained in section 3.2.3.

Testing
The test is also divided into cycles, in each of which one or more patterns are presented. The presentation time of a pattern is $T_{sample} = 1000$ms. Testing patterns may vary from one experiment to another. The network response will be evaluated in terms of frequencies.

5.1.3 Validation method

Performance assessment methods will be those used in most articles, namely the receptive field and pattern recognition. The receptive field shows the weight matrix associated with each output neuron after the learning period. Pattern recognition corresponds to the testing phase, during which the output neuron firing rate is measured when a pattern is presented. Its response is then compared to a threshold to decide whether or not the pattern is considered as learned by the network.

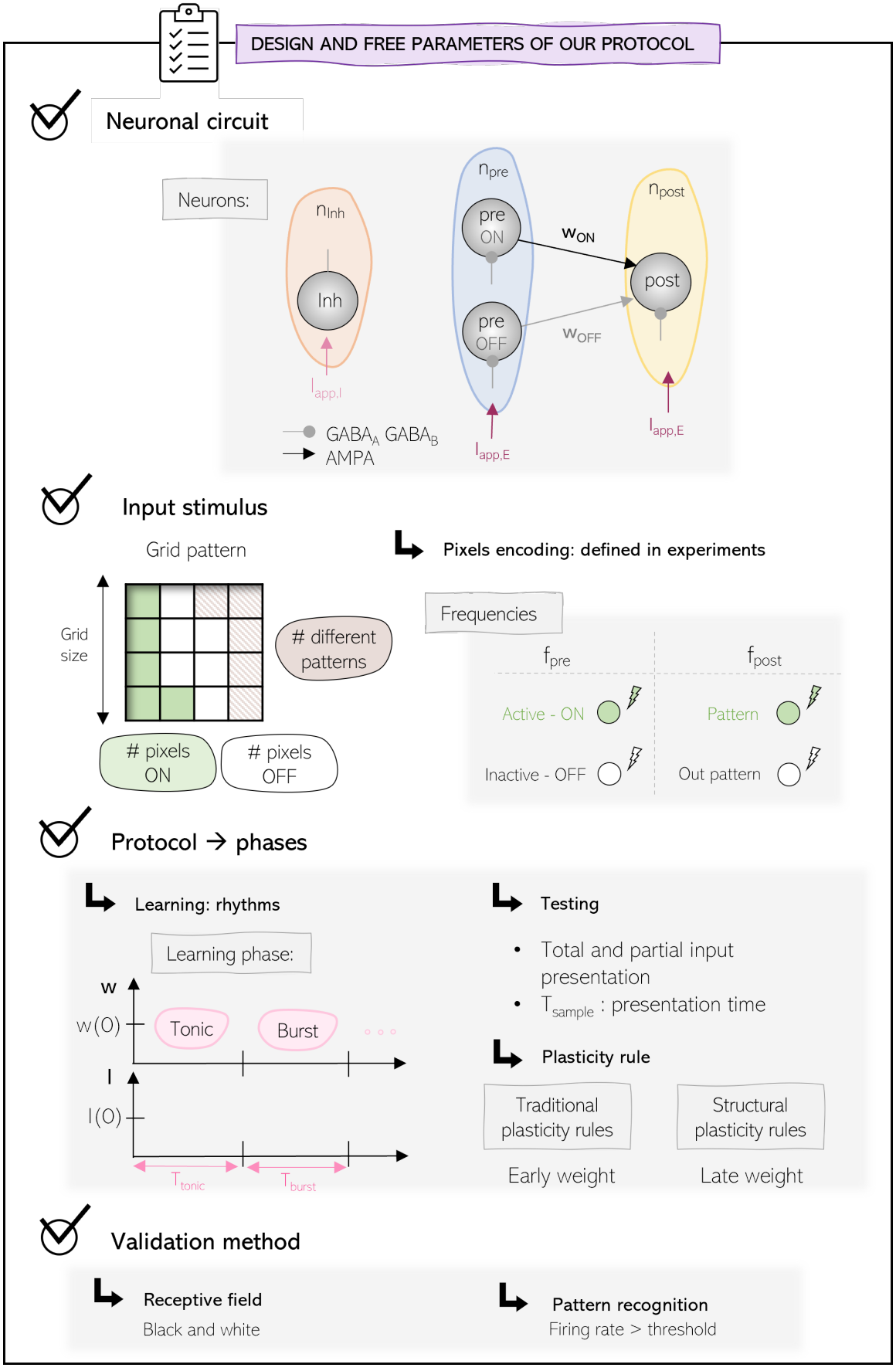

Figure 5.1 – **Design and free parameters of our learning protocol**: Details of the tools used here and the free parameters that can be chosen for each, with reference to the Figures 4.1 and 4.8 introduced in chapter 4.

5.2 Learning phase using our parameterization: frequency-encoded pixels

When doing learning tasks, most of the papers analyzed in Chapter 4 act on the frequencies imposed on the neurons to decide whether or not to learn a given pixel. Indeed, they consider correlated frequency activities as a mechanism for associating ON pixels, being part of the pattern, with the output neuron corresponding to this pattern. Meaning that the pixels ON were stimulated at the same time as the postsynaptic corresponding neuron. As for the OFF pixels (outside the pattern), they are often stimulated at very low frequencies or not at all. The design of the presynaptic f_{pre} and postsynaptic f_{post} frequencies will be explored to find a good combination of values leading to learning.

This simultaneous frequency association protocol will therefore be tested with the plasticity rules described above. Depending on the results we observe with these rules, hypotheses will be put forward in order to arrive at results consistent with consolidation mechanisms.

In this section, the generation of current pulses according to the encoded frequency takes place with a certain variability. In fact, the interval between spikes is not regular because each spike has an SD of 0.1 around its normal peak. The spike possibility interval is therefore 0.2 around the "regular" spike moment.

5.2.1 Frequency exploration in a simple protocol

To find the best set of frequencies, a protocol of learning is used and shown in Figure 5.2. Only one state is considered here, the tonic one lasting $T_{tonic} = 20000ms$. The architecture comprises an inhibitory neuron, a presynaptic neuron, and a postsynaptic neuron. The aim of this frequency exploration is to provide an experimental representation of the evolution of w as a function of the frequencies imposed on the neurons, for the calcium-based plasticity rule.

As illustrated in Figure 5.2(B), the choice of frequencies influences the convergence of w due to their modulation of the calcium oscillations of the 2 neurons. Depending on the frequencies chosen, calcium oscillations will be found at different levels of concentration. This means either below the depression threshold, between the depression and potentiation thresholds, or above the potentiation threshold. They may also be on either side of a threshold. The convergence value of w then depends on the balance between oscillation regions, as explained in Chapter 3. Since calcium dynamics is the same throughout the state, it is only shown in a short section ($1000ms$) to make it clearer.

A small experiment will also be carried out for the triplet rules, to see whether observations are the same when the rule is modified.

Calcium-based plasticity rules

Figure 5.3 illustrates that the modulation of synaptic strength, including both potentiation and depression, is influenced by the firing rates of the neurons involved. Three zones stand out separated by two boundaries. The lower left zone (colored in pale beige) corresponds to an unchanged value of w during the entire tonic state. The following zone (colored in lighter blue), is defining the depression of w up to a certain convergence value. The last zone (colored in darker blue) represents the combination of frequencies that will lead to the potentiation of w. The boundary between these last two zones is defined experimentally by interpolating the points shown on the graph.

The area around the zone boundaries will show less convergence than the rest of the zone. In more detail, the closer you get to the center of the depression zone, the lower the convergence value is. For the potentiation zone, the higher the frequency combination, the higher the convergence value.

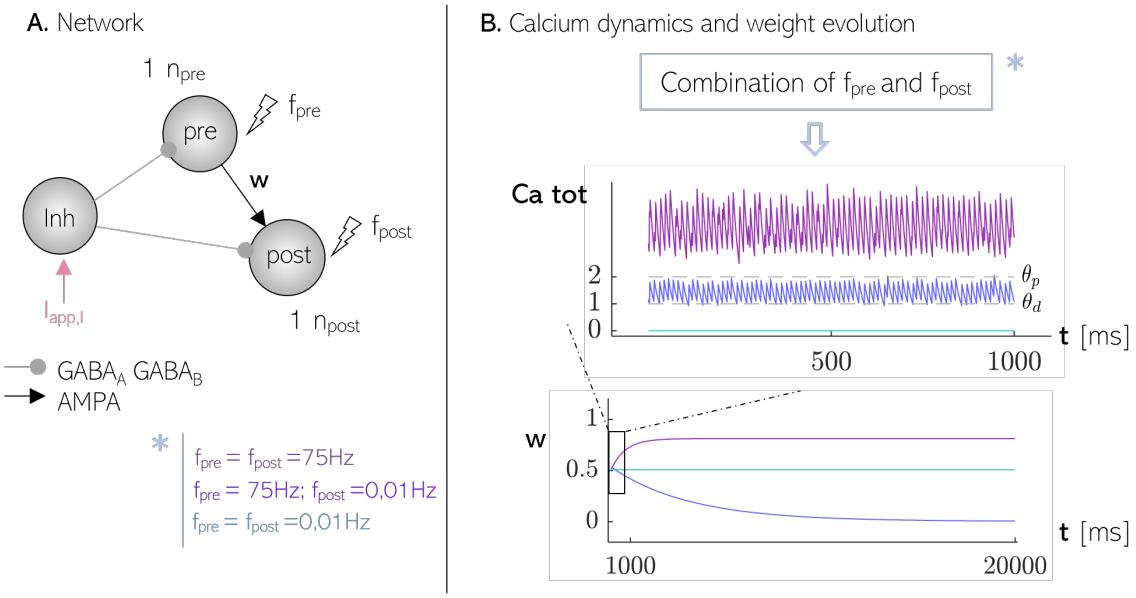

Figure 5.2 – **Simple protocol for the frequency exploration**. **A.** Architecture of the circuit and representation of the weight. **B.** Impact of the combination of f_{pre} and f_{post} on the calcium dynamics and consequently, on the weight.

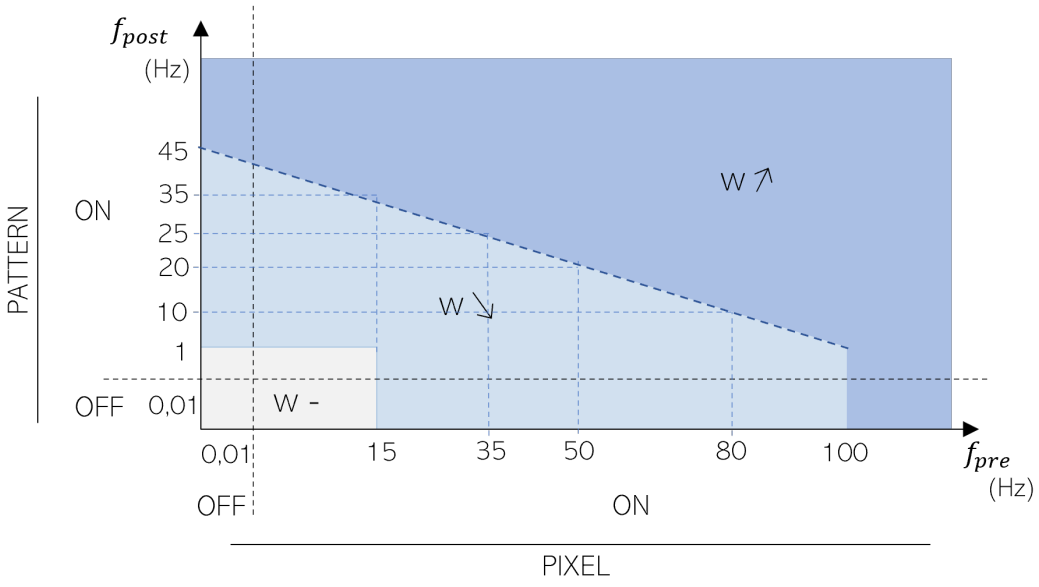

Figure 5.3 – **Influence of different frequency combinations on the evolution of the *early weight***: Three zones stand out as a function of the frequencies: the first zone (pale) corresponds to a stable value of w, the second one (lighter blue) leads to a decrease of the weight and the third one (darker blue) to its increase. Boundaries are experimentally defined.

The ON and OFF labels represent, for presynaptic neurons, the frequencies chosen to represent the ON and OFF pixels, and for postsynaptic neurons, ON is for the frequencies associated with the neuron that encodes the pattern and OFF for the others.

This graph shows a particular mechanism that may not be compatible with memory consolidation. Indeed, a postsynaptic firing alone at a frequency above $45Hz$ is capable of strengthening all the connections it has with presynaptic neurons, even those whose presynaptic activity is null (off pixels). This observation is indeed inconsistent with learning as it will lead, in the case of our pattern-based learning protocols, to an indistinction between the pixels to be 'learned' (making up the visual image to consolidate), and the rest of the pixels.

The representation of the phenomenon is illustrated in Figure 5.4 by taking two presynaptic neurons, one ON and one OFF, connected to the same postsynaptic neuron (all three are still connected to the inhibitor neuron). The frequencies of stimulation are set to $50Hz$ for the ON pixel, 0.01 Hz for the OFF pixel, and f_{post} is equal to $55Hz$.

The graphs show that whatever the value of f_{pre}, when f_{post} is greater than 45Hz, the calcium oscillations of both synapses are predominantly above the potentiation threshold. However, the average calcium concentration is lower at the second synapse, with only postsynaptic calcium contributing. Since the temporal evolution of the calcium total is predominantly above the potentiation threshold, we observe an increase in synaptic weight. The convergence value is different, however. This is explained by the fact that the region of Figure 5.3 corresponding to the connection between the OFF pixel and $f_{post} = 55Hz$ is close to a boundary, leading to a lower convergence value than the simultaneous high-frequency region. This result is because the calcium oscillation is on either side of the potentiation threshold and not completely above it. The convergence values can be calculated analytically using the equation 3.4.

Triplet plasticity rule

A similar result can also be observed with the triplet rule, but only when the f_{pre} is above $1Hz$. In fact, a postsynaptic frequency greater than approximately 40 Hz leads to a potentiation of synaptic weight, regardless of the value of the presynaptic frequency (as long as it is greater than 1). The convergence value in the case of triplet rules varies according to the timing of the spikes. The observed phenomenon is shown in Figure A.1 in Appendix 1.

Pair-based plasticity rule

En Pair-based, les protocoles d'apprentissage de correlation par haute-fréquences pré-post ne conviennent. En effet, lorsque l'encodage des pixels ne se fait pas par des spikes controlés, la valeur de w restera inchangée. En effet, si le neurone postsynaptique fire à haute fréquence, chaque spike pré synaptique arriver après et puis avant un spike postsynaptique. Cela mènera à une diminution de w, directement suivi d'une augmentation de même valeur.

Conclusion

The model used in the following experiments is the calcium-based model of Graupner et al. (2016). With this exploration, we found the right frequency ranges to impose on the neurons in our circuit to lead to the learning of the patterns presented in a sequence of learning cycles. These values can then be applied to a larger network to measure the impact of learning cycles on memory consolidation.

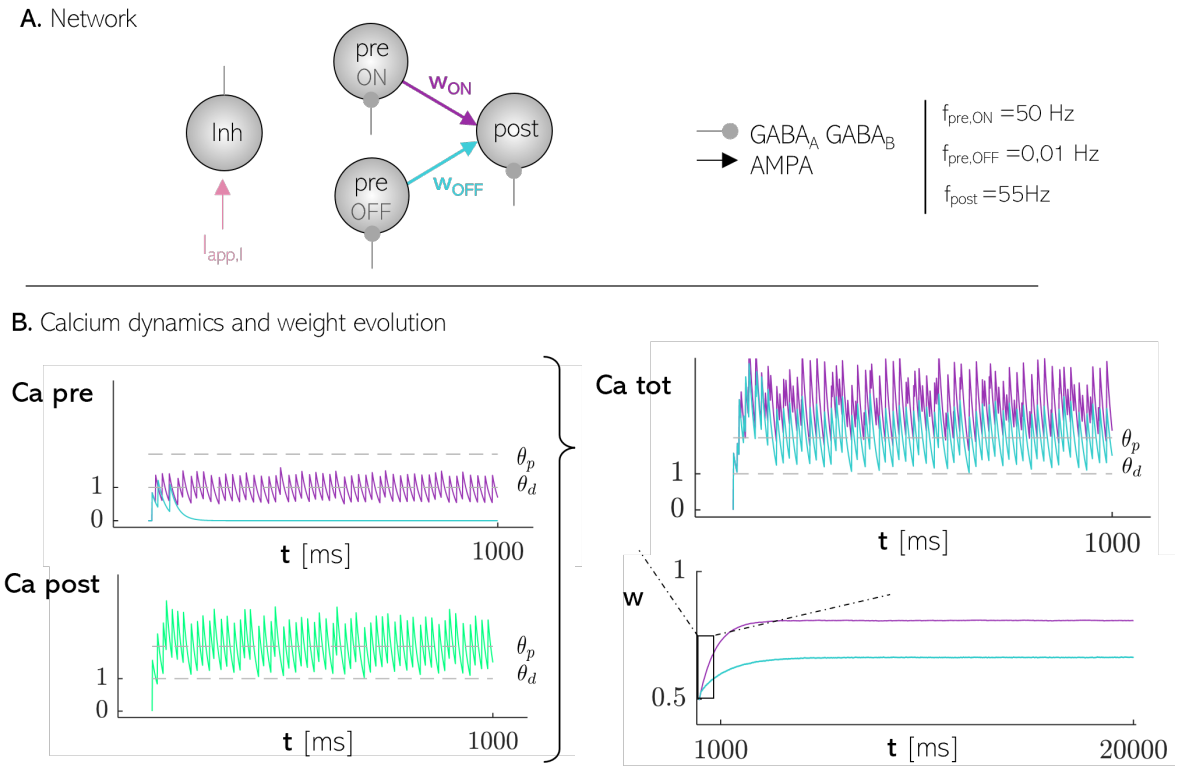

Figure 5.4 – **Illustration of the calcium-based rule limitation with a high postsynaptic firing rate**: **A.** Representation of the two different synapses, created by one presynaptic neuron (either ON or OFF) and the postsynaptic neuron. Different frequencies are used for each neuron. **B.** The evolution of the synaptic weight for the two connections is dependent on the calcium dynamics dictated by the rule implementation. Ca pre, Ca post, and Ca tot represent respectively the calcium presynaptic, the calcium postsynaptic and the calcium total (addition of both)

It should be noted, however, that with the current implementation of plasticity rules, at least for triplet and calcium, we observed an inconsistency with learning. Indeed, an increase in w occurred even when the post-synaptic neuron spiked alone. This observation will hereafter be referred to as *limitation A*.

5.2.2 Identification of the overconnectivity limitation

Network

The frequencies identified as corresponding to the learning mechanism during pattern presentation are now implemented in a larger network. The frequencies f_{pre} = 55 Hz and $f_{post} = 40Hz$ are chosen to represent the ON category. This combination is not the only possibility, but it ensures that the OFF pixels are not too strongly depressed (combination f_{pre} OFF and f_{post} ON). This would then have complicated the learning of these pixels, whose synaptic weight would have become too low, when presented with a different pattern.

The simulation consists of eight cycles of tonic and burst, of equal duration $T_{tonic} = T_{burst} = 15000ms$. During each tonic phase, a pattern is shown for the duration of this state. In this section, a single pattern is proposed for our circuit, consisting of 4 pixels ON and 5 pixels OFF. A total of $n_{pre} = 9$ (#pixels) is thus obtained, for a $n_{post} = 1$ (#pattern).

The traditional synaptic rule taken into account will be the calcium-based one. Initially, the

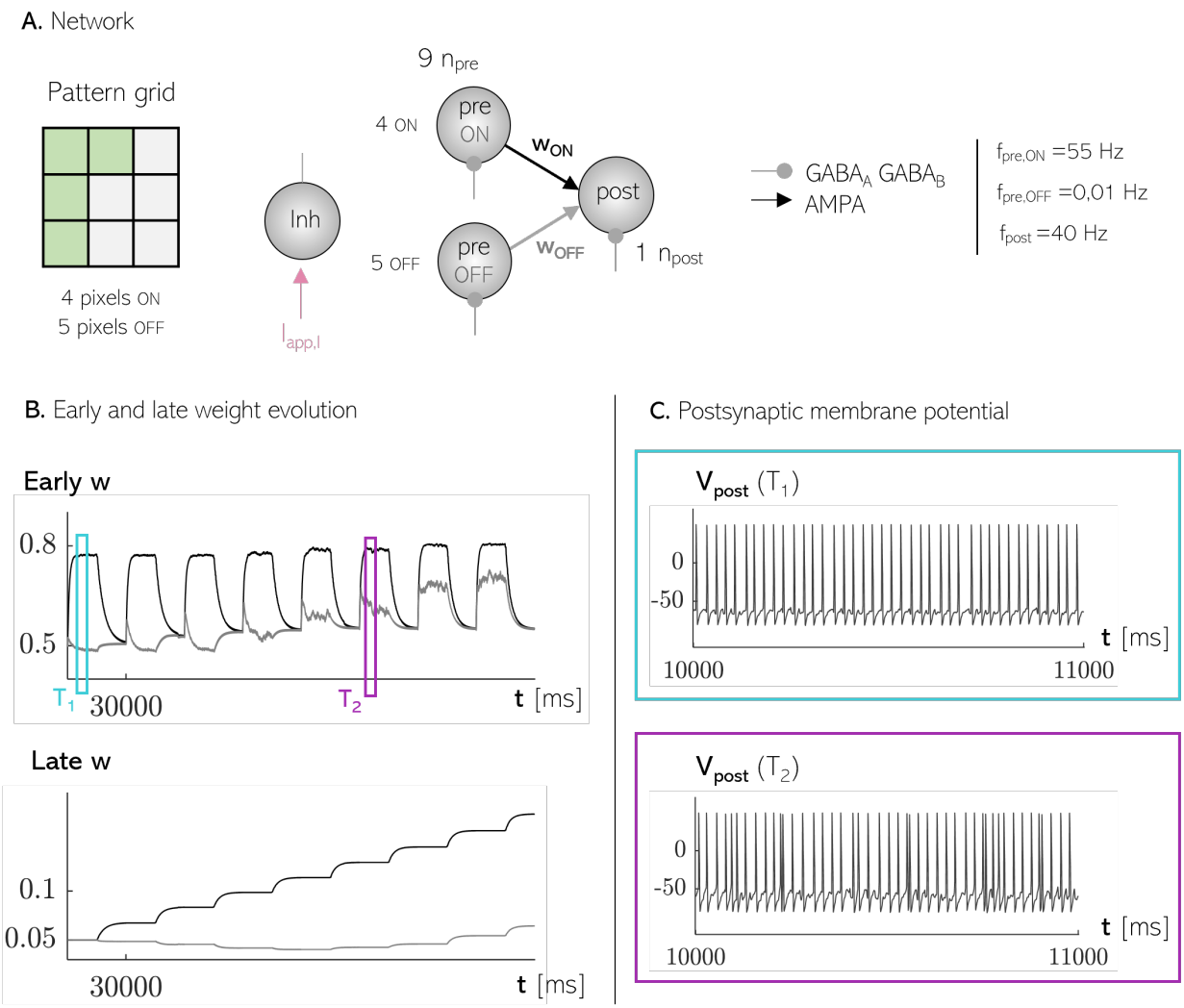

Figure 5.5 – **Learning phase in the circuit: spike transmission and overconnectivity**. **A.** Representation of the input pattern, the network and the frequencies of simulation. **B.** Graphs of early and late weights show an increase in synaptic strength for all pixels, including OFF pixels. This is called overconnectivity. **C.** Postsynaptic membrane in two time points revealed a higher frequency in T_2, due to the spike transmission.

parameters internal to the plasticity rules will not be modified, as they are fitted on experimental protocols.

Learning in the circuit

We observe in Figure 5.5 that from the fourth cycle on, the early weight of the OFF pixels has an increasingly high tonic convergence value. Consequently, the late w of these same pixels also starts to increase with each burst. This increase of connection strength for all pixels will be called *overconnectivity*. The reason why this effect is observed will therefore be investigated to find out whether it is a good or bad feature of memory consolidation.

Two time points, T1 (start of simulation) and T2 (when the phenomenon occurs), are chosen during the simulation to examine the membrane potential of the postsynaptic neuron. Looking at the graphs of postsynaptic potentials, we notice a much higher frequency at T2 than at T1. The phenomenon observed here will be referred to as *spike transmission*. This is due to the increase in synaptic weight.

The synaptic weight between neurons, corresponding to the product of w by l, has reached a value high enough to allow synaptic transmission of presynaptic action potentials to the postsynaptic neuron (section 5.2.3 will analyze the synaptic weight values at which this occurs). This transmission is added to the frequency f_{post} imposed on the postsynaptic neuron, resulting in a much higher value than the one chosen. Hence, this high activity leads to the *limitation A* identified in the section 5.2.1. As the postsynaptic frequency increases due to the transmission of spikes, the predominance of calcium oscillations eventually exceeds the potentiation threshold for all connections, inducing *overconnectivity*..

Cycles	Pixels	Freq (f_{pre}, f_{post})	Tonic w convergence	w_{reset}	Burst l convergence
#0	-	-	$w(0) = 0.5$	-	$l(0) = 0.05$
#1	ON	(55,40)	$w \longrightarrow 0.77$	0.51	$\nearrow : l \longrightarrow 0.067$
	OFF	(0.01,40)	$w \longrightarrow 0.48$		$\searrow : l \longrightarrow 0.048$
#2	ON	(55,40)	$w \longrightarrow 0.77$	0.53	$\nearrow : l \longrightarrow 0.084$
	OFF	(0.01,40)	$w \longrightarrow 0.48$		$\searrow : l \longrightarrow 0.045$
#3	ON	(55,40)	$w \longrightarrow 0.77$	0.54	$\nearrow : l \longrightarrow 0.1$ [1]
	OFF	(0.01,40)	$w \longrightarrow 0.48$		$\searrow : l \longrightarrow 0.041$
#4	ON	(55,43)	$w \longrightarrow 0.78$	0.55	$\nearrow : l \longrightarrow 0.114$
	OFF	(0.01,43)	$w \longrightarrow 0.54$		$\searrow : l \longrightarrow 0.040$
#5	ON	(55,45)	$w \longrightarrow 0.79$	0.55	$\nearrow : l \longrightarrow 0.13$
	OFF	(0.01,45)	$w \longrightarrow 0.62$ [2]		$\nearrow : l \longrightarrow 0.046$
...	...	...	...	...	...
#last	ON	(55,58)	$w \longrightarrow 0.8$	0.55	$\nearrow : l \longrightarrow 0.18$
	OFF	(0.01,58)	$w \longrightarrow 0.72$		$\nearrow : l \longrightarrow 0.067$

Table 5.1 – **Analysis of the spike transmission and overconnectivity link**: Cycle # 0 corresponds to the initialization of w and l. In the third cycle, the value of spike transmission is reached (and continues to increase over the cycles). Subsequent postsynaptic frequencies, therefore, become higher and higher, leading to a greater increase in early weight. By cycle five, this value is high enough to increase late weight. This is what we refer to as overconnectivity

The spike transmission and the overconnectivity are intimately linked. The analysis of these 2 mechanisms is detailed in Table 5.1. During the first two cycles, the late weight evolves as expected, increasing for ON pixels and decreasing for OFF ones. At the end of the third cycle, the value for spike transmission is reached. The postsynaptic frequencies of subsequent cycles will therefore be increasingly higher. By cycle five, the value of early weight is high enough to trigger the beginning of the overconnectivity phenomenon. In other words, the late-weight trend is reversed and will now rise. At the end of the cycles, the final value of late-weight is greater than $l(0)$, corresponding to the strong consolidation of

[1] Spike transmission allowed
[2] Overconnectivity begins

ON pixels, but the final value of early-weight is also greater than the initial value, showing a slight consolidation of OFF pixels. The reason for the change in the value of the reset is investigated in Justine Magis' thesis.

Problematic

Faced with these observations, the question that springs to mind is the following: *Does it make sense to avoid or limit the spike transmission to overcome the "limitation A"?*

In biological studies, the increase of postsynaptic neuron activity due the synaptic plasticity has been observed. Regulation mechanisms to adjust synaptic excitability have been discovered in neurons. These act to keep firing rates relatively constant and the phenomenon is known as homeostatic plasticity (Turrigiano and Nelson, 2004). The homeostasis of each neuron will set it to an excitation level depending on the excitation it receives (analogous to the number of ON pixels in our case). Biologically, spikes will be transmitted but if there are transmitted with our plasticity rules, the limitation A is encountered. These discoveries answer the question, confirming that it makes sense in our computational world to want to prevent the transmission of spikes.

The increase of synaptic plasticity is a computational problem because it leads to high postsynaptic activity and consequently to the consolidation of pixels OFF. This consolidation is detected through the increasing values of early weight during the tonic activity and, therefore, through the evolution of the late weight. To deal with this modeling problem of overconnectivity, various possible solutions are implemented. The first is the introduction of a maximum value for l, beyond which l cannot evolve. The second is a homeostasis approach, with the introduction of a processor to regulate the received excitation. The last one is based on the excitability of the postsynaptic neuron.

5.2.3 Solution 1: Threshold on the late weight

In this first approach, a maximum value (or *threshold*) that the late weight can attain will be implemented in the model. This addition can be seen, in a biological way, as reaching the maximum capacity of the synapse.

Firstly, tests without plasticity will be realized. They aim to find the minimum connection values, computationally expressed as the product of w and l, which will lead to spike transmission. Indeed, if the postsynaptic is not firing at a higher frequency than the defined one, the calcium dynamics will be what we wanted to achieve by defining the initial frequencies. In other words, depression for the OFF pixels and potentiation for the ON pixels.

Then, the value found by these static tests will be implemented as a threshold on the *late weight* to limit the consolidation under the spike transmission threshold.

By limiting the value of the memory consolidation, we observed a saturation after a small number of tonic/burst cycles, which is not consistent with biological learning. Therefore, parameter adjustments are done to slow down the threshold reach, such as the initial value of the *late* w or the time constant value τg.

Values of spikes transmission

Why does the product w and l influence the excitability of the postsynaptic neuron?

The explanation comes from the neuron model of (Hodgkin and Huxley, 1952). As a reminder, membrane potential contributions are the sum of ionic I_{ion}, applied I_{app}, and synaptic I_{syn} currents. We are interested here in the synaptic current I_{syn}, and more specifically that of the AMPAr, I_{AMPA}, since excitatory synaptic transmission from pre- to post-neurons is considered. Synaptic current can

be written as:

$$I_{\text{AMPA}} = wl\, s_{\text{AMPA}}\,(V_m - 0) \tag{5.1}$$

where V_m is the postsynaptic membrane potential and s_{AMPA} depends on the presynaptic voltage. In this equation, we can see how the contribution of the synaptic weight $w * l$ influences the synaptic current and therefore the excitability of the postsynaptic neuron. It can easily be deduced from this general equation that the addition of active presynaptic neurons will also contribute to the evolution of the synaptic current. In fact, the values of wl connections will be characterized and summed for each ON presynaptic neuron, according to:

$$I_{\text{AMPA}} = (\sum_i wl)\, s_{\text{AMPA}}\,(V_{pre})\,(V_m - 0) \tag{5.2}$$

Now, simple tests to find the values from which transmission occurs will be set up. As explained above, the number of pixels ON will influence the synaptic transmission. Tests will be done for different numbers of pixels ON and a logic will then be tried to generalize the transmission value as a function of the number of ON pixels chosen.

# pixels ON		1	2			4	
Spike simulation pattern		–	Simult.	Delayed	Random	Simult.	Random
l value (with w=0.5)	Spike transmission	0.4	0.2	0.3	0.35	0.1	0.15
	Frequency reproduction	0.9	0.5	0.5	0.5	0.3	0.3
	"Higher frequency"	–	–	0.6	0.5	–	0.9

Table 5.2 – **Test without plasticity to find the late weight maximum capacity**: Simult. stands for simultaneous simulation and corresponds to the timing of spikes exactly matched between presynaptic neurons, delayed corresponds to a 10ms offset between the same trains of presynaptic spikes, and random corresponds to spikes randomly distributed over the time period while retaining the imposed frequency. Spike transmission is the minimum required value for the transmission, frequency reproduction is the reproduction of the pre-spike frequency by the postsynaptic neuron, and higher frequency is the value for which most of the presynaptic spikes are reproduced, contributing at a higher frequency than the presynaptic ones (several transmissions).

The values for which the EPSP produced by the postsynaptic neuron in response to the presynaptic action potential will be transformed into a spike are given in Table 5.2. The table also includes the connection values for which the presynaptic frequency is exactly reproduced in the postsynaptic neuron. The last line of the table corresponds to the values for which the postsynaptic frequency is higher than the presynaptic frequencies, with transmission taking place for most pre-spikes (this value can only be obtained for different trains of presynaptic spikes, delayed or random).

When the number of ON pixels is greater than 1, we introduce the notion of a simulation pattern. This corresponds to the choice of the spike succession between presynaptic neurons, with the aim of seeing the different values obtained and being as rigorous as possible in our choice of threshold. Three different simulation patterns are used:

- Simultaneous simulation corresponds to the timing of spikes exactly matched between presynaptic neurons, delayed corresponds to a 10ms offset between the same trains of presynaptic spikes.

- Random simulation corresponds to spikes randomly distributed over the time period while retaining the imposed frequency.

- Delayed simulation describes a situation where the presynaptic spikes of the second neuron are delayed by 10ms compared to the spikes of the first neuron. Delayed simulation is only performed with 2 pre-spikes because the 4-pixel random simulation reduces the window of spike possibility so that the pre-synaptic spikes arrive close enough together in the same window.

Conclusion

By running several different simulations, we were able to consider a "perfect world" where the spikes occur exactly all at the same time, as well as a more "realistic" world where the spikes are not necessarily simultaneous. In the perfect world, the simultaneous spikes will result in the most restrictive value of the threshold.

The threshold value, which can be referred to as the late weight maximum capacity, will therefore be chosen according to the most restrictive transmission value so that transmission can also be prevented if all the pre-spikes arrive exactly at the same time. The choice of this value also enables us to adapt our maximum capacity to the number of ON pixels. In fact, since the contribution of each synaptic weight is additive, the value obtained for a single pixel (e.g., l=0.4 when w=0.5) can be divided by the number of ON pixels in the pattern.

Implementation of the threshold during learning patterns

The threshold found in the previous tests is now implemented in our circuit to limit the increase in late weight. The network used is the same as that shown in Figure 5.5. It is implemented in the coding by imposing that when the value of l exceeds the threshold, l is forced to this maximum value. Since the calculated threshold value of $l_{threshold} = 0.1$ was obtained with a $w = 0.5$ and that during tonic, w can rise above this value, the threshold is reduced to 0.08. A minimum value of 0 is also imposed (already present in previous simulations). The postsynaptic frequency has been reduced to better visualize changes in early and late weights. Indeed, with this frequency, the value of convergence in depression is lower and therefore allows a greater gap between it and the reset value, resulting in a greater decrease in late weight.

Figure 5.6 shows that this solution works and can be integrated into a learning protocol, by matching the threshold value to the number of active pixels in the simulation. We note that in the case of this figure, a saturation of the late weight occurs after a short number of cycles. This will depend on the model parameters, such as the initial value of the late weight $l(0)$ or the time constant associated with the late weight, τ_l (see equation 3.6).

Slower threshold reach

In the context of this threshold solution, and assuming progressive memory consolidation over several cycles, a slow-reaching threshold approach is envisaged.

To achieve this, a lower $l(0)$ and a higher τ_l can be implemented. A biological analogy can be drawn for both solutions. Indeed, the further away from the synapse's maximum capacity you begin the learning, the more it will be able to learn, and over a longer period of time if consolidation is more gradual.

5.2.4 Solution 2: Homeostasis mechanism implementation

Another solution to prevent the neuron from spiking at too high a frequency and generating the " limitation A " may be the implementation of a homeostatic mechanism. As a reminder, this process of input-dependent activity regulation has been observed biologically by Turrigiano and Nelson (2004).

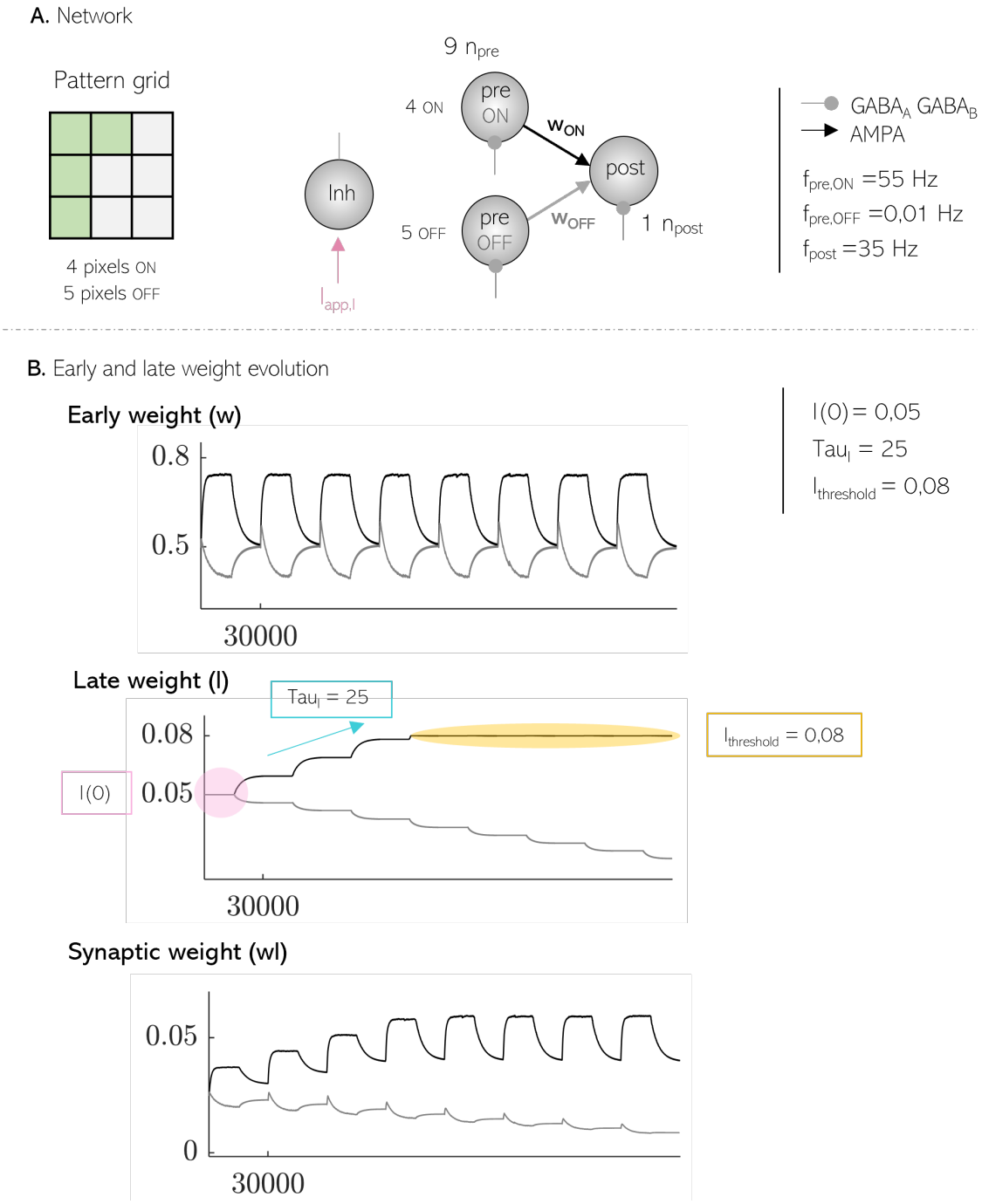

Figure 5.6 – **Implementation of late weight maximum capacity**: **A.** Network architecture simulated by a pattern of 4 active pixels **B.** The late weight threshold is set at $l_{\text{threshold}} = 0.08$. The parameters τ_l and $l(0)$ can be adapted to start learning further away from this maximum capacity.

Computationally, this approach can be seen as adding a variable to regulate the synaptic activity received. This variable will be identified by K in further development of this solution. Several different modelizations of this mechanism are tested and detailed below, from the "naive" approach to the more "realistic" one.

Implementation of K linearly increasing: "naive approach"

An initial approach was used to test feasibility. This model takes into account, in a very simplified way, the homeostatic scaling phenomenon described in the literature. Referring to equation 5.2, K is implemented as follows:

$$I_{\text{AMPA}} = \frac{\sum_i w_i l_i}{K} s_{\text{AMPA}}\left(V_{pre}\right)\left(V_m - 0\right) \tag{5.3}$$

In this naive model, K is simply updated linearly by constant increment at each ten time steps.

This technique works, as seen in Figure 5.7 but only for a $K(0)$ belonging to a very limited interval, and increasing with a precise increment according to the τ_l chosen. Indeed, a K too large prevents consolidation at any pixel, and a K too small does not prevent transmission. In this case, for a $l(0) = 0.03$ and $\tau_l = 25$, K started at 1 and was incremented by 0.000005. This approach is therefore highly parameterized and rather fragile to variability.

Implementation of K in function of the received excitability

The first implementation of an activity-level-dependent homeostatic mechanism is thought of as follows: The excitatory synaptic current received by the postsynaptic neuron in the context of this regulatory solution is described by the equation 5.3. The reasoning behind having an excitation-dependent K comes from the following assumption: the quotient $\frac{l}{K}$ must be below the threshold value defined in the previous section, denoted by l_{th}, in order to avoid spike transmission. To take the most restrictive case, the maximum value of l will be taken to update K according to

$$K(l) = \frac{max(l_i)}{l_{th}}$$

As the variable K now depends on l, it will be denoted $K(l)$. Putting the value of K back into the initial equation, we obtain:

$$I_{\text{AMPA}} = \frac{\sum_i w_i l_i}{max(l_i)} l_{th}\, s_{\text{AMPA}}\left(V_{pre}\right)\left(V_m - 0\right) \tag{5.4}$$

By looking at this equation we quickly note that, since the late-weight of all pixels ON is the same and therefore equal to $max(l_i)$, the fraction $\frac{l_i}{max(l_i)}$ is equal to 1. Therefore, The synaptic weight only corresponds to w_i scaled by the value of the threshold l_{th}. This solution is not compatible with our initial hypothesis of exploiting the homeostatic reset of early weights as a memory consolidation solution.

A second implementation is implemented, keeping the *mean* of l constant over the cycles. Indeed, l_i changes with learning, and K will evolve to keep their mean constant. The K is incorporated into the excitatory synaptic current in the same way as in the first approach, according to equation 5.3. The calculation of $K(l)$ can then be defined as follows:

$$\frac{mean(l(t))}{K(l(t))} = \frac{mean(l(t-1))}{K(l(t-1))} \Rightarrow K(l(t)) = \frac{mean(l(t))}{mean(l(t-1))} K(l(t-1)) \tag{5.5}$$

This definition of K requires an initial value, chosen at 1 in our case to have a neutral value. Since K is updated at each time step, this means that the ratio $\frac{mean(l)}{K}$ will always remain equal to the value of $l(0)$ defined at the start.

We observe that the solution works, but that the value of the convergence of $\frac{l}{K}$ depends on the initial value $l(0)$ (Figure 5.7). Indeed, when the $\frac{l}{K}$ of OFF pixels reaches 0, the mean will no longer change

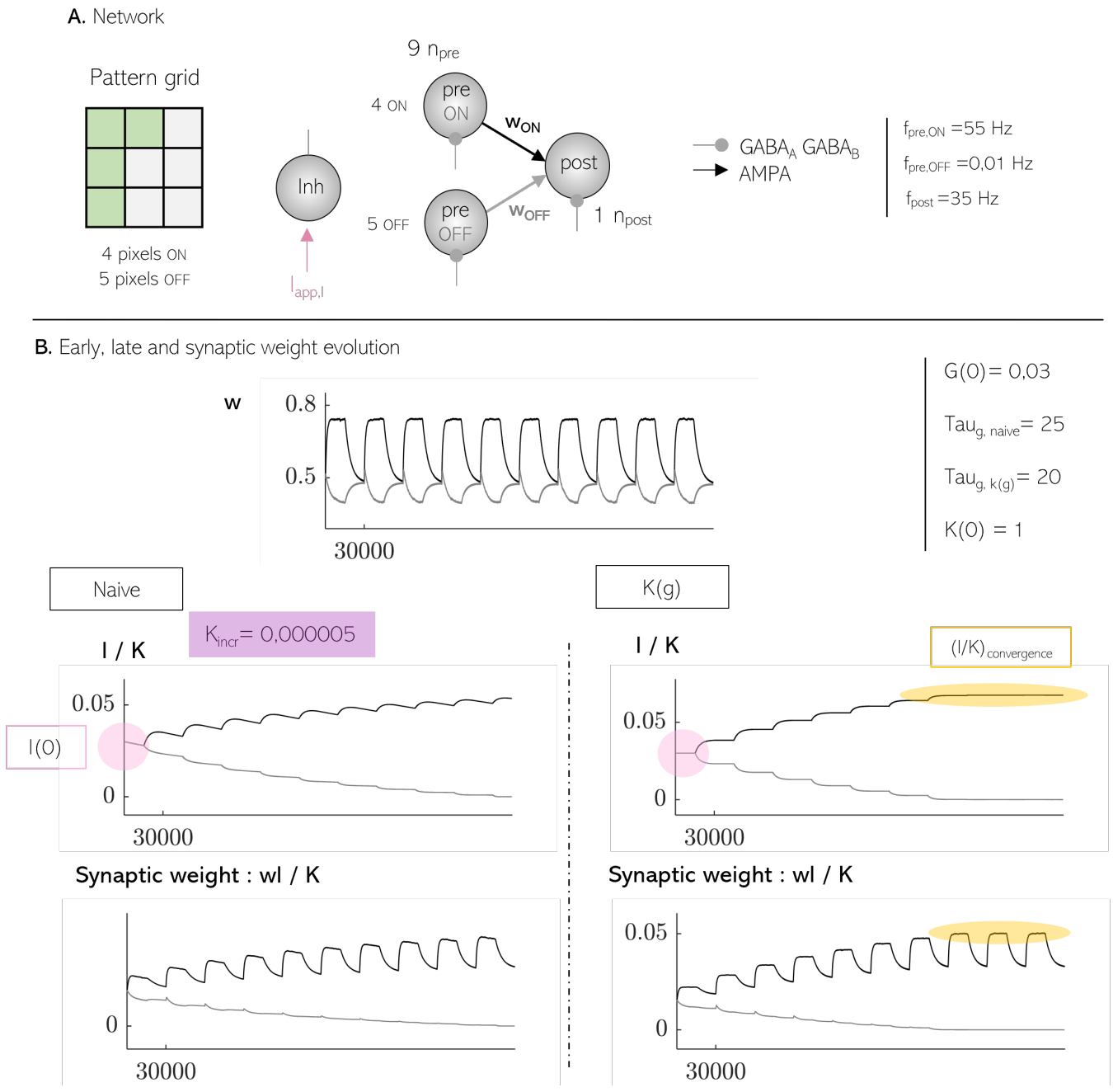

Figure 5.7 – **Implementation of solution based on homeostasis**: **A.** Network architecture simulated by a pattern of 4 active pixels **B.** Implementation of a variable K to regulate postsynaptic activity. The initial K is set to 1. **Naive** The parameters of the naive approach are the $l(0)$ value and the choice of K increment. **K(l)** In this implementation, K varies to keep the l average constant. The starting value, therefore, has a major influence on the convergence value

.

and we reach a stationary state, dependent on this $l(0)$. We therefore need to find a configuration where the initial value chosen does not result in a final $\frac{l}{K}$ convergence value lower than the spikes transmission threshold, or adapt K(0) accordingly. In this case, the maximum value reached will be equal to $l = 0.0675$, given that 4 active pixels contribute to keeping the average of 9 pixels at 0.03. The synaptic weight therefore reaches a lower maximum value than in the case of a ceiling.

5.2.5 Solution 3: Postsynaptic neuron excitability

The third approach to overcome the *limitation A* is the hypothesis of imposing a constant applied current I_{app} to the post-synaptic neuron in the tonic phase, instead of creating current pulses. This is represented in Figure 5.8

In the previous simulations, the postsynaptic neuron was hyperpolarized due to the inhibitory $GABA_A$ and $GABA_B$ currents of the inhibitory neuron in the circuit but had no current applied (I_{app}=0). The control of the excitability level is done differently than when it is a continuous applied current, as for the inhibitory neuron. In fact, the generation of spikes by excitatory neurons takes place, according to the chosen frequency, by current pulses with an intensity of 50 and lasting 3ms. The assumption is that the excitatory neuron is allowed to spike between pulses.

The intuition behind this solution is that if the postsynaptic neuron is supplied with a constant depolarizing current ($I_{app} > 0$), it may be less prone to the transmission of spikes from presynaptic neurons. A naive and rather unphysiological approach is implemented so that we can only see the impact of this current on spike transmission. To achieve this, the influence of the inhibitory neuron on the postsynaptic neuron is stopped and the current pulses are replaced by a constant depolarizing current of value $I_{app} = 1$. The previous homeostasis approach could have been applied in this case to regulate the value of the depolarizing current as a function of the excitation received.

Nevertheless, this approach still transmits spikes, so it fails to solve the problem of consolidating OFF pixels. Consequently, we shall not explore this solution any further. Had we wished to be more physiologically accurate, the postsynaptic neuron would still have had to be subjected to the currents of the inhibitory neuron, but their intensity could be reduced for this neuron in tonic. In fact, it is not very rigorous to cut off the influence of the inhibitory neuron only on the postsynaptic neuron in tonic, and then restore it during the burst.

5.2.6 Comparison of pattern class learning with and without overlap

After testing several approaches to get around the *overconnectivity*, the first solution will be implemented in the rest of the experiments. Indeed, this threshold approach is the one that seemed best to me, as it is the one for which we have the most control over the situation, and for which we can adapt the values according to our needs.

Still with the aim of understanding the role of burst in plasticity, we are going to increase the size of the network and introduce the notion of *pattern classes*. Like patterns, pattern classes are represented in the shape of a grid. They correspond to a defined region of the grid, in which several unique patterns are defined. A post neuron now codes for an entire class, not just a single pattern.

I chose to use pattern classes for several reasons. The first, to illustrate the reality, comes from the following thought. When we learn numbers, they can be represented in different fonts or writings. Taking a simplified approach, and comparing this real-life learning with our learning tasks, this would be analogous to varying the choice of ON and OFF pixels within the same class during simulation. The postsynaptic neuron stimulated would be the same, but it would be trained to a variation in simulation patterns within its associated class. This reason also applies to testing protocols, after the learning

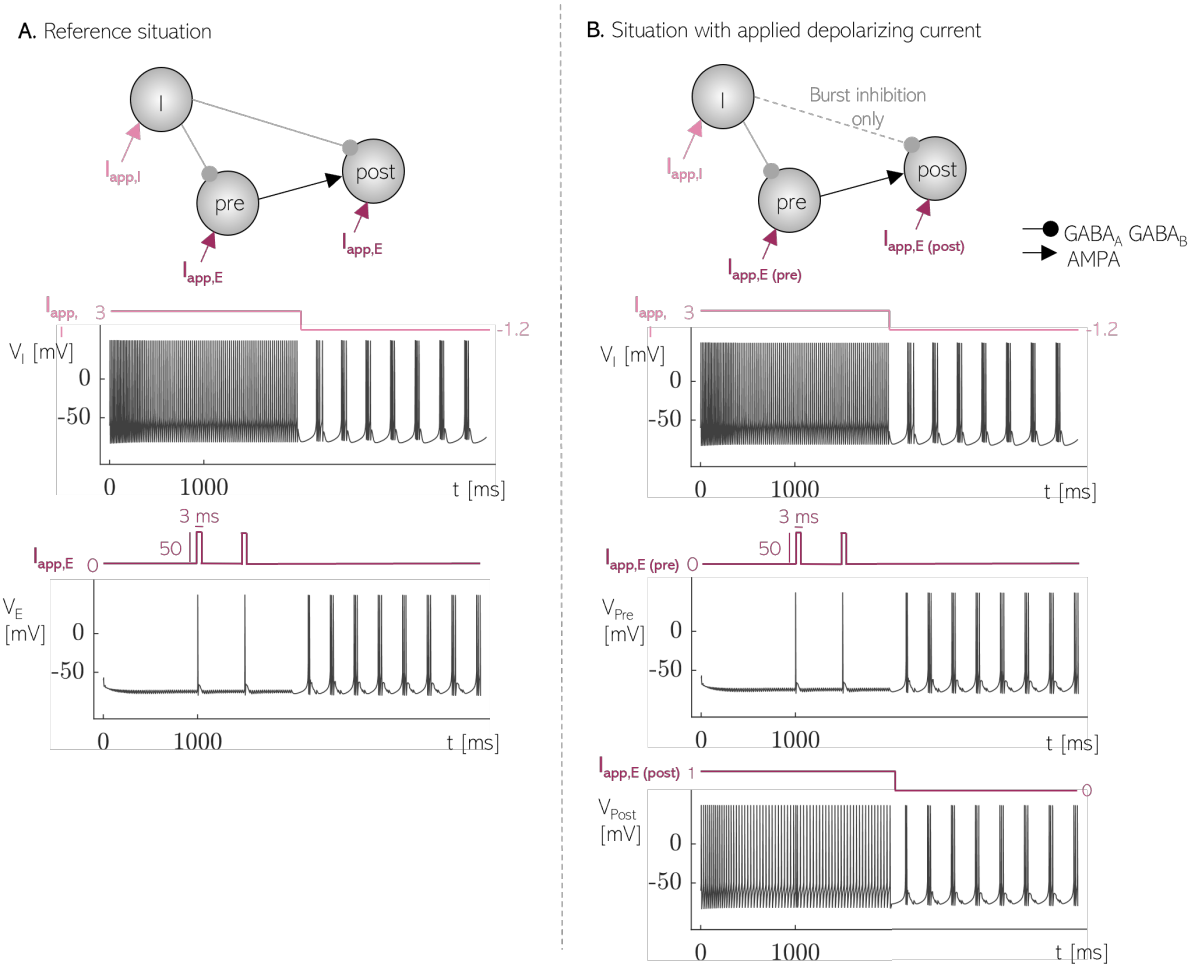

Figure 5.8 – **Simulation of the postsynaptic neuron with an applied depolarizing current in tonic firing**: **A.** Simulation of applied currents used in all experiments, explained in the section 3.2.3. **B.** The postsynaptic neuron no longer receives inhibitory current in tonic and is stimulated with an applied current $I_{app} = 1$. In burst, it is "reconnected" to the inhibitory neuron circuit.

phase. The postsynaptic neurons must be able to recognize several variations of the same class. The number of pixels activated during testing can be reduced or increased, which is not possible with a simple pattern.

Finally, if we focus on receptive fields, having several patterns making up a single class and therefore referring to a single postsynaptic neuron allows us to see the impact of pattern presentation on the consolidation of this neuron.

Patterns without overlap

One class of patterns on a 4x4 pixels grid

The first simulations are performed for patterns displayed on a 4x4 grid, with each pixel corresponding to a presynaptic neuron. Initially, a single pattern class is considered. The class, encoded by a unique postsynaptic neuron, is composed of 2 different patterns, as shown in Figure 5.9. The patterns are simply bars composed of 4 pixels. The frequencies used are the same as those found during frequency exploration, i.e. $f_{pre} = 55$Hz and $f_{post} = 40$Hz for the ON category, and 0.01Hz for the OFF category.

In terms of model parameters, the late-weight value is initialized to $l(0) = 0.02$, the associated time constant is $\tau_l = 50$ and the threshold is set to $l_{\text{threshold}} = 0.1$. In the learning protocol, patterns are presented alternately for each tonic. A total of 10 cycles of 30000ms are performed. One can see that the late weight, with these parameters, does not yet reach the threshold. This can obviously be changed by modifying the model variables and increasing the number of cycles.

In order to compare our results quantitatively with other learning protocols, two further scenarios are introduced. The one described above will be referred to as scenario $S3$ [3]. The validation method here will be the method of receptive fields (RF). As a reminder, the receptive field for each output neuron shows the values of the synaptic weights of each pixel with that specific neuron. This allows the evolution of weights to be visualized, showing the effect of pattern presentation on individual output neurons.

The first scenario introduced aims to investigate the impact of burst on learning. It will be called $S1$ and will consist of following tonic firing with a period of neuronal inactivation. This period is characterized by a very low spike frequency, equal to $f_{\text{rest}} = 1Hz$. Synaptic weight, therefore, remains almost constant during the transition to this state (it decreases extremely slightly). Biologically, it can be seen as an absence of stimulus or a blockade of neuromodulators, preventing neurons from spiking. The receptive fields obtained with scenario $S1$ show us that the learning of a new pattern during the tonic overwrites each previously consolidated pattern. The synaptic weights corresponding to one pattern will therefore increase during the presentation of this pattern, then return to their initial value during the next tonic when the other pattern is presented. Since plasticity does not change in bursts, this pattern is still retained throughout a cycle (consisting of 2 states). If the same pattern had been taught 2 times in succession, the weight would have just returned to its previous tonic value after its very slight decrease in rest, showing very limited memory consolidation.

The second scenario, called $S2$, illustrates the impact of structural changes on learning. It consists of a succession of bursts and tonics, with no structural changes to the synapse. In this case, the l variable remains unchanged, and only the early weight can evolve during the various states. As already demonstrated, the evolution of early weight into burst leads to the phenomenon of homeostatic reset, where previously stored information is erased. Looking at $S2$'s receptive field, we can clearly see an increase in synaptic weight during the tonic, followed by a total erasure of all traces of consolidation during the burst. Learned patterns are therefore forgotten at the end of each cycle.

For scenario $S3$, the receptive fields associated with the synaptic weight values at each state are shown on the Figure 5.9. We observe the effect expected by the definition of our frequencies, namely a progressive consolidation of the class to which the two bars learned during tonic belong. This scenario thus avoids the erasure of patterns during the burst ($S2$) and also the overwriting of the receptive field ($S1$). In fact, previously learned patterns are retained and pixels corresponding to newly learned patterns are simply added to the receptive field.

Two classes of patterns

1.Patterns on a 4x4 pixels grid

Next simulations are done with two classes of patterns, and therefore 2 output neurons. There will now be 2 receptive fields, each representing the synaptic weights of an output neuron with each presynaptic neuron. The two classes each comprise two 4-pixel bars. With the use of these classes, we will be able to analyze how the presentation of a pattern associated with a specific neuron, as well as

[3]Notations were introduced by Jacquerie (2023) and are repeated here to maintain the same formalism

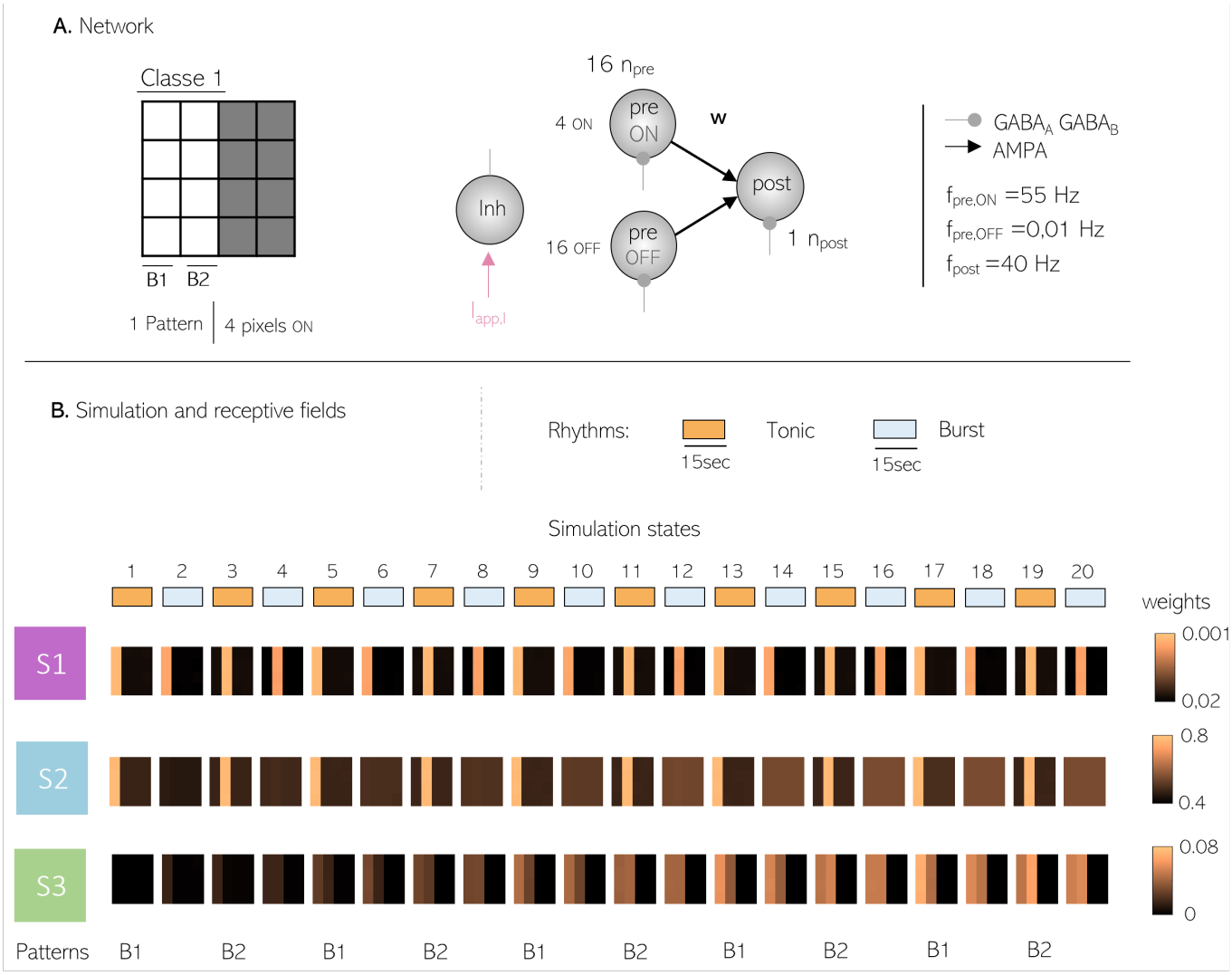

Figure 5.9 – **One classe of patterns without overlap**: **A.** The class of pattern is composed of the two first bars. Only one output neuron is considered. **B.** S1. Learning of a new pattern during the tonic overwrites each previously consolidated pattern. S2. Consolidation in tonic but pattern erasure during the burst. S3. Progressive consolidation of the class of pattern.

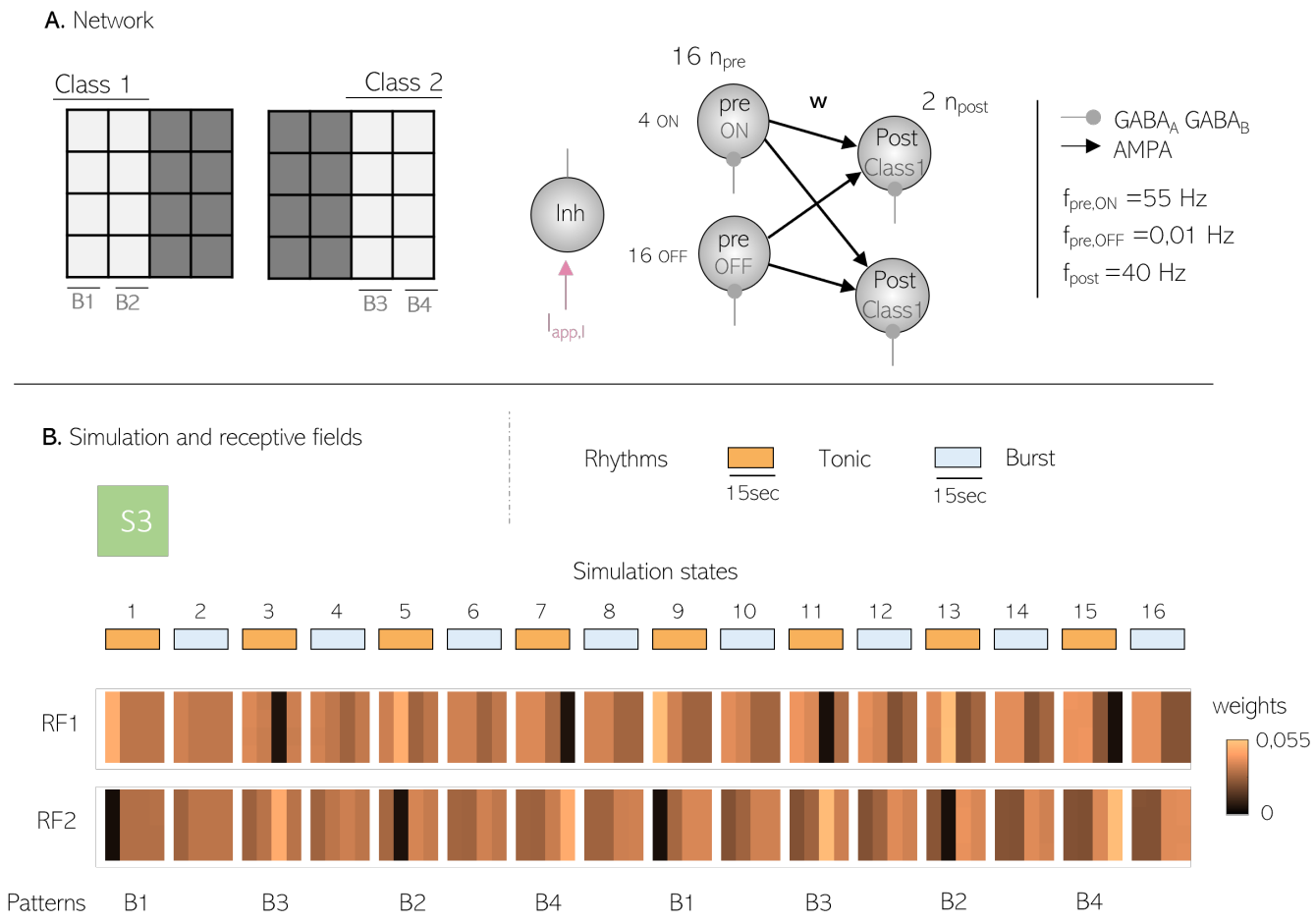

Figure 5.10 – **Two classes of patterns without overlap: A.** The two classes of patterns are composed respectively of the two first and last bars. Two output neurons are now considered, one for each class**B.** Pixel consolidation when patterns from the good class (the same one as the output neuron considered) are presented. Pixel depression occurs when a pattern from the other class is presented.

a pattern associated with the other neuron, affects the receptive field. During each tonic, a random pattern from one class is presented in alternation with a pattern from the other class. A total of 8 cycles is run.

Looking at the receptive fields in Figure 5.10, we notice that on the neuron associated with the presented pattern, the synaptic weight increases when the pattern is learned, and this consolidation is maintained (with a lower weight) over the cycles. If we look at the other neuron when the same bar is presented, we observe a strong depression, linked to the choice of frequencies $f_{pre,on}$ and $f_{post,off}$. This depression seems rather positive, as it helps to highlight the consolidation of the class associated with the pattern, by creating a greater difference in synaptic weight. Indeed, when we look at the last image for the 2 output neurons, we can see an overall consolidation of the class associated with them.

2. Increase of the grid size

Grid size is increased to 5x5 pixels. The results, unsurprisingly, remain similar to those obtained in 4x4. Bars of the first class are consolidated on the first pattern, while those of the other class are depressed. We can see that the middle bar is between the two extremes of synaptic weight value.

Patterns with overlap

Two classes of patterns on a 4x4 pixels grid

To now make overlapping patterns and see what happens when certain pixels are shared by several patterns, we will consider two classes, the first containing the first two bars (vertical) and the second containing the first two lines (horizontal). For the simulation, the same frequencies as those used when presenting patterns without overlap are retained, i.e. $f_{\text{pre,ON}} = 55\text{Hz}$ and $f_{\text{pre,OFF}} = 40\text{Hz}$. The number of cycles will be set at 4, because as shown in Figure 5.10, the receptive field in the 8^{th} state is the same as in the 16^{th} state. The only difference is the gap between the weights.

We realize, by looking at the receptive fields on Figure 5.11, that when a bar is displayed, the weights of its pixels are depressed on the neuron coding for lines. This means that the weights of active pixels on the wrong post neuron are highly depressed compared to the potentiation on the good neuron. This raises the question of whether or not this is a good thing. If the depression is too strong, it will prevent the consolidation of pixels over the depression. But the fact that there is a depression can be qualified as good, because the overlap pixels will be less consolidated than the areas unique to the neuron. This means that when we activate only the overlap pixel and ask it to associate it with an output neuron (and therefore 1 pattern class), it will not know how to do so. It will need to activate an additional single pixel in order to make this association. This response can be considered analogous to that of a human. Indeed, if we are presented with a horizontal bar and asked to associate it with a square or a triangle, we will not be able to do so.

The frequency range must therefore be fine-tuned to ensure that this weight does not decrease too much. This sharp decrease in synaptic weight for pixels did not seem problematic at first glance when there was no overlap, as it had no impact on the consolidation of pixels to be learned. Here, when we look at the end of the learning process, overlap pixels are less consolidated than pixels that are not part of any pattern, which does not seem normal. The weight value becomes too low to be consolidated afterward. This situation of excessively depressed pixels in the receptive field of the wrong output neuron (relating to the pattern not containing these pixels) is called *limitation B*.

To remedy this, the pre-frequency is reduced to 35Hz (Figure 5.12). With this frequency, the tonic depression convergence value of w when combining ($f_{\text{pre,ON}}$, $f_{\text{post,OFF}}$) will be lower than that obtained previously with 55Hz (we are closer to a limit on the 5.3 diagram).

MNIST

To test the model's parameterization on a larger, more complex network, we are moving on to the digits of the MNIST dataset. As seen in the Capone et al. (2019) experiment, we will only use 3 digits, namely 0, 1 and 2.

In the simulation, we see on the receptive field of the first neuron coding for 0, that the digit begins to consolidate in the first state it is presented (Figure 5.11 A). However, when other digits are presented, this will lead to depression of the corresponding pixels on our neuron coding for 0. The same phenomena are observed for the receptive fields of other neurons, leading us to conclude that depression is too great in this rule.

In an article by Litwin-Kumar and Doiron (2014) an analysis similar to that of this thesis concerning frequency exploration was carried out for several plasticity rules. When we look at the results they obtained with the calcium-based rule of Graupner and Brunel (2012), the central depression zone is much smaller than the one I obtained with that of Graupner et al. (2016), see appendix XX. The frequencies selected are those that will lead to potentiation when active frequencies are combined, but to a neutral zone when a pre- or postsynaptic neuron is activated alone, namely $f_{\text{pre}} = 40$ Hz and $f_{\text{post}} = 40$ Hz. When displaying the receptive field, we can see the clear appearance of each digit for each

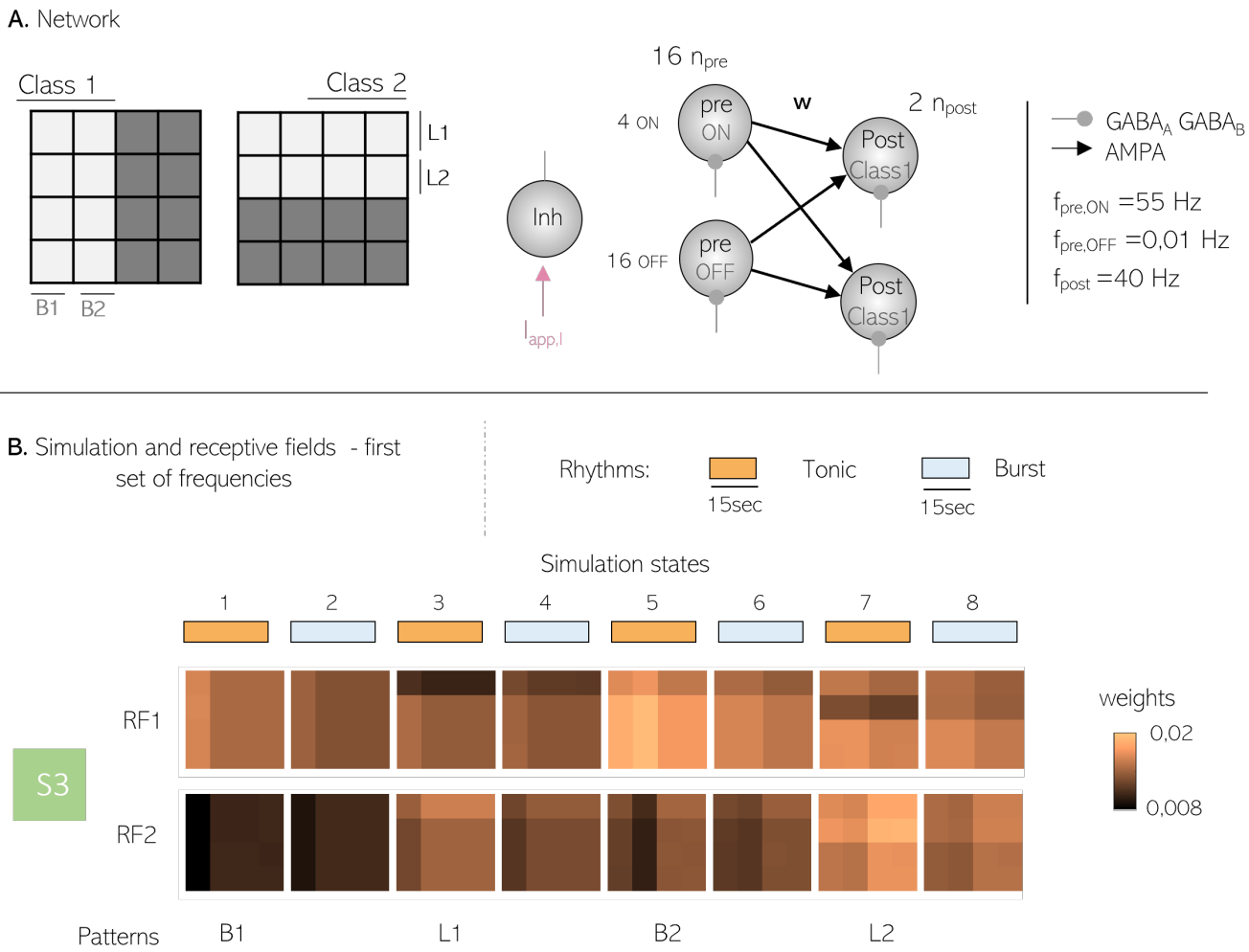

Figure 5.11 – **Two classes of patterns with overlap**: **A.** The two classes of patterns are composed respectively of the two first bars and two first lines. Two output neurons are considered, one for each class. **B.** Weights of active pixels on the wrong post neuron are highly depressed compared to the potentiation on the good neuron

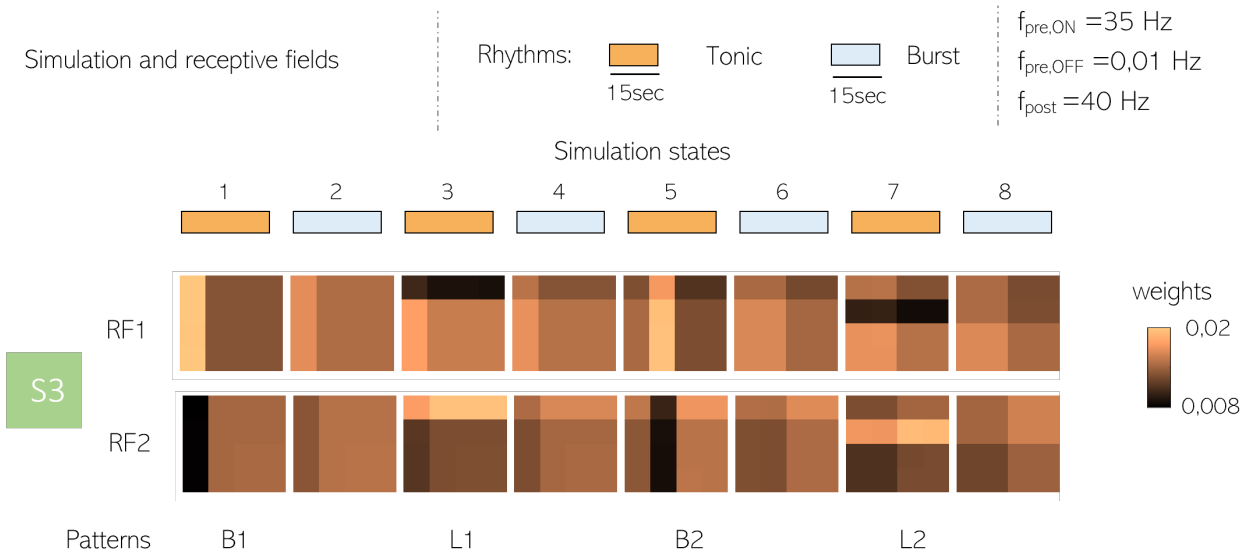

Figure 5.12 – **Reduced frequency to avoid high depression** : With f_{pre} equals to 35Hz, the tonic depression convergence of w is lower, leading to a lower overall depression

corresponding neuron output.

With these two implementations of the same plasticity rule leading to completely different results, we can see the importance and relevance of parameterization in task design.

5.3 Learning phase using our parameterization: pixel encoding by spike correlation

Since we do not know what is going on in the brain and we are doing computational exploration, another learning protocol will be implemented. This protocol is inspired by one of Gjorgjieva et al. (2011)'s experiments, in which the hypothesis of pixel consolidation is not based on simulation frequency, but on spike correlation. Hence, to cause an increase in synaptic weight, the spikes of the pre-neurons will arrive a time Δt before the spikes of the post-neuron. We will call this causal activity. Conversely, to induce a decrease in synaptic weight, spikes from pre-neurons will arrive a time Δt after postsynaptic spikes. We call it anticausal activity. Causal activity will be used to encode ON pixels, and anticausal activity for OFF pixels.

In this section, we will use a lower frequency for pixel reinforcement than in the previous section. The presynaptic and postsynaptic frequencies of the good neuron output will also all be set to the same value since this is no longer the parameter determining pixel consolidation. The post neuron not matching the pattern will however be simulated with a frequency of 0.01Hz, as in all previous experiments. The free parameters to be redefined during this learning phase are the applied frequency and the Δt. This interval is chosen to give the greatest increase in calcium when neuron activity is causal. For this, we refer to the D parameter of the calcium rule model, corresponding to the time-delayed increase of calcium after a presynaptic spike. The point at which the addition of calcium peaks will be greatest is when the postsynaptic spike arrives a time D after the presynaptic spike. As this D parameter is 9.54, we round off our Δt to a value of 10sec.

When we applied the calcium rule to this new way of learning, we realized that the minimum frequency to be imposed on neurons is 15Hz for the causal activity to start leading to potentiation. However, this firing rate in anti-causal activity already leads to strong depression. So we are still

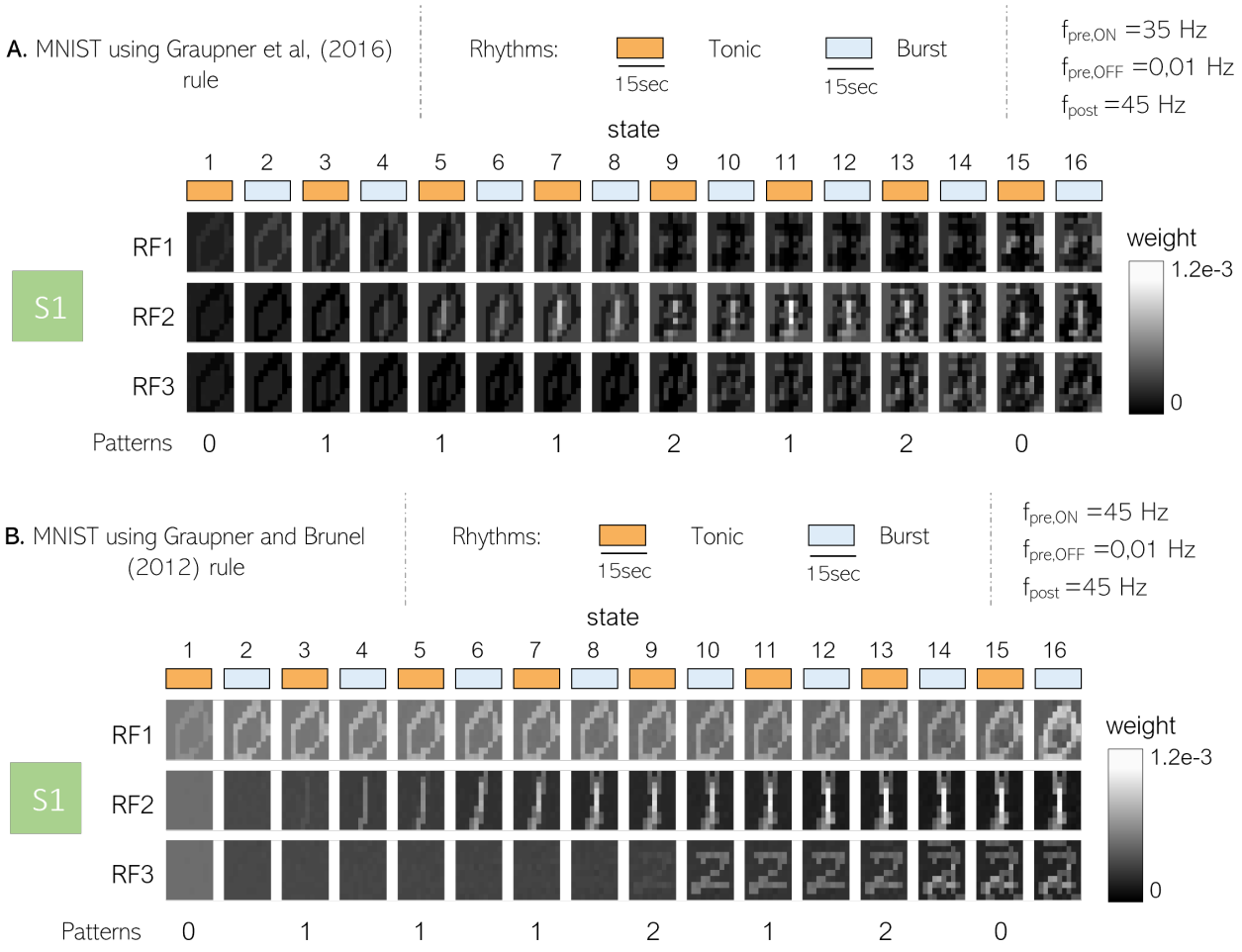

Figure 5.13 – **MNIST digits task: With the parametrization of Graupner et al. (2016) used in this project. For the RF1 (associated with digit 0), when other digits are presented, depression occurs. With the rule of Graupner and Brunel (2012), we see a clear appearance of each digit for each corresponding RF**

confronted with the *limitation B* identified in overlapping patterns.

There are several possible solutions to this limitation. They will be divided into 2 categories, the first being the modification of the calcium rule parameters and the second being the use of another plasticity model, namely the pair-based model.

5.3.1 Solution 1: Modification of the calcium model parameters

Concerning the internal parameters of the calcium model, one possible solution to the problem is to change the value of the depression convergence threshold, Ω_d. This solution can also be approached by decreasing the time of the tonic state, as the depressant weights would have converged to a lower value. However, this does not seem particularly meaningful from a physiological point of view. Replacing Ω_d with a higher value was therefore evaluated on learning 4x4 overlapping patterns. This implementation brought almost no change to the RF. On the contrary, the RF is less significant because the difference between the synaptic weight values of the ON and OFF pixels is smaller than before.

Another solution could have been to reduce the parameter $C_{mathrmpost}$, the value of the calcium increase following a postsynaptic spike. This is set at 1.62, which is quite high in the depression zone of calcium oscillations (between 1 and 2). This parameter could have been reduced either below the depression threshold or to a value slightly higher than the depression threshold, still causing depression, but less severe than previously. This keeps the "positive" side of pixel overlap less consolidated than pixels unique to a pattern. This would also potentially have led to a solution to our *limitation A*, or at least to a higher value of postsynaptic frequency leading alone to potentiation.

5.3.2 Solution 2: changing the synaptic plasticity model

Here, we abandon the calcium model in favor of the pair-based model. This involves checking the evolution of early weights in causal and anticausal activity. The frequencies chosen here are 10Hz and the Δt is 10sec, as before. If we observe the impact of causal and anticausal activity on the "good" neuron output (associated with the pattern presented), it conducts, as intended, to an increase in w for ON pixels and a decrease in w for OFF pixels. For the "wrong" output, simulated with a frequency of 0.01Hz, the value of w does not vary for all pixels. This is logical, as there is no longer any notion of causality, and both have a firing rate of 10Hz, effectively leading to no change in early weight.

This learning mechanism is implemented in a neuronal circuit, with 4x4 overlapping patterns. On the RF we observe that the pixel overlap does not deconsolidate, but the receptive field is indicative of the patterns learned for each neuron.

5.4 Testing phase using our parameterization

Most experiments in the literature also include a post-training network testing phase. This phase will also be run on our protocol. The test phase serves as an additional "validation" step, in addition to the RF. The most commonly used validation method is pattern recognition, where the post-neuronal response is compared with a threshold. The threshold is set at 20Hz, and the pattern is considered learned when this frequency is exceeded. This threshold allows to ignore the noise and to be sure that the activation of the post neuron is indeed in response to the activation of the pattern associated with it.

However, the mechanisms implemented to prevent transmission lead to a "trade-off" in the test phase. Indeed, the pattern recognition phase is precisely based on the fact that when pre-neurons with high enough synaptic weights are stimulated, it generates synaptic transmission, enabling a response in the form of action potential generation from the postsynaptic neuron. Here, given that this transmission

is prevented when a certain number of pixels encoded at a certain frequency are presented, we are going to play on these parameters to obtain a response.

In order to generate synaptic transmission, either the frequency of pixel activation or the number of activated pixels in a class must be increased. A combination of the two is also possible. Given that our synaptic weight always arrives at the same maximum consolidation value (the w of strengthened pixels varying only between 0.5 and 0.8 and the l being locked at 0.08), the learning protocol is of little importance in this case. We will take here the weights matrix obtained when training the class of patterns made up of 2 bars (on a 4x4 pixel grid).

The results show that if we keep the activation frequency at 55Hz, 6 active pixels of a class are required for a postsynaptic response above the threshold. In the opposite case, if we keep only 4 pixels active, the frequency to be applied to these 4 neurons is around 90Hz. Logically, the greater the number of active pixels in the pattern class, the higher the synaptic current received, and therefore the higher the response in terms of firing rate. The same applies to higher frequencies.

Part IV

Conclusion and perspectives

Chapter 6

Conclusion and perspectives

6.1 Thesis summary

With the objective of understanding the link between activity switches and memory consolidation, my project is based on the use of biophysical models in memory tasks. More precisely, its aim was to parameterize a protocol for analyzing learning as a function of different brain states through computational neuroscience.

The results of this research question are as follows:

1. Firstly, during the first stage of protocol design, we realized that each article had its own way of designing the experiment. A checklist was drawn up to identify common features and tools. A choice of frequencies also had to be specified to avoid the consolidation of neutral pixels.

2. Having parameterized the network as we saw fit, we tested it on a simple simulation. During this simulation, we observed a first phenomenon that was not consistent with our approach to consolidation: the transmission of spikes. This spike transmission refers to the increase in postsynaptic frequency when the synaptic weight reaches a certain value. Given that the frequencies were chosen to induce the desired plasticity, i.e. potentiation for ON pixels and depression for OFF pixels, the increase in postsynaptic frequency overturns this parameterization. As a result, a phenomenon of increased synaptic weight also occurs for presynaptic neurons not activated during pattern presentation. This is known as overconnectivity, as all connections are potentiated regardless of the pixel considered.

This spike transmission could be avoided via two main mechanisms:

- The implementation of a ceiling on the late weight, which can refer to the maximum capacity of the synapse.
- The implementation of a homeostasis mechanism to regulate neuronal activity according to the stimuli received.

3. Once our parameterization was complete, including the first spike non-transmission mechanism, the focus was on pattern consolidation with the introduction of pattern classes. A first approach without overlap was carried out. We observe a unique consolidation of the pixels making up the patterns, which shows a result consistent with learning. A second approach with overlap was then carried out, first with simple patterns and then with 3 digits from the MNIST dataset.

The results suggest two possibilities for consolidating overlapped pixels: Either their consolidation on the RF of each neuron output is done in the same way as the ON pixels. This results in a clearly

distinct RF representative of the patterns or pattern class associated with that neuron. However, in the testing phase, if only the overlapped pixel is activated, both outputs will activate simultaneously. It is as if all patterns with this overlap pixel could be identified by it alone. Either there is a partial consolidation of the overlap pixel, leading to a less distinct RF, whose highest synaptic weight values will be those corresponding to the pattern's single pixels. However, in the testing phase, if only the overlap pixel is activated, neither of the two output neurons will activate. In the same way as a human being, the network will need the additional activation of a pixel unique to the pattern to be able to predict the pattern presented to it.

Therefore, the question of the right learning method remains open and merits further investigation. The results of this thesis can serve as a computational tool for other researchers wishing to design their own tasks and study learning mechanisms.

6.2 Perspectives

6.2.1 Combining plasticity rules to represent biological mechanisms

A promising perspective of my work is to explore different synaptic plasticity rules to improve the representation of biological reality in our models. The aim would be to develop plasticity implementations that accurately combine biological processes. We have already begun to address this perspective by exploring the mechanism of homeostasis to regulate neuronal activity.

However, the field of synaptic plasticity research is highly complex and the exact biological mechanisms of plasticity and learning are not fully understood. The question that arises if we go further in this direction is: how can we combine these plasticity rules in our models? Which rules should we choose to get the best results? Moreover, the introduction of new plasticity rules would also entail an increased need for parameterization, adding another dimension of complexity to our work...

6.2.2 Impact of parameterization

Another important perspective highlights the crucial role of parameterization in plasticity rules. We found that a considerable amount of time had to be devoted to finding the most appropriate parameters to ensure coherent logic in the learning process.

This observation can be interpreted in two different ways:

On the one hand, this requirement for precise parameterization can be seen as an inherent fragility of the models, requiring a specific set of parameters to function optimally. Impressively, even slight variations in plasticity parameters can lead to completely different results. The question then arises as to whether this parameter sensitivity is physiological or not. In this case, it would be essential to continue accumulating more results to determine a solid consensus on protocols and establish benchmarks, as is done for standardized tasks such as MNIST

On the other hand, it is possible to envisage that each configuration of parameters leads to a different situation, but that these situations all occur in the brain under the influence of various external parameters or neuromodulators. For example, the level of calcium required to trigger synaptic plasticity would not be fixed, but modulated by neuromodulators such as dopamine. So our emotional state, such as being in a good mood, could influence the pattern of parameterization and, consequently, consolidation.

6.2.3 Combining results at multiple neuroscience interfaces

There are advantages and disadvantages in every field, whether cognitive or computational neuroscience. In neuroscience, there are well-known and classified tasks, but there can be a degree of subjectivity in assessing memory scores and reaction times. These measures often depend on the researchers' interpretation and can vary according to the criteria chosen. Despite this, cognitive neuroscience provides us with a solid basis for studying the mental processes and neural correlates associated with memory.

Computational approaches offer increased flexibility by allowing controlled manipulation of experimental parameters and variables. This makes it possible to run computational simulations and explore a wide range of scenarios. However, computational approaches require accurate modeling of biological mechanisms to be reliable and representative. Yet the complexity of biological systems imposes additional modeling challenges.

By combining these approaches, it would be possible to gain a deeper understanding of the mechanisms of memory and learning, drawing on the strengths of each field.

Part V

Appendix

Appendix A

Triplet rule experiment

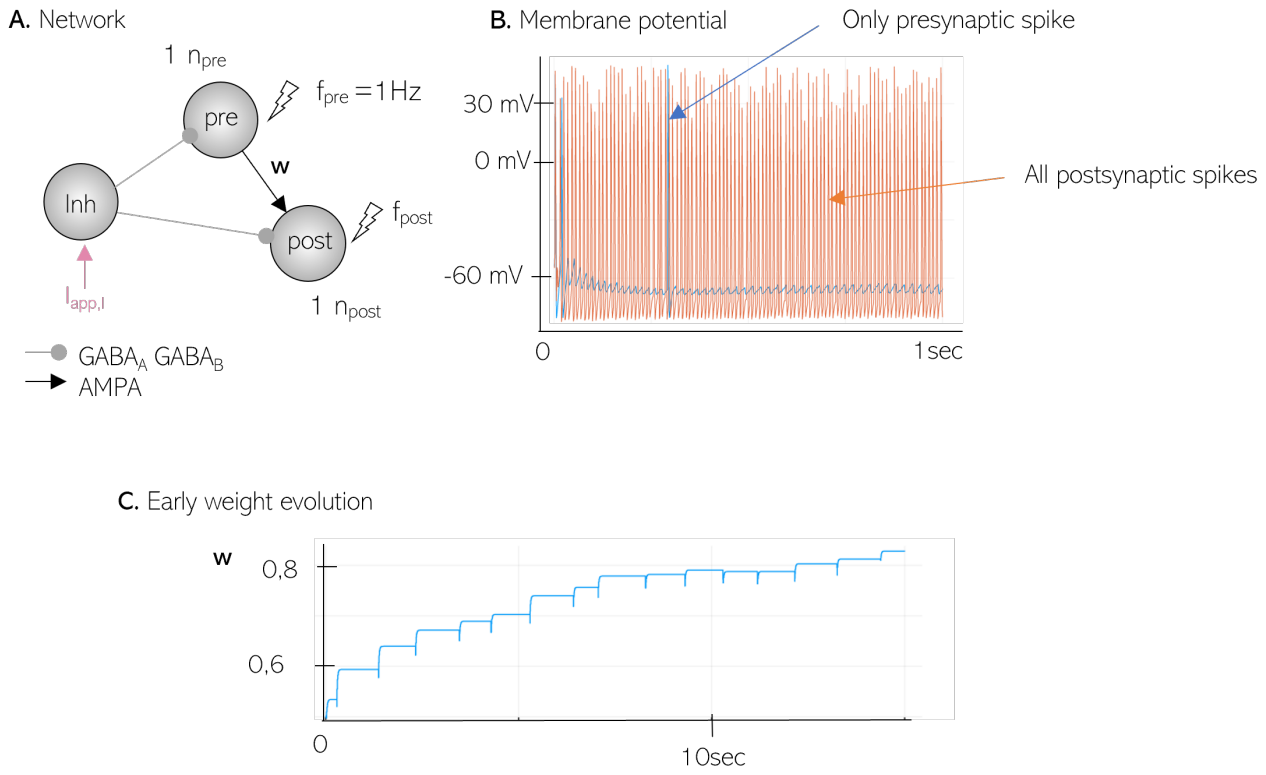

Figure A.1 – **Triplet frequency experiment**: Potentiation of synaptic weight, regardless of the value of the presynaptic frequency

Appendix B

Literature review - extended versions

B.1 GURUNATHAN 2020

B.1.1 Title

"Spurious learning in networks with Spike Driven Synaptic Plasticity", (Gurunathan and Iyer, 2020).

B.1.2 Goal

In this article, they used the SDSP (spike-driven synaptic plasticity) to study the spurious and incomplete learning of patterns in SNNs (Spiking Neural Networks). Their goal was to use simple network architecture and simple patterns to better understand the rule, which is not widely used at the moment. The SDSP is derived from the STDP rule, where the weight of a synapse is increased when a spike from a postsynaptic neuron occurs after a presynaptic one. In the SDSP rule, the change in weight does not depend on the timing of spikes but on the state of the postsynaptic membrane potential when a presynaptic neuron spikes. However, the learning is not straightforward as in the STDP rule, where more input current increase the probability of a postsynaptic spike, increasing weight.

The learning here depends on a probability ρ of the postsynaptic membrane potential V_m to reach a certain voltage threshold V_{th}^w when a pattern is presented, according to the following equation

$$W = \begin{cases} W + a, & \text{if } V_m \geq V_{th}^w \\ W - b, & \text{otherwise} \end{cases}$$

With a, the increment value, and b, the decrease value, such that a>b. However, the probability of the membrane potential is not proportional to the amount of input current reaching the output neuron. Thus, they introduce the notions of *incomplete* and *spurious* learning. Spurious learning is associated with *false positive* learning. This is defined as a large increase in weight even when the input current is low, due to a large probability. Incomplete learning, inversely, reflects the cases when there is no learning where it should normally happen. These 2 incorrect learning depend on the parameters of the model. This paper aimed to find out the impact of two parameters on spurious and incomplete learning, namely the voltage threshold V_{th}^w and the time membrane constant τ_M. The latter is a parameter of the neuron model used (LIF) and corresponds to the "rate at which the membrane potential decays towards its resting potential in response to a small input current".

B.1.3 Experiments

They did five experiments, the first one aimed to show how the network works with simple data, and the following ones were focusing on the understanding of spurious learning with the plasticity rule.

First experiment specific features and methods:

- *Patterns* : 5 random patterns on a 3x3 grid with different overlaps. Each pattern is composed of 5 inactive and 4 active pixels and is associated with 1 output neuron, which brings the total to 5 output neurons.
- *Dataset*: The datasets for the learning and test phase are generated from the 5 initial random patterns with different frequency spike trains. In total, 2000 training patterns and 100 test patterns are obtained.
- *Input neuron frequencies - f_{pre}*: Poisson spike trains of high (30Hz) and low (2Hz) frequency are respectively assigned to active or inactive pixels.
- *Output frequencies - f_{post}*: The first experiment is composed of 5 output neurons: a high-frequency spike train of 400Hz will be used for the output neuron associated with the presented pattern ("good" output), and a low-frequency spike train of 20Hz for the 4 other ("wrong") output neurons.
- *Simulation*: Each pattern runs for 400 ms and "between them, all voltages and current traces are reset"
- *Validation method*: Check of the pattern (in testing phase): The pattern associated with the output neuron that fires the most spikes is considered as the pattern predicted by the network. They obtained a mean accuracy of 99.97%

In the four other experiments, they took

- *Patterns*: 1 output neuron, encoding a pattern class. The pattern class in this article represents the entire grid and is composed of 2 patterns. This is to specifically study spurious learning. The pattern C^+ will be presented with a signal T^+, and C^- with a signal T^-, as explained in the network architecture. These categories are just representing the patterns that are supposed to be consolidated (C^+), associated with a high frequency, or not (C^-).
- *Dataset*: They used 2000 training patterns during the training of the network. Then, the network is tested on 100 testing patterns.
- *Input neuron frequencies - f_{pre}*: Poisson spike trains of high (30Hz) and low (2Hz) frequency are respectively assigned to active or inactive pixels.
- *Output frequencies - f_{post}*: 400Hz will be used as the T^+ signal (assigned to the C^+ pattern) and 20Hz as the T^- signal (for the C^- pattern).

Second experiment: For which values of V_{th}^w and τ_M (the time membrane constant) do spurious or incomplete learning (grouped under the notion of "incorrect learning") occur? The network is run with different values of these two parameters, and they used two ways to check the incorrect learning: The first one is focused on the ratio of patterns C^+ and C^- learned. They look at the frequency of spikes fired by the output neuron for the two classes of patterns and check if the difference between

the learning of C^+ and C^- is significant. They can also gather the results and have a fraction of the pattern with incorrect learning.

The second one focuses on the learned weights on a receptive field. The receptive field is built by looking at which portion of weight in the wrong category has learned (spurious learning) and those in the good category who did not learn. They showed the weights in the receptive field with different colors, corresponding to the different ranges of values of the weights.

Third experiment: In this experiment, they find out the cause of spurious learning. As weight changes depending on the probability ρ (that $V_m \geq V_{th}^w$), they compute ρ as the number of time steps for which $V_m \geq V_{th}^w$ divided by the total number of time steps. They first prove that high values of ρ do not always correspond to high input into the neuron. Then, they study the impact of this phenomenon on the results, for different parameter values.

Fourth experiment: Can the implementation of a learning stop condition avoid spurious learning? A stop learning condition will be useful if the correct learning of the weight is happening before the spurious learning. In order to answer this question, a time lag between correct and spurious learning is done with different parameter values. Therefore, in some cases where time lag is sufficient, a stop learning condition can actually be utilized.

Fifth experiment: In this experiment, the period of learning is tested. A longer training time is implemented by taking 5000 patterns instead of 2000. They checked the fraction of the pattern with incorrect learning and compared it to the second experiment.

B.1.4 Conclusion

All those experiments have the goal to understand how the network is learning and how the neurons behave with the SDSP rule, and especially how the evolution of weights is directed by the values of the parameters. They made a review of V_{th}^w and τ_M parameters that were impacting this rule, for SDSP users to be able to use it properly.

This article has given me a better overview of the different patterns that can be taught to a circuit. Indeed, it proposes a simulation based on a pattern class comprising several patterns, thus showing that not all patterns are uniquely associated with a neuron output. The receptive field proposed is also interesting, as it demonstrates the usefulness of using classes to better understand consolidation mechanisms within a single neuron as a function of imposed frequencies. The first simulation carried out also informed me about network testing methods, and in particular about prediction and accuracy calculation.

B.2 ZENKE 2015

B.2.1 Title

"Diverse synaptic plasticity mechanisms orchestrated to form and retrieve memories in spiking neural networks", (Zenke et al., 2015).

B.2.2 Goal

The goal of this paper is to show that a combination of different plasticity rules is sufficient to form and recall assemblies in spiking neural networks. In particular, it concerns here a spiking recurrent

neural model of inhibitory and excitatory neurons.
The different types of plasticity considered are the Hebbian homosynaptic and non-Hebbian (heterosynaptic and transmitter-induced) plasticity, combined with structural, short-term, and homeostatic plasticity. The latter are used to represent slow homeostatic changes and consolidation.

B.2.3 Experiments

Orchestrate plasticity to form stable cell assemblies
The paper first discusses the concept of orchestrated plasticity in the formation of cell assemblies in a recurrent neural network. Orchestrate plasticity reflects a model that contains different forms of plasticity. The authors describe the unstable formation of cell assemblies occurring through Hebbian plasticity at excitatory synapses. Network architecture :

- *Network*: 5120 LIF neurons: 4096 excitatory and 1024 inhibitory randomly connected. Cell assemblies are of 400 excitatory neurons.

Stability is restored through the interplay of homosynaptic (triplet STDP), transmitter-induced potentiation, and heterosynaptic depression. Stability refers to a state in which the firing rate of neurons in the network remains relatively constant over time. The authors show through simulations that the network reaches two stable fixed points of weight dynamics, which correspond to the activity fixed points of neurons in cell assemblies. The firing rate at the stable states depends on the initial synaptic weights and on the strength of heterosynaptic and transmitter-induced plasticity. Network architecture for bistability:

- *Inputs*: 1 postsynaptic neuron received simultaneous inputs from an active pathway composed of 80 presynaptic neurons activated at 10 Hz and a control pathway with 80 background neurons at 1 Hz.
- *Protocol*: Localized stimulus that changes its position on average once every 20 s
- *Results*: Mean firing rate of a postsynaptic neuron over time
- *Validation method*: Postsynaptic neuron develops a localized receptive field accorded to its stimulus

Assembly formation and recall
This experiment investigate whether inhibitory and excitatory plasticity could work together to enable stable assembly formation and recall.
In this neural network model, each excitatory neuron received input from both other neurons in the network and from sensory neurons that represented specific locations in space. These small patches of sensory neurons are defining the receptive field of the excitatory neuron. The network was then stimulated with different patterns of input, and the plasticity allowed certain groups of neurons to become more strongly connected to each other, forming assemblies that responded to specific input patterns.

- *Network*: Composed of 5120 LIF neurons, including 4096 excitatory and 1024 inhibitory neurons randomly connected, with an overall connection probability of 10%.
- *Input*: Excitatory neurons receive stimulation from an external input. The inout is a 64x64 Poisson units, where cells from a circular area (R=8) are projected to an individual input neuron. The center of the circle is randomly selected into the input space and associated with one

excitatory neuron. All input neurons stimulated during activation of the circular area, go on to excite the excitatory neuron corresponding to the center of the circle.

- *Stimulation/Patterns*: The stimuli are 4 different geometric patterns, randomly presented and alternated with periods without stimulation. The patterns can overlap, which means that some neurons corresponding to the first pattern, can also fire for another pattern.

- *Protocol*: Only one phase with ongoing plasticity throughout the phase, allowing synapses to evolve freely. This phase is "separated" into 2 parts, wherein the first one, the network is stimulated by applying "repeatedly and stochastically one of four possible full-filed input patterns". Then in the second part, the network is stimulated with partial input (up to three-quarters of the input field can be occluded). The identity and duration of the stimulus, as well as the time between successive stimuli, were randomized. However, the intensity of the stimulus remained constant.

- *Results* : The activity they record is the mean activity of all neurons *responding* to the stimulus

- *Validation method* : they count the postsynaptic neuron as coding for the stimulus when its stimulus-evoked firing rate is $\geq$ 10Hz

Results show that these assemblies could maintain their connection even after the input had stopped, and could be reactivated later by partial input that matched the original pattern. The authors found that the assemblies were stable over long periods of time and did not degrade and that the network could spontaneously transition between different assemblies without external input. The network shows working memory states that correlate with the learned patterns. Despite distractor stimuli and ongoing plasticity, these states are stable.

By looking at the different timescales of plasticity mechanisms and how they contribute to stability in the model, they also proved that this stability is a result of the coordinated interplay of multiple plasticity mechanisms on different timescales.

Other small experiments were done to see the effect of simulation parameters on learning. For example, one experiment aimed to see the effect of individual plasticity on the network (by blocking it). Another focused on increasing the learning time or adding new learning patterns.

B.2.4 Conclusion

This article allowed me to see patterns made with particular motifs (not just randomly activated pixels). Another interesting point is their test phase, where patterns are reactivated in full but also partially (up to three-quarters of the input field can be occluded). As a validation method, they do not just compare frequencies with each other to find the post neuron with the highest frequency but consider that the frequency must exceed a certain defined threshold. It also highlights the importance of having several plasticity mechanisms, taking into account both short- and long-term changes, in order to better represent reality.

B.3 CAPONE 2019

B.3.1 Title

"Sleep-like slow oscillations improve visual classification through synaptic homeostasis and memory association in a thalamo-cortical model", (Capone et al., 2019).

B.3.2 Goal

The main idea of this paper is to explore the role of slow oscillations (SO) during sleep, and how they contribute to memory consolidation and restoration, from a computational point of view. Experimental studies have shown that this oscillation activity is beneficial for memory consolidation and task performances optimization.
The authors investigate the impact of deep-sleep-like slow oscillation activity on a simplified thalamo-cortical model that performs tasks related to handwritten digit images. They demonstrate the interesting effects of this activity on the model's performance in encoding, retrieval, and classification tasks. They used Adex neurons in a thalamo-cortical network model and the STDP (or pair-based) for the plasticity rule.

B.3.3 Experiments

Network architecture and protocol

- *Patterns*: The patterns shown to the network are handwritten digits from the MNIST dataset, including 28x28 pixels images. An algorithm is used to transform each image into a vector of 324 binary features. The number of images will be specified for the 2 different runs of the paper.
- *Network*: Number of thalamic neurons $N_{th} = 324$. Number of cortical neurons $N_{cort} = 20$ neurons for each image. Number of inhibitory neurons: $N_{in} = 200$ and $N_{re} = 200$, corresponding respectively to the cortical and the thalamic inhibition. All neurons are interconnected.
- *Frequencies*: The frequencies of input signals vary according to the stimulation and the target population. The thalamic neurons receive a visual stimulus, formed by a Poisson spike train with an average firing rate of $30kHz$ when the element of the vector is 1. An external stimulation ("contextual signal") provides a $2kHz$ Poisson spike train to cortical neurons.
- *Protocol*: The protocol is divided in 4 successive phases : *Training*, *pre-sleep testing*, *sleeping (slow-oscillation)*, *post-sleep testing*:
  - *Training phase*: In the training phase, the thalamic population receives a visual stimulus. More precisely, this stimulus is a Poisson spike train with an average firing rate of 30Hz only when the element of the vector is 1. At the same time, an external stimulus is applied to a subset of 20 cortical neurons, which allows them to code for this specific image. The STDP rules change the weight of connections in the network.
  - *Testing*: Images are presented without the contextual signal on the cortical neurons. Only the thalamic neurons are stimulated. The success of this phase is achieved when the population of cortical neurons responding to this stimulation is the same as in the training phase.
  - *Slow oscillation (SO) phase*: To obtain the slow oscillations of this phase, the parameters of the model are modulated. Especially, a non-specific stimulus of low frequency (700Hz Poisson spike-train) is provided inside the cortex. The network is disconnected from sensory stimuli, and driven by its internal activity. This phase lasts 600 seconds.

First set of run
In this first set of runs, 9 images are presented to the network in the training phase. More precisely, 3 instances for each chosen digit (0,1,2) are used. They demonstrate that the slow oscillations enable the creation of stronger synapses between groups of neurons belonging to the same digit category.

The importance of cortico-thalamic connections during this activity is also demonstrated. Indeed, the SO of the network leads to the spontaneous event of *Up states* in the cortical population. Up states refers to a high firing rate regime of a subset of neurons. This particular event causes the activation of thalamic neurons, similar to those responsible for activating the population in the retrieval phase. It's called *top-down prediction*. When thalamic neurons are active, they stimulate all cortical neurons associated with similar thalamic input.
This demonstrates that thanks to the cortico-thalamo-cortical pathways, populations have a tendency to recruit other populations with corresponding thalamic representations.

Second set of run
In the second group of runs, the network was presented with images from all ten-digit classes in the MNIST dataset, with three examples per digit. A total of 30 training instances are randomly picked from an initial dataset of 250 images. The goal here was to prove the post-sleep improvement for the classification task. The classification was achieved by identifying the pattern associated with the neuron with the highest firing rate. The accuracy of the classification task goes from 58% to 64% after sleep.

B.3.4 Conclusion

This article introduced me to different protocol variants. In this case, a slow oscillation phase is added to the testing and learning phases. In addition, the patterns use several output neurons to encode a single image. The network validation method is therefore based on the response of the entire output population. Here, they use a fairly high pattern complexity with the MNIST dataset. However, as we can observe, it is also possible to select just a few digits from the dataset to train our network.

B.4 GARG 2022

B.4.1 Title

"Voltage-Dependent Synaptic Plasticity (VDSP): Unsupervised probabilistic Hebbian plasticity rule based on neurons membrane potential ", (Garg et al., 2022).

B.4.2 Goal

The authors of this paper propose a new unsupervised learning rule, *Voltage-Dependent Synaptic Plasticity* (VDSP), and test it by using a spiking neural network (SNN) for the recognition of handwritten digits (MNIST dataset). The motivation for this rule was mainly the memory requests for the use of the STDP rule, involving the storage of spike traces of both presynaptic and postsynaptic neurons. Conversely to the STDP, defined as the relation between the change in weight (Δw) (resp. *"weight conductance" in the paper*) and the time interval between pre- and postsynaptic spike (Δt), the VDSP is relating Δw to the presynaptic membrane potential at the moment when a postsynaptic spike occurs, $v(t_{post})$. To simplify the STDP rule by using only the presynaptic membrane potential $v(t_{post})$, the presynaptic neurons must be supplied with a constant positive current. This current allows the spike dynamics to be predicted.

The network and learning protocols for the classification task are described as follows:

- *Neuron model*: LIF input neurons and ALIF output neurons. The "A" stands for *adaptive* because an adaptation mechanism is included in the post-neurons to avoid the instability caused

by excessive firing.

- *Patterns*: The patterns showed for the classification task are 28x28 images from the MNIST dataset. The training set is composed of 60000 images and the test set contains 10000 images, different from those of the training set.

- *Network*: The number of input neurons equals the total number of pixels in an image, i.e. 784. The number of output neurons varies according to the experiment. The input neurons are fully connected to every output neuron.

- *Input*: The magnitude of the input current used to stimulate the input neurons vary according to the intensity of the pixel, but goes from a magnitude of 0 (black pixel) to 1 (white pixel).

- *Protocol*: During the learning phase, the images are presented to the SNN for 350ms. Every instance of digits is shown without a wait time between them. During the testing phase, the synaptic weights are fixed and the samples from the test set are proposed to the trained network.

- *Results/Validation method*: After the learning phase, a weight matrix for each of the ten output neurons is obtained and represented on a receptive field. To obtain the accuracy of the network in the recognition of patterns, a testing phase is done. The digit predicted by the network is assigned based on the output neuron class that had the highest number of spikes during the presentation of the sample. Accuracy is then obtained by comparing this predicted digit with the digit actually presented.

B.4.3 Experiments

First experiment To evaluate the efficiency of the VDSP rule in pattern recognition, they conduct a performance analysis by recognizing handwritten digits. In this experiment, the number of output neurons is equal to the number of digits of the MNIST dataset, i.e. 10. The accuracy they obtained for the recognition is about 61.4%. The reason for the approximation is the utilization of five distinct initial conditions during the experiment.

Second experiment
Here, they test the impact of the network size and training time on the efficiency of the implemented learning rule. The network size is modified by changing the number of output neurons, ranging from 10 to 500. The training time is modulated by increasing the number of epochs (the number of times the dataset is run in its entirety) until 5. The accuracy achieved for 50 neurons after 3 epochs is about 84.74%. For 500 neurons and a training time of 5 epochs, the accuracy increase until reaching about 90.56%.

B.4.4 Conclusion

This article uses a protocol quite similar to that of (Capone et al., 2019). However, the validation phase is based on the cumulative frequency of all output neurons coding for the same digit, when several neurons are associated with 1 digit. Interestingly, they also show synaptic weights on a receptive field, giving a clearer, more visual representation of what is going on in our network. We note that this paper also uses pattern classes, as there is only one output neuron each time.

B.5 GJORGJIEVA 2011

B.5.1 Title

"A triplet spike-timing–dependent plasticity model generalizes the Bienenstock–Cooper–Munro rule to higher-order spatiotemporal correlations", (Gjorgjieva et al., 2011).

B.5.2 Goal

The main goal of the research is to explore and overcome the limitations of the BCM learning rule by introducing the triplet model, which considers sets of three spikes instead of pairs. Indeed, the BCM rule is not able to account for the timing of pre-and postsynaptic spikes and has difficulty distinguishing input patterns based on temporal spiking structure. The researchers demonstrate that the triplet model improves the explanation of synaptic plasticity. The triplet model also offers insights into the role of higher-order correlations in neural coding.

B.5.3 Experiments

Some network features are common for all experiments, and will be specified in each of their descriptions:

- *Network*: Feedforward network with n_{pre} input neurons as Dirac delta spike train and 1 output neuron.
- *Input*: The number of patterns differs in all experiments. The first 10 are rate-based patterns, defined by different input firing rates. The second 10 are correlated-based patterns, associated with different correlation strengths between groups of input neurons in a pattern. The last 2 patterns are "third-order correlation"-based patterns. These patterns are defined by 3 specific input neurons (spatial correlation) having a spike exactly at the same time during the pattern presentation (temporal correlation).
- *Protocol*: Every 200 ms, the network was presented with a new randomly-chosen pattern.

First experiment: Selectivity with Rate-Based Patterns
To examine the level of pattern selectivity of the feedforward network, the authors designed the following experiment: 100 input neurons are divided into groups of 10, with each group coding for a specific pattern. The patterns are rate-based patterns, which means they differentiate by their input's firing rates. The input patterns presented to the network are 10 Gaussian profiles with different ratios of the background firing rate (r_{min}) to the peak firing rate (r_{max}), and different standard deviations (SD), resulting in different amounts of overlap. In this experiment, r_{min} was between 0 and 10 Hz, r_{max} was set at 55Hz and the SD could vary from 5 to 15.

The amount of selectivity of the postsynaptic neuron is computed. They observed that higher selectivity is associated with higher values of the ratio (r_{min}/r_{max}) and lower standard deviation (SD).

Second experiment: Selectivity with Correlation-Based Patterns
In this context, correlation-based patterns refer to patterns with identical firing rates but varying degrees of correlation strength. The firing rate of all inputs is thus set to 10Hz. There are 100 input neurons, each group of 10 coding for 1 pattern, as in the first experiment. The correlation strength was done by selective potentiation of a group of inputs. Weight of 10 input from 1 pattern potentiated while the other depressed at each time we show a new pattern.

The calculation of the average change in synaptic weights, in the function of the firing of the post-synaptic neuron, is performed for various levels of correlation among the inputs. The results revealed that the network with a higher correlation displayed a larger region of potentiation.

Third experiment: Selectivity driven by third order correlations
The goal is to prove that the selectivity driven by third-order correlations of input can be achieved by using the triplet rule, but not the pair-based. Two patterns are presented to the network: P1 and P2. A total of 6 input neurons is used. The patterns consist of 2 pools of 3 input neurons. The first pattern P1 contained a third-order correlation in inputs 1 to 3, while inputs 4-6 had no third-order correlations. For the second pattern P2, it is the opposite. Inputs 4-6 comprised third-order correlations.

The analysis focuses on how the probability of Pattern 1 winning varies with the probability of presenting this pattern to the network, and also with the level of input correlation. They examined the evolution of weights for the 6 input neurons to determine the winning pattern. Weights are increased due to the third-order correlation and decreased in the other case, which reveals the winning pattern according to the group of neurons with higher weights.

B.5.4 Conclusion

This article has shown me that pixel consolidation can also be achieved in ways other than frequency-based association. Here, patterns can be defined in several ways. Either by a priori reinforcement of the connection between several input neurons or by a simulation pattern made up of correlated spikes for the inputs corresponding to the pattern we want to consolidate.

B.6 DELAMARE 2022

B.6.1 Title

"Intrinsic neural excitability induces time-dependent overlap of memory engrams", (Delamare et al., 2022).

B.6.2 Goal

The main goal of the study is to understand the mechanisms underlying the formation and linking of memory engrams in neural circuits, with a focus on the role of synaptic plasticity and intrinsic excitability. Indeed, memories are stored in neural ensembles called engrams, which are reactivated during memory recall. Engrams have been identified across multiple brain regions as the neural basis for memory storage and retrieval. They are defined as *" a subpopulation of neurons that is initially activated during the presentation of a stimulus, followed by transient physical and/or chemical changes that lead to its specific reactivation during memory recall"*.

The exact process behind engram overlaps, which are important for memory allocation, is still unclear. However, it has been suggested that intrinsic excitability, mediated by neural activity, may serve as a complementary mechanism for the formation of memory engrams.

For this purpose, the researchers developed a computational model that integrates synaptic plasticity and intrinsic excitability to explain the dynamics of overlapping memory ensembles. They are using a rate-based Recurrent Neural Network with feed-forward and recurrent connections and Hebbian plasticity and excitability for plasticity mechanisms.

B.6.3 Experiments

Description of the network and protocol used in this study.

- *Network*: The network is divided into the input layer and the main region. The input layer is composed of 30 neurons and is projected to the main layer, which contains 60 neurons. Weights are then initialized to form 3 diagonal blocks in the receptive field.
- *Inputs*: The inputs are one layer of neurons divided into 3 subsets, forming groups for different context presentations. Groups are formed by 10 consecutive neurons from the input layer.
- *Protocol*: Training and testing phases:
  - Training phase: Simulation of the network by presenting different contexts. One group of input neurons is activated by setting their firing rate to 4Hz. Each activation is repeated 20 times during 40ms, with an interstimulus interval of 150ms. The "active" threshold, where the neurons are classified as active, is set to 6Hz.
  - Testing phase (resp. *"memory retrieval phase"*: this phase test the ability of the network to do pattern recognition task. Some neurons from the assembly, that were tagged as active, are stimulated again during 40ms. The results are presented in the form of a firing rates graph..

Formation of a single memory engram
After showing the first context, only the firing rate of neurons associated with this context is above the active threshold. The weight matrix revealed that learning leads to the formation of an assembly of highly interconnected neurons. The memory retrieval phase is using only 4 of the 7 active neurons for pattern completion. It displays that memories can be retrieved even when stimulated by a partial signal. This finding demonstrates that activating a subgroup of neurons within the assembly is enough to stimulate other neurons in the same assembly due to robust intra-assembly connections.

Link of intrinsic neural excitability and overlapped memory engrams
To study the overlap of memory engram, another experiment is made. During the learning, 2 different contexts are shown to the network to form 2 different memories. The contexts are spaced by time intervals of 6h or 24h. The memory retrieval phase happens 24h after the last learning and consists in showing the 2 contexts, separated by 25min. The intrinsic neuronal excitability is added in this experiment such that after learning, the neural excitability of the neurons involved in the newly established assembly is enhanced.

They found that when the contexts are presented with a 6h interval, the two memories are stored using overlapping neural representations. This is not the case in 24h intervals. The overlap between the 2 assemblies can be quantified by the number of active neurons for both context recalls.

B.6.4 Conclusion

This article is characterized by a synaptic weight initialization process prior to learning. This step makes it possible to observe the impact of this initialization on consolidation. As for the patterns, no overlap is implemented and, as with those of (Capone et al., 2019; Garg et al., 2022), several output neurons represent the same neuron group. In the test phase, only certain neurons in the group are activated for simulation. The choice of these neurons is interesting in that it is made according to their activation, among the neurons considered to be active (whose firing rate is greater than a certain threshold).

With regard to plasticity, this study highlights the importance of considering not only synaptic plasticity but also intrinsic excitability in order to understand the mechanisms of memory formation and neuronal connectivity.

Appendix C

Supplementary figures

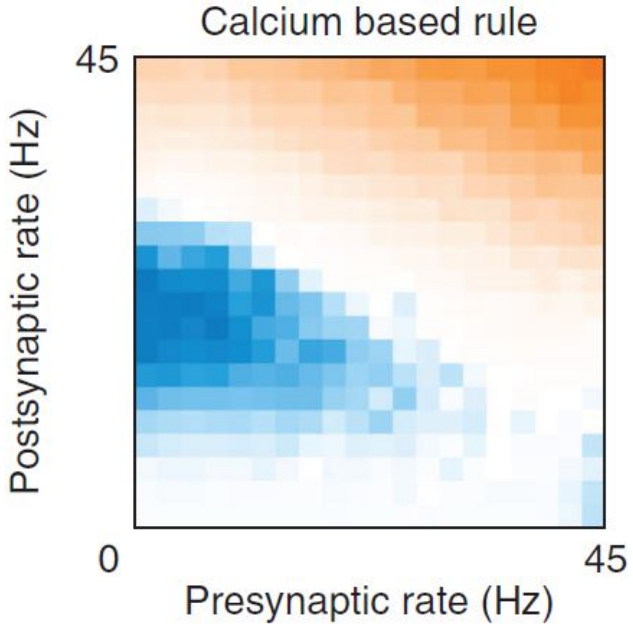

Figure C.1 – **Frequency exploration from Litwin-Kumar and Doiron (2014)**: Figure représentant les zones de dépression (bleu), non changement (blanc) ou potentiation (orange) du poids synaptique selon les fréquences pré et post synaptiques.

Bibliography

Abbott LF, Nelson SB (2000) Synaptic plasticity: taming the beast. *Nature Neuroscience* 3:1178–1183.

Abraham WC, Jones OD, Glanzman DL (2019) Is plasticity of synapses the mechanism of long-term memory storage? *npj Science of Learning* 4:9.

Anderson C, Craik F (1974) The effect of a concurrent task on recall from primary memory. *Journal of Verbal Learning and Verbal Behavior* 13:107–113.

Badin AS, Fermani F, Greenfield SA (2017) The Features and Functions of Neuronal Assemblies: Possible Dependency on Mechanisms beyond Synaptic Transmission. *Frontiers in Neural Circuits* 10.

Baltaci SB, Mogulkoc R, Baltaci AK (2019) Molecular Mechanisms of Early and Late LTP. *Neurochemical Research* 44:281–296.

Becker MFP, Tetzlaff C (2021) The biophysical basis underlying the maintenance of early phase long-term potentiation. *PLOS Computational Biology* 17:e1008813.

Beurrier C, Congar P, Bioulac B, Hammond C (1999) Subthalamic Nucleus Neurons Switch from Single-Spike Activity to Burst-Firing Mode. *The Journal of Neuroscience* 19:599–609.

Bi Gq, Poo Mm (1998) Synaptic Modifications in Cultured Hippocampal Neurons: Dependence on Spike Timing, Synaptic Strength, and Postsynaptic Cell Type. *The Journal of Neuroscience* 18:10464–10472.

Bi Gq, Poo Mm (2001) Synaptic Modification by Correlated Activity: Hebb's Postulate Revisited. *Annual Review of Neuroscience* 24:139–166.

Bosch M, Hayashi Y (2012) Structural plasticity of dendritic spines. *Current Opinion in Neurobiology* 22:383–388.

Bradley C, Nydam AS, Dux PE, Mattingley JB (2022) State-dependent effects of neural stimulation on brain function and cognition. *Nature Reviews Neuroscience* 23:459–475.

Butz M, Wörgötter F, Van Ooyen A (2009) Activity-dependent structural plasticity. *Brain Research Reviews* 60:287–305.

Buzsáki G (2010) Neural Syntax: Cell Assemblies, Synapsembles, and Readers. *Neuron* 68:362–385.

Capone C, Pastorelli E, Golosio B, Paolucci PS (2019) Sleep-like slow oscillations improve visual classification through synaptic homeostasis and memory association in a thalamo-cortical model. *Scientific Reports* 9:1–11.

Chistiakova M, Bannon NM, Bazhenov M, Volgushev M (2014) Heterosynaptic Plasticity: Multiple Mechanisms and Multiple Roles. *The Neuroscientist* 20:483–498.

Citri A, Malenka RC (2008) Synaptic Plasticity: Multiple Forms, Functions, and Mechanisms. *Neuropsychopharmacology* 33:18–41.

Clopath C, Büsing L, Vasilaki E, Gerstner W (2010) Connectivity reflects coding: a model of voltage-based STDP with homeostasis. *Nature Neuroscience* 13:344–352.

Cotman CW, McGaugh JL (1980) Synaptic Transmission In *Behavioral Neuroscience*, pp. 151–208. Elsevier.

Daoudal G, Debanne D (2003) Long-Term Plasticity of Intrinsic Excitability: Learning Rules and Mechanisms. *Learning & Memory* 10:456–465.

Debanne D, Inglebert Y, Russier M (2019) Plasticity of intrinsic neuronal excitability. *Current Opinion in Neurobiology* 54:73–82.

Debas K, Carrier J, Orban P, Barakat M, Lungu O, Vandewalle G, Tahar AH, Bellec P, Karni A, Ungerleider LG, Benali H, Doyon J (2010) Brain plasticity related to the consolidation of motor sequence learning and motor adaptation. *Proceedings of the National Academy of Sciences* 107:17839–17844.

Delamare G, Feitosa Tomé D, Clopath C (2022) Intrinsic neural excitability induces time-dependent overlap of memory engrams preprint, Neuroscience.

Deolindo CS, Kunicki ACB, Da Silva MI, Lima Brasil F, Moioli RC (2018) Neuronal Assemblies Evidence Distributed Interactions within a Tactile Discrimination Task in Rats. *Frontiers in Neural Circuits* 11:114.

Feldman DE (2020) Spike timing–dependent plasticity In *Neural Circuit and Cognitive Development*, pp. 127–141. Elsevier.

Fioravante D, Regehr WG (2011) Short-term forms of presynaptic plasticity. *Current Opinion in Neurobiology* 21:269–274.

Fon EA, Edwards RH (2001) Molecular mechanisms of neurotransmitter release. *Muscle & Nerve* 24:581–601.

Garg N, Balafrej I, Stewart TC, Portal JM, Bocquet M, Querlioz D, Drouin D, Rouat J, Beilliard Y, Alibart F (2022) Voltage-Dependent Synaptic Plasticity (VDSP): Unsupervised probabilistic Hebbian plasticity rule based on neurons membrane potential Publisher: arXiv Version Number: 6.

Gjorgjieva J, Clopath C, Audet J, Pfister JP (2011) A triplet spike-timing–dependent plasticity model generalizes the Bienenstock–Cooper–Munro rule to higher-order spatiotemporal correlations. *Proceedings of the National Academy of Sciences* 108:19383–19388.

Graupner M, Brunel N (2012) Calcium-based plasticity model explains sensitivity of synaptic changes to spike pattern, rate, and dendritic location. *Proceedings of the National Academy of Sciences* 109:3991–3996.

Graupner M, Wallisch P, Ostojic S (2016) Natural Firing Patterns Imply Low Sensitivity of Synaptic Plasticity to Spike Timing Compared with Firing Rate. *The Journal of Neuroscience* 36:11238–11258.

Gu J, Wang Z, Kuen J, Ma L, Shahroudy A, Shuai B, Liu T, Wang X, Wang G, Cai J, Chen T (2018) Recent advances in convolutional neural networks. *Pattern Recognition* 77:354–377.

Gurunathan A, Iyer LR (2020) Spurious learning in networks with Spike Driven Synaptic Plasticity In *International Conference on Neuromorphic Systems 2020*, pp. 1–8, Oak Ridge TN USA. ACM.

Hayashi Y, Majewska AK (2005) Dendritic Spine Geometry: Functional Implication and Regulation. *Neuron* 46:529–532.

Hebb Do (1949) *The Organization of Behavior: a Neurophysiological Theory* A Wiley book in clinical psychology. John Wiley.

Hodgkin AL, Huxley AF (1952) A quantitative description of membrane current and its application to conduction and excitation in nerve. *The Journal of Physiology* 117:500–544.

Holtmaat A, Svoboda K (2009) Experience-dependent structural synaptic plasticity in the mammalian brain. *Nature Reviews Neuroscience* 10:647–658.

Holz R, Fisher SK (1999) Synaptic Transmission In Siegel G, Agranoff B, Albers R, Fisher SK, Uhler MD, editors, *Basic Neurochemistry: Molecular, Cellular and Medical Aspects*. Philadelphia: Lippincott-Raven, 6th edition.

Jacquerie K (2023) Modeling brain-state dependent memory consolidation Ph.D. diss., Univeristy of Liège, Liège.

Jacquerie K, Minne C, Ponnet J, Benghalem N, Sacré P, Drion G (2022) Switches to slow rhythmic neuronal activity lead to a plasticity-induced reset in synaptic weights preprint, Neuroscience.

Jenkins JG, Dallenbach KM (1924) Obliviscence during Sleep and Waking. *The American Journal of Psychology* 35:605.

Knapp R, Rubenzik M, Malatynska E, Varga E, Roeske WR, Yamamura HI (2003) Neurotransmitter Receptors In *Encyclopedia of the Neurological Sciences*, pp. 602–614. Elsevier.

Lamprecht R, LeDoux J (2004) Structural plasticity and memory. *Nature Reviews Neuroscience* 5:45–54.

Lee SH, Dan Y (2012) Neuromodulation of Brain States. *Neuron* 76:209–222.

Litwin-Kumar A, Doiron B (2014) Formation and maintenance of neuronal assemblies through synaptic plasticity. *Nature Communications* 5:5319.

Magee JC, Grienberger C (2020) Synaptic Plasticity Forms and Functions. *Annual Review of Neuroscience* 43:95–117.

Miehl C, Onasch S, Festa D, Gjorgjieva J (2022) Formation and computational implications of assemblies in neural circuits. *The Journal of Physiology* p. JP282750.

Morrison A, Diesmann M, Gerstner W (2008) Phenomenological models of synaptic plasticity based on spike timing. *Biological Cybernetics* 98:459–478.

Muller D, Nikonenko I, Jourdain P, Alberi S (2002) LTP, Memory and Structural Plasticity. *Current Molecular Medicine* 2:605–611.

Musen G, Treisman A (1990) Implicit and explicit memory for visual patterns. *Journal of Experimental Psychology: Learning, Memory, and Cognition* 16:127–137.

Pedrosa V, Clopath C (2017) The Role of Neuromodulators in Cortical Plasticity. A Computational Perspective. *Frontiers in Synaptic Neuroscience* 8.

Peirano PD, Algarín CR (2007) Sleep in brain development. *Biological Research* 40.

Pereira Jr A (2007) What The Cognitive Neurosciences Mean To Me. *Mens Sana Monographs* 5:158.

Pfister JP, Gerstner W (2006) Triplets of Spikes in a Model of Spike Timing-Dependent Plasticity. *The Journal of Neuroscience* 26:9673–9682.

Ponnet J (2022) Master thesis : Neuromodulation of calcium-based plasticity rules Ph.D. diss., Univeristy of Liège, Liège.

Poulet JFA, Crochet S (2019) The Cortical States of Wakefulness. *Frontiers in Systems Neuroscience* 12:64.

Rauchs G, Feyers D, Landeau B, Bastin C, Luxen A, Maquet P, Collette F (2011) Sleep Contributes to the Strengthening of Some Memories Over Others, Depending on Hippocampal Activity at Learning. *The Journal of Neuroscience* 31:2563–2568.

Regehr WG (2012) Short-Term Presynaptic Plasticity. *Cold Spring Harbor Perspectives in Biology* 4:a005702–a005702.

Shajun Nisha S, Nagoor Meeral M (2021) Applications of deep learning in biomedical engineering In *Handbook of Deep Learning in Biomedical Engineering*, pp. 245–270. Elsevier.

Shim HG, Lee YS, Kim SJ (2018) The Emerging Concept of Intrinsic Plasticity: Activity-dependent Modulation of Intrinsic Excitability in Cerebellar Purkinje Cells and Motor Learning. *Experimental Neurobiology* 27:139–154.

Smolen P (2007) A Model of Late Long-Term Potentiation Simulates Aspects of Memory Maintenance. *PLoS ONE* 2:e445.

Sun L, Zhou H, Cichon J, Yang G (2020) Experience and sleep-dependent synaptic plasticity: from structure to activity. *Philosophical Transactions of the Royal Society B: Biological Sciences* 375:20190234.

Takeuchi T, Duszkiewicz AJ, Morris RGM (2014) The synaptic plasticity and memory hypothesis: encoding, storage and persistence. *Philosophical Transactions of the Royal Society B: Biological Sciences* 369:20130288.

Timofeev I, Chauvette S (2019) Sleep-Wake and Cortical Synaptic Plasticity In *Handbook of Behavioral Neuroscience*, Vol. 30, pp. 443–454. Elsevier.

Toni N, Buchs PA, Nikonenko I, Bron CR, Muller D (1999) LTP promotes formation of multiple spine synapses between a single axon terminal and a dendrite. *Nature* 402:421–425.

Turrigiano GG, Nelson SB (2004) Homeostatic plasticity in the developing nervous system. *Nature Reviews Neuroscience* 5:97–107.

Vandeginste B, Massart D, Buydens L, De Jong S, Lewi P, Smeyers-Verbeke J (1998) Artificial Neural Networks In *Data Handling in Science and Technology*, Vol. 20, pp. 649–699. Elsevier.

Vitureira N, Letellier M, Goda Y (2012) Homeostatic synaptic plasticity: from single synapses to neural circuits. *Current Opinion in Neurobiology* 22:516–521.

Wamsley EJ (2019) Memory Consolidation during Waking Rest. *Trends in Cognitive Sciences* 23:171–173.

Zenke F, Agnes EJ, Gerstner W (2015) Diverse synaptic plasticity mechanisms orchestrated to form and retrieve memories in spiking neural networks. *Nature Communications* 6:6922.

Zhang LI, Tao HW, Holt CE, Harris WA, Poo Mm (1998) A critical window for cooperation and competition among developing retinotectal synapses. *Nature* 395:37–44.

Zucker RS, Regehr WG (2002) Short-Term Synaptic Plasticity. *Annual Review of Physiology* 64:355–405.